MICROCOPY RESOLUTION TEST CHART

NATIONAL BUREAU OF STANDARDS-1963-A

RADC-TR-76-377
Final Technical Report
December 1976

RESEARCH STUDIES ON TUNABLE OPTICAL PARAMETRIC OSCILLATORS

W. W. Hansen Laboratories of Physics
Stanford University

DDC
MAR 3 1977
RECEIVED
C

Approved for public release;
distribution unlimited.

ROME AIR DEVELOPMENT CENTER
AIR FORCE SYSTEMS COMMAND
GRIFFISS AIR FORCE BASE, NEW YORK, 13441

Professor S. E. Harris is the responsible investigator for this contract. Audun Hordvik (ETSL), is the RADC Project Engineer.

This report has been reviewed by the RADC Information Office (OI) and is releasable to the National Technical Information Service (NTIS). At NTIS it will be releasable to the General public, including foreign nations.

This technical report has been reviewed and approved for publication.

APPROVED: *Audun Hordvik*
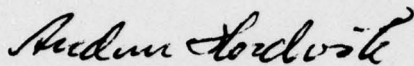
AUDUN HORDVIK
Project Engineer

APPROVED: *Robert M. Barrett*
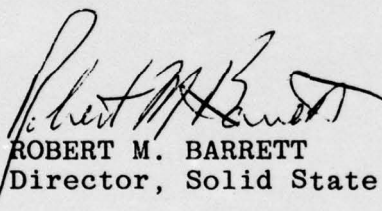
ROBERT M. BARRETT
Director, Solid State Sciences Division

FOR THE COMMANDER: *John P. Huss*

Plans Office

REPORT DOCUMENTATION PAGE		READ INSTRUCTIONS BEFORE COMPLETING FORM
1. REPORT NUMBER RADC-TR-76-377	2. GOVT ACCESSION NO.	3. RECIPIENT'S CATALOG NUMBER
4. TITLE (and Subtitle) RESEARCH STUDIES ON TUNABLE OPTICAL PARAMETRIC OSCILLATORS		5. TYPE OF REPORT & PERIOD COVERED Final Report 1 Oct. 1974—30 Sept 1976
		6. PERFORMING ORG. REPORT NUMBER G.L. 2630
7. AUTHOR(s) Stephen E. Harris James F. Young		8. CONTRACT OR GRANT NUMBER(s) F19628-75-C-0046 DAAG29-74-C-0033
9. PERFORMING ORGANIZATION NAME AND ADDRESS Edward L. Ginzton Laboratory W. W. Hansen Laboratories of Physics Stanford University, Stanford, CA 94305		10. PROGRAM ELEMENT PROJECT TASK AREA & WORK UNIT NUMBERS 62204F 56340902
11. CONTROLLING OFFICE NAME AND ADDRESS Deputy for Electronic Technology (RADC(ESTL)) Hanscom AFB, MA 01731 Monitor: Audun Hordvik		12. REPORT DATE December 1976
		13. NUMBER OF PAGES 256
14. MONITORING AGENCY NAME & ADDRESS(if different from Controlling Office)		15. SECURITY CLASS. (of this report) UNCLASSIFIED
		15a. DECLASSIFICATION DOWNGRADING SCHEDULE

16. DISTRIBUTION STATEMENT (of this Report)

Approved for public release; distribution unlimited

17. DISTRIBUTION STATEMENT (of the abstract entered in Block 20, if different from Report)

18. SUPPLEMENTARY NOTES

19. KEY WORDS (Continue on reverse side if necessary and identify by block number)

Excimer Lasers
IR Up-Conversion and Imaging
Infrared to Visible Frequency Converters

20. ABSTRACT (Continue on reverse side if necessary and identify by block number)

The primary goal of this contract is to pursue research studies of tunable optical sources, to develop coherent sources in new spectral regions, and to conceive and to investigate new nonlinear optical devices of interest to the Air Force. During this contract our efforts have been concentrated on two primary projects: experimental studies of possible metal vapor excimer laser systems, and a unique cesium vapor infrared to visible frequency converter for imaging.

DD FORM 1 JAN 73 1473   EDITION OF 1 NOV 65 IS OBSOLETE

409640

EVALUATION

1. This is the Final Report on the contract. It covers research done on metal vapor excimer laser systems and a cesium vapor infrared to visible frequency converter for imaging. The contract period was 1 Oct. 1974 – 30 Sep. 1976. The objective of the research has been to develop coherent sources in new spectral regions and to investigate new applications of non-linear optical effects. Under this contract a new technique for upconverting infrared radiation to the visible has been demonstrated. An image illuminated by 2.9μ radiation has been upconverted to 4550 Å using a cesium vapor with a power conversion efficiency of 20% and over 1000 resolvable spots.

2. The work performed under this contract has shown that metal vapors are considerably superior to non-linear crystal upconverters. In addition, since short laser pulses are used in the upconversion process, time resolved imaging and range gating can be done. These upconverter devices have potential application for reconnaissance and surveillance.

AUDUN HORDVIK
Project Engineer

SCIENTIFIC PERSONNEL

S. E. Harris	Professor
J. F. Young	Adjunct Professor
G. W. Bekkers	Research Assistant
J. H. Newton	Research Assistant
E. A. Stappaerts	Research Assistant

SUMMARY OF SCIENTIFIC WORK

The primary goal of this contract is to pursue research studies of
tunable optical sources, to develop coherent sources in new spectral re-
gions, and to conceive and to investigate new nonlinear optical devices
of interest to the Air Force. During this contract our efforts have been
concentrated on two primary projects: experimental studies of possible
metal vapor excimer laser systems, and a unique cesium vapor infrared to
visible frequency converter for imaging.

Early in this program a number of metal vapor excimer laser systems
were investigated experimentally with the hope of demonstrating net opti-
cal gain. Based on a number of factors, it was hoped that such excimer
systems might prove useful as high efficiency, high power density ampli-
fiers or lasers in the visible or near infrared portion of the spectrum.
Because of the lack of detailed knowledge of the interatomic potential of
such systems, our investigation was primarily experimental. Na-Ze, Li-Xe,
and Na-Na systems were studied, but no net gain was observed in any case.
In addition, these experiments revealed a number of severe technical prob-
lems related to the construction of high temperature, high pressure cells
containing reactive metals. In addition, the uniform optical pumping of
such highly absorbing and dispersive atomic vapors proved very difficult.
In view of these problems, along with the very small optical gains available,

- 3 -

we subsequently devoted our entire efforts to the cesium infrared image up-converter project.

The IR image up-conversion technique employs a three-photon sum process in cesium vapor. High efficiencies are achieved by two-photon pumping a non-allowed transition in order to produce a resonantly enhanced nonlinearity; using this large nonlinearity, image up-converters having high efficiency and resolution can be constructed using only moderate pump powers. The solid state pumping laser, Nd:lanthanum beryllate, has a natural two-photon coincidence with the cesium $6s^2S-7s^2S$ transition, resulting in a simple, practical system with a number of potential applications for communications, reconnaissance, and the imaging of rapid events.

An evaluation of IR imaging technologies sponsored by the Air Force Avionics Laboratory[*] concludes that the overall performance of such metal vapor techniques is considerably superior to crystal systems, and is comparable to proposed direct IR detection methods. A particular advantage of the nonlinear technique is the high instantaneous conversion efficiency achieved; this makes time resolved imaging of fast events possible, a capability notably lacking in direct detection devices which require long integration times. In addition, the relative timing of an illuminating source and the up-converter pump can be used for range-gated imaging, both to determine range, and to reduce interference from undesired objects. Other attractive features of these systems include scalability to large

_____

[*] Kamala S. Krishnan and John S. Ostrem, "Evaluation of Technologies for Infrared Imaging," Stanford Research Institute Project ISE 4047 for AFAL/TEO Contract F33615-75-C-1142 (January 1976).

- 4 -

apertures and collection angles, high transmission throughout the IR, and the ability to withstand high incident power densities without damage.

Our experimental work has demonstrated a number of these device characteristics. We have recently demonstrated the up-conversion of $2.9\,\mu$ IR images to $4550\,\overset{\circ}{A}$ in cesium vapor. A power conversion efficiency of 20% with over 1000 resolvable spots was achieved using a pump power of only 8 kW. In addition, an extensive theoretical study of the factors influencing image up-converter efficiency, resolution, and image aberrations has been performed. This work, including details of the experimental measurements, and optimized designs for higher performance up-converters, is included as Appendix A.

The publications resulting from work under this contract are listed in Appendix B; previous related contracts and their publications are listed in Appendix C. Portions of this work were jointly supported by the Army Research Office and the Joint Services Electronics Program.

APPENDIX A

INFRARED IMAGE UP-CONVERSION IN

ALKALI METAL VAPORS

by

E. A. Stappaerts

G. L. Report No. 2569

May 1976

Internal Memorandum

Edward L. Ginzton Laboratory
W. W. Hansen Laboratories of Physics
Stanford University
Stanford, California

ABSTRACT

Two-photon-resonant frequency converters are shown to offer an attractive method for up-converting infrared images into the visible and ultraviolet. It is found that for this application they are far superior to crystal up-converters. Experimental results, including the first images produced with this technique, are presented.

A theoretical analysis of two-photon-resonant processes is performed, both for the cases of Q-switched and mode-locked lasers. General results are obtained for efficiency, two-photon absorption probabilities, and the Kerr contribution to the index of refraction. A new method for measuring linewidths of non-allowed transitions, based on the results of this analysis, and experimental results demonstrating this method, are presented.

Finally, harmonic generation and mixing processes at high intensities are discussed. It is shown how the resonances of nonlinear processes are intensity-dependent. The effect of these "frequency shifts" on the efficiency of VUV and soft x-ray generators is discussed.

ACKNOWLEDGEMENTS

I would like to thank the many people who surrounded me during the course of this work. I am particularly indebted to Professor Stephen E. Harris, for his guidance and his enthusiastic support. The experience of working with him for these few years will undoubtedly be of great value for my professional career.

I must also thank the Belgian American Educational Foundation, the European Space Research Organization, and the National Aeronautics and Space Administration for their generous financial support.

Dr. James F. Young has also made a substantial contribution to my education. His "Fingerspitzgefuhl" for mechanical gadgets with n degrees of freedom $(n \rightarrow \infty)$ was most valuable for the eventual product of this thesis.

Suzanne Bennett has helped me on numerous occasions, and her friendship, dedication, and expertise are greatly appreciated.

Thanks also go to R. L. Byer, G. C. Bjorklund, D. M. Bloom, and all the students in the group for many stimulating discussions during the course of this work. This does not only include the more technical discussions, but also the lunch-hour ones on politics, American lifestyle, etc. I consider these an integral part of the fine education Stanford offered me.

TABLE OF CONTENTS

LIST OF FIGURES

LIST OF TABLES

CHAPTER I

INTRODUCTION

This dissertation presents a theoretical and experimental study of the feasibility of using two-photon-resonant frequency conversion processes in metal vapors as a technique for up-converting infrared images into the visible or near UV. The experimental results include (the first) images obtained using this technique. The superiority of the technique over up-conversion in nonlinear crystals is clearly demonstrated.

Also presented is a theoretical analysis of the dependence of the efficiency of two-photon-resonant frequency converters on the laser and atomic linewidths. A new technique for measuring linewidths of non-allowed transitions, based on the results of this analysis, and which has been experimentally demonstrated, is also discussed.

Finally, a theoretical analysis is presented of the interaction of atoms with very intense laser fields as are used for the generation of wavelengths in the VUV range of the spectrum.

The concept of up-conversion in nonlinear crystals is a number of years old.[1,2] The merits of such systems for infrared imaging applications were discussed in a review paper by F. Milton.[3] Two severe

drawbacks of such systems are the very high powers required, together with the poor optical and mechanical properties of most nonlinear crystals. Recently, however, a new technique for frequency up-conversion has been demonstrated,[4-6] which makes use of the strong non-linearities of alkali metal vapors when the pump radiation is tuned to a two-photon resonance. Because of the resonant nature of the interaction, the powers required for high efficiency high resolution imaging are typically more than two orders of magnitude less than those required when making use of the best available crystals, while damage problems do not exist. The price to pay for these improvements is that a pump laser is required which either has an accidental resonance with a non-allowed transition in an alkali metal, or which can be tuned to such a resonance. Also, the choice of IR wavelengths that can be up-converted is limited because the generated sum frequency has to come fairly close to an allowed transition of the vapor. In Chapter III, infrared imaging with such an up-converter is discussed in detail. The various aspects involved are explained using the example of 3μ up-conversion in atomic cesium, for which a very convenient pump source is available.

The efficiency of a two-photon-resonant frequency converter is, in the most general case, a function of the laser spectrum, the pressure broadened linewidth and the Doppler width. General expressions are derived for this efficiency for two cases. In the first case the modes of the laser are assumed to be independent (Q-switched laser), while in the second case they are assumed to be all zero (mode-locked

laser). The results of the first case suggest a new simple way for measuring pressure broadened linewidths, requiring only a tunable laser that may be several orders of magnitude wider than the linewidth being measured. This has to be contrasted with other existing techniques which all require a laser narrower than the atomic linewidth.[7-10] The technique also is able to measure linewidths which are more than an order of magnitude narrower than the Doppler width. The analysis of two-photon-resonant processes, together with experimental results for the pressure broadening by He of the $3s^2S-3d^2D$ transition of Na, are presented in Chapter II.

Chapter IV, which is unrelated to the rest of this dissertation, discusses harmonic generation (mixing) processes which require very high intensities. These processes offer a promising technique for the generation of radiation in the wavelength range of a few hundred angstroms. At the very high intensities involved, the resonances of the nonlinear process are not the same as in the weak field case, but they become dependent on the power of the laser(s). Although these "frequency shifts" can in principal be compensated for, e.g., by tuning to the new resonance frequency in the case of a two-photon-resonant frequency converter, this is often very hard in practice because of the pulse-to-pulse fluctuations of the lasers used for such experiments. At the present time an effort is underway in the laboratory of Dr. Harris to generate 625 Å radiation in He by a third order mixing process of the seventh harmonic, the ninth harmonic, and the fundamental of the 1.064 μ line of the Nd:YAG laser.

CHAPTER II

LINEWIDTH DEPENDENCE OF TWO-PHOTON-RESONANT PROCESSES.

APPLICATION TO THE MEASUREMENT OF LINEWIDTHS OF

ELECTRIC DIPOLE FORBIDDEN TRANSITIONS

A.   INTRODUCTION

Two-photon-resonant processes have been shown to offer a very ef-
ficient technique for the generation of UV as well as IR radiation.[4-6]
They also offer a way for populating atomic or molecular energy levels
via two-photon absorption to some higher level, followed by rapid de-
cay to the level of interest.[11] In the first application these pro-
cesses are attractive because they suffer far less from absorption and
dispersion at the pump and the generated wavelength than do single- or
three-photon-resonant processes. In the second application they are
sometimes preferred over direct population of the pertinent level be-
cause of the possibility to excite a certain small volume inside the
medium by appropriate focusing of the pumping radiation, and also be-
cause the longer wavelengths required are often more easily available.
In this chapter the calculation of such processes is considered in de-
tail. First the basic relations are presented from which the effi-
ciency of frequency converters, two-photon absorption probabilities,

and the quadratic Kerr effect can be calculated. Obviously there is a large number of cases that can be considered, depending on the properties of the incident radiation, i.e., continuous or discrete spectrum, independent or coupled modes, etc. Two cases are treated in detail. In the first one, the incident radiation is assumed to consist of a set of discrete modes with independent phases. The second case is that of a time-bandwidth limited pulse with a continuous spectrum. Sources which produce pulses having a spectrum of the first kind usually have pulselengths that are long compared to the atomic dephasing times, and as a consequence build-up times can and will be neglected in these calculations. For the second case, which is typically that of a very short pulse switched out of a mode-locked train, an exact solution is presented, taking into account the transitory behavior. Finally, based on the results of the first case, a new method is presented for measuring linewidths of electric dipole forbidden transitions, requiring for the measurement a laser source which can be <u>several orders of magnitude wider</u> than the pressure or Doppler broadened atomic linewidth being measured.

B.   BASIC RELATIONS FOR THE CALCULATION OF TWO-PHOTON-RESONANT PROCESSES

1.   The Nonlinear Polarization in Terms of the Incident Fields

The general expression for the 3-d order nonlinear susceptibility is given by Butcher.[12] For the case of two-photon-resonant processes, the polarization at the third harmonic and the back-polarization at the

fundamental frequency can be calculated from the following set of ex-pressions:

$$P^{(3)}(t) = \iiint\limits_{-\infty}^{\infty} d\omega_1 d\omega_2 d\omega_3 \; \chi^{(3)}(\omega_1, \omega_2, \omega_3)$$

$$\times \; E(\omega_1)E(\omega_2)E(\omega_3) \; e^{-i(\omega_1+\omega_2+\omega_3)t}$$

where

$$\chi^{(3)}(\omega_1, \omega_2, \omega_3) = -\frac{N}{\hbar^3} \sum_{\text{paths}} \rho_{00}\mu_{01}\mu_{12}\mu_{23}\mu_{30}$$

$$\times \left\{ \frac{1}{(\omega_{10}-\omega_1)(\omega_{20}-\omega_1-\omega_2-i\gamma/2)(\omega_{30}-\omega_1-\omega_2-\omega_3)} \right.$$

$$+ \frac{1}{(\omega_{10}+\omega_1)(\omega_{20}+\omega_1+\omega_2+i\gamma/2)(\omega_{30}+\omega_1+\omega_2+\omega_3)}$$

$$+ \frac{1}{(\omega_{10}-\omega_1)(\omega_{20}-\omega_1-\omega_2-i\gamma/2)(\omega_{30}+\omega_3)}$$

$$\left. + \frac{1}{(\omega_{10}+\omega_1)(\omega_{20}+\omega_1+\omega_2+i\gamma/2)(\omega_{30}-\omega_3)} \right\}$$

and

$$E(\omega_k) = \frac{1}{2\pi} \int\limits_{-\infty}^{\infty} dt \; E_k(t) \; e^{i\omega_k t} \tag{2.1}$$

In the case of 3-d harmonic generation, the contribution of the last two terms in the susceptibility is small, and we will neglect it in what follows. Assuming that the process is only two-photon-resonant, combination of the expressions under (2.1) gives the following result:

$$P^{(3)}(t;3\omega_0) = -\frac{N}{\hbar^3} \times \frac{\mu_{01}\mu_{12}\mu_{23}\mu_{30}}{(\omega_{10} - \omega_0)(\omega_{30} - 3\omega_0)} \times E_3(t)$$

$$\times \left\{ \int\!\!\!\int_{-\infty}^{\infty} \frac{d\omega_1 d\omega_2 E(\omega_1)E(\omega_2) \; e^{-i(\omega_1 + \omega_2)t}}{(\omega_{20} - \omega_1 - \omega_2 - i\gamma/2)} \right.$$

$$\left. + \int\!\!\!\int_{-\infty}^{\infty} \frac{d\omega_1 d\omega_2 E(\omega_1)E(\omega_2) \; e^{-i(\omega_1 + \omega_2)t}}{(\omega_{20} + \omega_1 + \omega_2 + i\gamma/2)} \right\} \qquad (2.2)$$

where a summation over paths is implicit. Note that although all the calculations will be done for third harmonic generation, the results will be independent of the field used in the third step.

In the case of the back-polarization at the fundamental frequency, the third and fourth terms in the susceptibility are equal respectively to the first and second terms. Assuming again that the process is only two-photon-resonant, the expression for the polarization can be written

- 28 -

as

$$P^{(3)}(t;\omega_0) = -\frac{2N}{\hbar^3} \times \frac{\mu_{01}\mu_{12}\mu_{23}\mu_{30}}{(\omega_{10} - \omega_0)(\omega_{30} - \omega_0)} \times E_3(t)$$

$$\times \left\{ \int\!\!\!\int_{-\infty}^{\infty} \frac{d\omega_1 d\omega_2 E(\omega_1) E(\omega_2)\, e^{-i(\omega_1 + \omega_2)t}}{(\omega_{20} - \omega_1 - \omega_2 - i\gamma/2)} \right.$$

$$\left. + \int\!\!\!\int_{-\infty}^{\infty} \frac{d\omega_1 d\omega_2 E(\omega_1) E(\omega_2)\, e^{-i(\omega_1 + \omega_2)t}}{(\omega_{20} + \omega_1 + \omega_2 + i\gamma/2)} \right\} \qquad (2.3)$$

where again a summation over paths is implicit. In this case the dominant term in the summation over the 3-d level is the one where the 3-d level is the same as the first level. In what follows we will only keep that term.

2. The Generated Electric Field in Terms of the Nonlinear Polarization

The relation between polarization and radiated electric field is given by the wave equation. Neglecting loss:

$$\nabla^2 \overline{E} - \frac{1}{v^2} \frac{\partial^2 \overline{E}}{\partial t^2} = \mu_0 \frac{\partial^2 \overline{P}}{\partial t^2} \qquad (2.4)$$

If the polarization is expanded in a set of plane waves, a traveling wave equation can be written for the complex envelope quantities of each wave. In one dimension:

$$\frac{\partial E_m}{\partial z} = -\frac{i\omega_m \eta_m P_m}{2} \quad \text{for} \quad \text{mode} \quad m \tag{2.5}$$

Because of the linearity of the wave equation, the total field is found by summing the contributions of the individual modes:

$$E(z,t) = \text{Re} \left\{ \sum_m E_m e^{i(\omega_m t - k_m z)} \right\} \tag{2.6}$$

3. The Two-Photon Absorption Probability in Terms of the Back-Polarization

From energy conservation:

$$-\dot{P}E = \hbar\omega_{20} N W^{(2)} \tag{2.7}$$

where P is the back-polarization, N is the number density, and $W^{(2)}$ is the two-photon absorption probability per second. From this expression an average absorption rate can be calculated:

$$W^{(2)} = -\frac{1}{N\hbar\omega_{20}} \times \lim_{T\to\infty} \left[\frac{1}{T} \int_0^T \dot{P}E \, dt \right] \tag{2.8}$$

- 30 -

Often it is more meaningful to talk about the total absorption probability during a pulse:

$$\int_{-\infty}^{\infty} W^{(2)} \, dt \;=\; - \frac{1}{N \hbar \omega_{20}} \int_{-\infty}^{\infty} \dot{P} E \, dt \qquad (2.9)$$

4. The Quadratic Kerr Effect in Terms of the Back-Polarization

The in-phase component of the back-polarization gives a contribution to the index of refraction. For infinite plane waves, this in-phase component can be written as:

$$P^{(3)}_{\text{in phase}} \;=\; \epsilon_0 \chi(\omega) E \qquad (2.10)$$

where E is the amplitude of the wave at frequency ω . The index of refraction is then given by (from Maxwell's equations):

$$(n - 1)_{\text{Kerr}} \;=\; \frac{1}{2} \chi(\omega) \qquad (2.11)$$

For short pulses, the effect on pulse propagation through the medium is found by solving the T.W.E.:

$$\frac{\partial E}{\partial z} + \frac{1}{v} \frac{\partial E}{\partial t} \;=\; - \frac{i \omega \eta P}{2} \qquad (2.12)$$

- 31 -

C. EFFICIENCY OF TWO-PHOTON-RESONANT FREQUENCY CONVERTERS

1. Electric Field With a Discrete Spectrum of Independent Modes

We calculate the tripling efficiency for an incident electric field of the form:

$$E(t) = \sum_m E_m \cos \left[(\omega_0 + m\Delta\omega)t - \varphi_m \right] \qquad (2.13)$$

where the phases φ_m are independent random variables. First we will calculate the polarization at the 3-d harmonic frequency using (2.2). From this we can find the generated electric field using the T.W.E. (2.5). The efficiency is then calculated as the ratio of the power in the third harmonic field to the power in the fundamental field.

Substituting the expression for the electric field (2.13) in the expression for the transform of the field (2.1), we find:

$$E(\omega) = \frac{1}{2} \sum_m E_m \left[e^{i\varphi_m} \delta(\omega - \omega_0 - m\Delta\omega) + e^{-i\varphi_m} \delta(\omega + \omega_0 + m\Delta\omega) \right] \qquad (2.14)$$

Substituting this in the expression for the polarization (2.2):

$$P^{(3)}(t) = -K_1 E_3(t) \times \sum_{m,n} E_m E_n$$

$$\times \left\{ \frac{e^{-i[2\omega_0 + (m+n)\Delta\omega]t + i(\varphi_m + \varphi_n)}}{[\omega_{20} - 2\omega_0 - (m+n)\Delta\omega] - i\gamma/2} + c.c. \right\}$$

where

$$K_1 = \frac{N}{4\hbar^3} \times \frac{\mu_{01}\mu_{12}\mu_{23}\mu_{30}}{(\omega_{10} - \omega_0)(\omega_{30} - 3\omega_0)} \tag{2.15}$$

To incorporate Doppler broadening in the theory we note that, for an observer traveling with the incident electric field, atoms moving at different velocities have different apparent resonance frequencies $\omega_{02}(x) = \omega_{02} + x$. For a Maxwellian velocity distribution, the frequency deviation x has a Gaussian probability density function:

$$p(x) = \frac{1}{\sqrt{2\pi\gamma_D^2}} e^{-x^2/2\gamma_D^2}$$

where

$$\gamma_D = \sqrt{\frac{kT\omega_{20}^2}{Mc^2}} \tag{2.16}$$

There are $N \times p(x) \times dx$ atoms with (apparent) resonance frequencies between $\omega_{20} + x$ and $\omega_{20} + x + dx$. The total polarization is found by summing over all velocity classes. The result is:

$$P^{(3)}(t) = -\frac{2K_1 E_3(t)}{\sqrt{2\pi\gamma_D^2}} \times \sum_{m,n} E_m E_n$$

$$\times \left\{ F_R(k) \cos\left[(2\omega_0 + k\Delta\omega)t - (\varphi_m + \varphi_n)\right] \right.$$

$$\left. + F_I(k) \sin\left[(2\omega_0 + k\Delta\omega)t - (\varphi_m + \varphi_n)\right] \right\}$$

where

$$k = m + n$$

$$F_R(k) = \int_{-\infty}^{\infty} \frac{(\omega_{20} - 2\omega_0 + x - k\Delta\omega)\, e^{-x^2/2\gamma_D^2}\, dx}{(\omega_{20} - 2\omega_0 + x - k\Delta\omega)^2 + (\gamma/2)^2}$$

$$F_I(k) = \int_{-\infty}^{\infty} \frac{\gamma/2\, e^{-x^2/2\gamma_D^2}}{(\omega_{20} - 2\omega_0 + x - k\Delta\omega)^2 + (\gamma/2)^2} \qquad (2.17)$$

The functions $F_R(k)$ and $F_I(k)$ are the real and imaginary parts of the plasma dispersion function.[13] Substituting the expression for $E_3(t)$ in (2.17), the polarization can finally be written as:

$$P^{(3)}(t) = -\frac{K_1}{\sqrt{2\pi\gamma_D^2}} \times \sum_{m,n,p} E_m E_n E_p$$

$$\times \left\{ F_R(k) \cos\left[(3\omega_0 + (k+p)\Delta\omega)t - (\varphi_m + \varphi_n + \varphi_p)\right] \right.$$

$$\left. + F_I(k) \sin\left[(3\omega_0 + (k+p)\Delta\omega)t - (\varphi_m + \varphi_n + \varphi_p)\right] \right\}$$

$$(2.18)$$

Using the T.W.E. (2.5), the electric field generated by each term in the sum (2.18) can now be calculated. The total electric field is found by summing all these contributions. Assuming the same k-vector mismatch for all the terms in the sum (which may not be exact at intensities where the Kerr effect becomes important, see Section II-E),

the T.W.E. for an arbitrary term of the sum is:

$$\frac{\partial E_{m,n,p}}{\partial z} = - \frac{i(3\omega_0)\eta_0 P_{m,n,p} e^{i\triangle kz}}{2}$$

where

$$P_{m,n,p} = - \frac{K_1}{\sqrt{2\pi\gamma_D^2}} E_m E_n E_p [F_R(k) - iF_I(k)] \qquad (2.19)$$

Integrating this equation over the length L of the medium:

$$E_{m,n,p} = - \frac{i(3\omega_0)\eta_0 L}{2} \times P_{m,n,p} e^{i\triangle kL/2} \text{ sinc } (\triangle kL/2) \qquad (2.20)$$

Finally, the total generated field is given by:

$$E^{(3)}(t) = \text{Re} \left\{ \sum_{m,n,p} E_{m,n,p} e^{i\psi} \right\}$$

$$= \frac{(3\omega_0)\eta_0 K_1 L}{2\sqrt{2\pi\gamma_D^2}} \times \text{ sinc } (\triangle kL/2)$$

$$\times \sum_{m,n,p} E_m E_n E_p [F_I(k) \cos \psi - F_R(k) \sin \psi]$$

where

$$\psi = [3\omega_0 + (k + p) \triangle\omega]t - k_s L - (\varphi_m + \varphi_n + \varphi_p) \qquad (2.21)$$

Because the phases $(\varphi_m + \varphi_n + \varphi_p)$ for different terms of the sum are independent, the time average value of the square of the electric field waveform is simply given by one-half the sum of the squares of the amplitudes of the terms:

$$\langle [E^{(3)}(t)]^2 \rangle = \frac{(3\omega_0)^2 \eta_0^2 K_1^2 L^2}{16 \pi \gamma_D^2} \times \text{sinc}^2 (\Delta k L/2)$$

$$\times \sum_p E_p^2 \sum_{k,n} E_n^2 E_{k-n}^2 [F_R^2(k) + F_I^2(k)] \qquad (2.22)$$

(Note that, since terms with different p values have different frequencies, this result is true no matter what the relation is between the φ_p's ; hence the third field could be anything). Since the time averaged value of the square of the incident field is simply $\sum_p E_p^2/2$, the efficiency, in the plane wave approximation, is given by:

$$\mathcal{E} = \frac{P_{\text{harmonic}}}{P_{\text{fundam.}}} = \frac{\langle [E^{(3)}]^2 \rangle}{\langle (E)^2 \rangle}$$

$$= \frac{(3\omega_0)^2 \eta_0^2 K_1^2 L^2}{8 \pi \gamma_D^2} \times \text{sinc}^2 (\Delta k L/2)$$

$$\times \sum_{k,n} E_n^2 E_{k-n}^2 [F_R^2(k) + F_I^2(k)] \qquad (2.23)$$

If we define the normalized auto-convolution of the power spectrum of

the incident field:

$$G(k) = \frac{\frac{1}{4} \sum\limits_{n} E_n^2 E_{k-n}^2}{\left[\sum\limits_{n} (E_n^2/2) \right]^2} \equiv \frac{1}{4\eta_0^2} \sum\limits_{n} \frac{E_n^2 E_{k-n}^2}{I_{av}^2} \qquad (2.24)$$

where I_{av} is the average intensity of the incident field, this can be rewritten as:

$$\mathcal{E} = \frac{2(3\omega_0)^2 \eta_0^4 K_1^2 L_c^2 I_{av}^2}{\pi^3 \gamma_D^2} \times \sin^2 (\Delta kL/2) \times \sum\limits_{k} G(k) [F_R^2(k) + F_I^2(k)]$$

$$(2.25)$$

This expression is very general in that it gives the lineshape of the two-photon-resonance for any power spectrum with independent modes, both in the Doppler and the pressure broadened regime. In an arbitrary case, (2.25) can be evaluated numerically (see Appendix A). Two special cases are of particular interest, because they occur often in practice, and because they also suggest a new way of measuring linewidths of non-allowed transitions. They are the cases when either pressure or Doppler broadening dominates, while the mode spacing is much smaller than and the laser bandwidth is much wider than the atomic linewidth of the case being considered. We will now derive closed form expressions for the efficiency in both these cases, assuming a Gaussian

power spectrum for the incident radiation:

$$E_n^2 = E_0^2 \, e^{-4n^2 \Delta\omega^2/\delta^2} \tag{2.26}$$

where $\delta = (\ln 2)^{-\frac{1}{2}}$ times the F.W.H.M. of the laser spectrum. Using this definition one easily finds, by substitution in (2.24):

$$G(k) = \sqrt{\frac{2}{\pi}} \; \frac{\Delta\omega}{\delta} \; e^{-2k^2\Delta\omega^2/\delta^2} \tag{2.27}$$

a. <u>Pressure broadened regime, $\Delta\omega < \gamma < \delta$</u>

On resonance, one finds in this limiting case:

$$F_R(k) = \sqrt{2\pi\gamma_D^2} \; \frac{(-\, k\Delta\omega)}{(k\Delta\omega)^2 + (\gamma/2)^2}$$

$$F_I(k) = \sqrt{2\pi\gamma_D^2} \; \frac{\gamma/2}{(k\Delta\omega)^2 + (\gamma/2)^2} \tag{2.28}$$

Substituting (2.27) and (2.28) in the summation over k appearing in (2.25), we find for this sum:

$$\sum_k = 2\pi \sqrt{\frac{2}{\pi}} \times \frac{\gamma_D^2 \Delta\omega}{\delta} \times \sum_k \frac{e^{-2k^2\Delta\omega^2/\delta^2}}{(k\Delta\omega)^2 + (\gamma/2)^2} \tag{2.29}$$

Since the laser bandwidth is assumed to be much wider than the atomic linewidth, the exponential in the sum can be set equal to one. Because

the mode spacing is much less than the linewidth, the sum can be approximated by an integral. The final result is:

$$\mathcal{E} = \frac{8}{\pi} \frac{\sqrt{2}}{\sqrt{\pi}} \times \frac{(3\omega_0)^2 \eta_0^4 K_1^2 L_c^2 I_{av}^2}{\gamma\delta} \times \sin^2(\Delta kL/2) \qquad (2.30)$$

which shows an inverse linear dependence on both the laser bandwidth and the pressure broadened atomic linewidth.

b. Doppler broadened regime, $\Delta\omega < \gamma_D < \delta$

In this limiting case, on resonance:[13]

$$F_R(k) = -2\sqrt{\pi} \; e^{-x^2} \int_0^x e^{t^2} dt$$

$$F_I(k) = \pi \; e^{-x^2}$$

where

$$x = \frac{k\Delta\omega}{\sqrt{2} \; \gamma_D} \qquad (2.31)$$

Again we have to evaluate the sum over k appearing in (2.25). Using (2.27) and (2.31):

$$\sum_k G(k) F_I^2(k) = \pi^2 \sqrt{\frac{2}{\pi}} \times \frac{\Delta\omega}{\delta} \times \sum_k e^{-k^2\Delta\omega^2[(2/\delta^2) + (1/\gamma_D^2)]}$$

$$(2.32)$$

- 39 -

Because the laser is assumed to be much wider than the Doppler width, the term involving the laser width can be neglected in the exponential. Because the mode spacing is much less than the Doppler width, the sum can be approximated by an integral. The result is:

$$\sum_k = \pi^2 \sqrt{2} \; \frac{\gamma_D}{\delta} \tag{2.33}$$

Using (2.27) and (2.31):

$$\sum_k G(k)F_R^2(k) = 4 \sqrt{2\pi} \times \frac{\Delta\omega}{\delta}$$

$$\times \sum_k \left\{ e^{-(k^2 \Delta\omega^2/\delta^2)} \left[e^{-x^2} \int_0^x e^{t^2} \, dt \right]^2 \right\} \tag{2.34}$$

For the same reasons as above, this can be approximated by:

$$\sum_k = 16 \sqrt{\pi} \times \frac{\gamma_D}{\delta} \times \int_0^\infty dv \left[e^{-v^2} \int_0^v e^{t^2} \, dt \right]^2 \tag{2.35}$$

The value of the integral in this expression is 0.5. So the final result is:

$$\sum_k = 8 \sqrt{\pi} \; \frac{\gamma_D}{\delta} \tag{2.36}$$

Substituting (2.33) and (2.36) in (2.25), we find for the efficiency

in this case:

$$\mathcal{E} = \frac{2(\pi^2 \sqrt{2} + 8 \sqrt{\pi})}{\pi^3} \times \frac{(3\omega_0)^2 \eta_0^4 K_1^2 L^2 I_{c\,av}^2}{\gamma_D \delta} \times \sin^2 (\Delta k L/2) \qquad (2.37)$$

which shows, similar to the pressure broadened case, an inverse lin-ear dependence on the laser bandwidth and the Doppler broadened atomic linewidth.

Remarks

The inverse linear dependence of the efficiency on δ and γ (2.30), and δ and γ_D (2.37) can easily be arrived at using simple arguments. Assume that the incident field consists of N modes of equal amplitude E . In the pressure broadened regime, the response at $2\omega_0$, and hence the electric field generated by a pair of modes (m,n) is proportional to E^2/γ . Since the contributions of dif-ferent pairs have independent phases, powers have to be added. So we just have to multiply the power for one pair of modes by the number of pairs. This number can easily be found as follows. If we keep the mode used in the first perturbation step fixed, then there are $\gamma/\Delta\omega$ (for $\Delta\omega < \gamma < \delta$) possibilities for the mode in the second step. This can be done using any of the N modes in the first step. Thus the total power and hence the efficiency is proportional to:

$$\mathcal{E} \propto \left(\frac{E^2}{\gamma}\right)^2 \times \frac{\gamma}{\Delta\omega} \times N$$

- 41 -

In terms of the average intensity $I_{av} \propto NE^2$, this can be written as:

$$\mathcal{E} \propto \frac{I_{av}^2}{\gamma \delta}$$

In the Doppler broadened regime, the atoms can be divided into packets of width γ . All the atoms in one packet are mainly driven by the same set of modes, while atoms in different packets are driven by independent sets of modes. Hence in this case the total radiated power will be proportional to the number of packets, while in the pressure broadened regime, where all atoms respond identically, it varies as the square of the <u>total</u> number density. This means that compared to the other case, the efficiency is down by the number of packets, i.e.:

$$\mathcal{E} \propto \frac{I_{av}^2}{\gamma \delta} \Bigg/ \frac{\gamma_D}{\gamma} = \frac{I_{av}^2}{\gamma_D \delta}$$

Note that in this last derivation the result of the pressure broadened regime was used, which means that it is only valid if $\Delta \omega < \gamma$, not just $\Delta \omega < \gamma_D$. In the exact derivation we did not have to make this stronger assumption. It should be noted however that, if the mode spacing is larger than the linewidth of individual atoms, we have a non-homogeneous situation where certain atoms are driven much harder than others. The result (2.37) gives the efficiency for the total ensemble of atoms. In using it under non-homogeneous conditions one should check however whether the response of strongly driven atoms is

- 42 -

not saturating (a similar remark can be made for two-photon absorption, where bleaching can occur).

If the laser spectrum consists of only a few modes, then the general expression for the efficiency (2.25) should be looked at as an ensemble average, i.e., it represents the average efficiency for a large number of laser shots.

2. Time-Bandwidth-Limited Pulses

We calculate the tripling efficiency for an electric field of the form:

$$E(t) = E_0 \, e^{-t^2/\tau^2} \cos \omega_0 t \tag{2.38}$$

Substituting this expression in (2.1):

$$E(\omega) = \frac{E_0 \tau}{4 \sqrt{\pi}} \left\{ e^{-[(\omega - \omega_0)^2 \tau^2/4]} + e^{-[(\omega + \omega_0)^2 \tau^2/4]} \right\} \tag{2.39}$$

The polarization set up at the third harmonic frequency is found by

substituting (2.39) into (2.2):

$$P^{(3)}(t) = -4K_1 E_3(t) \times \left(\frac{E_0 \tau}{4\sqrt{\pi}}\right)^2$$

$$\times \left\{ \iint_{-\infty}^{\infty} \frac{d\omega_1 d\omega_2 \, e^{-(\tau^2/4)[(\omega_1-\omega_0)^2 + (\omega_2-\omega_0)^2]} \, e^{-i(\omega_1+\omega_2)t}}{\omega_{20} - \omega_1 - \omega_2 - i\gamma/2} \right.$$

$$\left. + \iint_{-\infty}^{\infty} \frac{d\omega_1 d\omega_2 \, e^{-(\tau^2/4)[(\omega_1+\omega_0)^2 + (\omega_2+\omega_0)^2]} \, e^{-i(\omega_1+\omega_2)t}}{\omega_{20} + \omega_1 + \omega_2 + i\gamma/2} \right\}$$

(2.40)

The two integrals can be greatly simplified by making two successive changes of variables:

First Change

First Integral	Second Integral
$x = \omega_1 - \omega_0$	$x = \omega_1 + \omega_0$
$y = \omega_2 - \omega_0$	$y = \omega_2 + \omega_0$

Second Change

$$u = x + y$$
$$v = x - y$$

The result is:

$$P^{(3)}(t) = -\frac{K_1}{4\pi} \times E_0^2 \tau^2 E_3(t)$$

$$\times \left\{ e^{-i2\omega_0 t} \int_{-\infty}^{\infty} dv\, e^{-(\tau^2 v^2/8)} \int_{-\infty}^{\infty} \frac{du\, e^{-(\tau^2 u^2/8)}\, e^{-iut}}{\omega_{20} - 2\omega_0 - u - i\gamma/2} \right.$$

$$\left. + e^{i2\omega_0 t} \int_{-\infty}^{\infty} dv\, e^{-(\tau^2 v^2/8)} \int_{-\infty}^{\infty} \frac{du\, e^{-(\tau^2 u^2/8)}\, e^{-iut}}{\omega_{20} - 2\omega_0 + u + i\gamma/2} \right\}$$

(2.41)

The integral with respect to v is trivial, while the ones with respect to u can be quite easily done if looked at as Fourier transforms of products. The result is:[14]

$$P^{(3)}(t) = -2K_1 E_0^2 E_3(t)$$

$$\times \left\{ ie^{-i2\omega_0 t} \left[e^{-2t^2/\tau^2} * e^{-\gamma t/2}\, H(t)\, e^{-i(\omega_{20} - 2\omega_0)t} \right] + c.c. \right\}$$

(2.42)

where $H(t)$ is the unit stepfunction and the star denotes convolution. One can show that in the rotating wave approximation, this expression

can also be written as:

$$P^{(3)}(t) = -8K_1E_3(t)$$

$$\times \left[\left(E_0 \, e^{-t^2/\tau^2} \right)^2 \cos 2\omega_0 t * e^{-\gamma t/2} H(t) \sin \omega_{20} t \right] \qquad (2.43)$$

In this form the response can immediately be recognized as the con-
volution of the impulse response of the system with an effective
driving field, completely analogous to the case of a single photon
process. If we substitute the expression (2.38) for $E_3(t)$ in (2.42),
we finally find for the polarization at the third harmonic frequency:

$$P^{(3)}(t) = -2K_1E_0^3 \, e^{-t^2/\tau^2} [C_R(t) \sin 3\omega_0 t + C_I(t) \cos 3\omega_0 t]$$

where

$$C(t) \equiv C_R(t) + iC_I(t) = e^{-2t^2/\tau^2} * e^{-\gamma t/2} H(t) e^{i(\omega_0 - 2\omega_0)t} \qquad (2.44)$$

The complex envelope of the generated third harmonic field is easily
found using the T.W.E. (2.5). The result is:

$$E^{(3)}(t) = \frac{2}{\pi} \eta_0(3\omega_0)K_1L_cE_0^3 \, e^{-t^2/\tau^2} (C_R + iC_I) \, e^{i(\Delta kL/2)} \sin(\Delta kL/2)$$

$$(2.45)$$

- 46 -

Since we are dealing with a pulse with a certain profile in time, the most meaningful definition for the efficiency in this case is as the ratio of the energy in the third harmonic pulse to the energy in the fundamental pulse. In the plane wave approximation, where all beams have the same area:

$$\mathcal{E} = \frac{\int\limits_{-\infty}^{\infty} [E^{(3)}(t)]^2 \, dt}{\int\limits_{-\infty}^{\infty} (E_0 \, e^{-t^2/\tau^2})^2 \, dt}$$

$$\boxed{\mathcal{E} = \frac{32}{\pi^3} \frac{\sqrt{2}}{\sqrt{\pi}} \, D_1 (3\omega_0)^2 \eta_0^4 K_1^2 L_c^2 \times (J/A)^2 \times \sin^2 (\Delta k L/2)}$$

where

$$D_1 = \frac{1}{\tau^2} \int\limits_{-\infty}^{\infty} e^{-2v^2} |C(\tau v)|^2 \, dv$$

$$J/A = \frac{1}{2} \sqrt{\frac{\pi}{2}} \frac{E_0^2 \tau}{\eta_0} \tag{2.46}$$

The quantity D_1 is a dimensionless quantity, while J/A is the energy density in the incident pulse. The expression (2.46) gives the shape of the resonance profile, assuming no Doppler broadening (see later). On resonance, in the usual case that the pulselength is much shorter than the atomic dephasing time, the function $C(t)$ reduces to

- 47 -

the probability integral, and D_1 can easily be calculated numerically

giving the result $D_1 = 0.67$. Hence, on resonance:

$$\mathcal{E} = 0.55 \ (3\omega_0)^2 \eta_0^4 K_1^2 L_c^2 \times (J/A)^2 \times \sin^2 (\Delta k L/2) \qquad (2.47)$$

As mentioned before, this result neglects Doppler broadening. For the

case where the laser bandwidth is considerably wider than the Doppler

width, which is usually the case for pulses generated by a mode-locked

laser, it can simply be argued however that Doppler broadening is not

going to affect the result (2.47). The reason is that in the mode-

locked case, in contrast to the case of independent modes, all the

phases are zero, and hence <u>all</u> the atoms are excited in phase, even

though different packets are driven by different bands of frequencies.

Remarks

The dependence of (2.46) on laser linewidth can easily be under-

stood as follows. Applying a short optical pulse with center frequency

ω_0 is by definition equivalent to applying a monochromatic wave of

frequency ω_0 for a time equal to the pulselength τ . The polar-

ization set up by a monochromatic wave on resonance is proportional to

E_0^3/γ . However, the build-up time on resonance is T_2 , and since

we assume that this time is much longer than the pulselength, the

polarization will only build up to a fraction (τ/T_2) of the value

for an infinite wave. Thus the value of the polarization for a short

- 48 -

pulse is:

$$P \propto \frac{E_0^3}{\gamma} \times \frac{\tau}{T_2} \propto E_0^3 \tau$$

The energy in the polarization pulse and hence in the radiated electric field is then proportional to $(E_0^3 \tau)^2 \times \tau$. Hence the efficiency is proportional to:

$$\mathcal{E} \propto \frac{E_0^6 \tau^3}{E_0^2 \tau} \propto (J/A)^2$$

D.   TWO-PHOTON ABSORPTION

1.   Electric Field With a Discrete Spectrum of Independent Modes

We calculate the two-photon absorption probability per second for an electric field of the form (2.13), using (2.8). First we calculate the back-polarization at the fundamental frequency, using (2.3). The result is an expression very similar to (2.18), except that the temporal variation is at ω_0 , and the constant K_1 gets replaced by a constant K_2 , where:

$$K_2 = \frac{N}{2\hbar^3} \times \frac{\mu_{01}^2 \mu_{12}^2}{(\omega_{10} - \omega_0)^2}$$

Hence:

$$
P^{(3)}(t) = -\frac{K_2}{\sqrt{2\pi\gamma_D^2}} \sum_{m,n,p} E_m E_n E_p
$$

$$
\times \left\{ F_R(k) \cos\left[(\omega_0 + (m+n-p)\Delta\omega)t - (\varphi_m + \varphi_n - \varphi_p)\right] \right.
$$

$$
\left. + F_I(k) \sin\left[(\omega_0 + (m+n-p)\Delta\omega)t - (\varphi_m + \varphi_n - \varphi_p)\right] \right\} \qquad (2.48)
$$

Using this expression we can calculate $\dot{PE}$. Keeping only the slowly varying terms, which are the only ones that will contribute to the time averaged absorption rate, we find:

$$
\dot{PE} \approx -\frac{K_2\omega_0}{2\sqrt{2\pi\gamma_D^2}} \sum_{m,n,p,q} \left[-F_R(k)\sin\psi + F_I(k)\cos\psi\right]
$$

where

$$
\psi = (m+n-p-q)\Delta\omega t - (\varphi_m + \varphi_n - \varphi_p - \varphi_q) \qquad (2.49)
$$

According to (2.8), we now have to calculate the time averaged value of this quantity, i.e.:

$$
\langle \dot{PE} \rangle = \lim_{T\to\infty} \left[\frac{1}{T}\int_0^T \dot{PE}\, dt\right]
$$

- 50 -

We find immediately the condition $(m+n) = (p+q)$, and hence:

$$\langle \dot{PE} \rangle = -\frac{K_2 \omega_0}{2\sqrt{2\pi \gamma_D^2}} \sum_{\substack{m,n,p,q \\ m+n=p+q}} E_m E_n E_p E_q F_I(k) \cos(\varphi_m + \varphi_n - \varphi_p - \varphi_q)$$

$$(2.50)$$

Because of the independence of the phases, the only terms which do not average out in this quadruple sum are those for which $\varphi_m + \varphi_n - \varphi_p - \varphi_q = 0$, such that the cosine factor is unity. This is only possible if:

$$\begin{cases} \varphi_m = \varphi_p \\ \varphi_n = \varphi_q \end{cases} \quad \text{or} \quad \begin{cases} \varphi_m = \varphi_q \\ \varphi_n = \varphi_p \end{cases}$$

which says that the same pair of modes has to be used in going from dc to frequency $2\omega_0$ and in coming back down from $2\omega_0$ to dc. The expression (2.50) then simplifies to a double sum:

$$\langle \dot{PE} \rangle = -\frac{K_2 \omega_0}{\sqrt{2\pi \gamma_D^2}} \times \sum_{k,n} E_n^2 E_{k-n}^2 F_I(k) \qquad (2.51)$$

This expression can be rewritten in terms of the auto-convolution function $G(k)$, and substituted into (2.8). This gives the final general result:

$$\boxed{W^{(2)} = \frac{2K_2 \eta_0 I_{av}^2}{\hbar N} \times \frac{1}{\sqrt{2\pi \gamma_D^2}} \sum_k G(k) F_I(k)} \qquad (2.52)$$

- 51 -

As it should be, this expression only contains the coefficients $F_I(k)$ of the quadrature component of the back-polarization. We will now again, as in the previous section, derive closed form expressions for the special cases where the laser bandwidth is much larger than and the mode spacing is much smaller than the atomic linewidth, and *either* pressure or Doppler broadening dominates.

a. Pressure broadened regime, $\Delta\omega < \gamma < \delta$

On resonance:

$$\frac{1}{\sqrt{2\pi\gamma_D^2}} \, F_I(k) = \frac{\gamma/2}{(k\Delta\omega)^2 + (\gamma/2)^2} \tag{2.53}$$

This expression, together with (2.27), can be used to evaluate the summation over k appearing in (2.52). Using identical arguments as in Section C, one finds:

$$\frac{1}{\sqrt{2\pi\gamma_D^2}} \, \sum_k G(k) F_I(k) = \frac{\sqrt{2\pi}}{\delta} \tag{2.54}$$

Substituting this expression and the expression for K_2, we find for the two-photon absorption rate:

$$W^{(2)} = \frac{\sqrt{2\pi} \, \eta_0^2 \mu_{01}^2 \mu_{12}^2 I_{av}^2}{\hbar^4 (\omega_{10} - \omega_0)^2 \delta} \tag{2.55}$$

Note that this expression does <u>not contain the atomic linewidth</u>.

b. <u>Doppler broadened regime, $\Delta\omega < \gamma_D < \delta$</u>

On resonance:

$$\frac{1}{\sqrt{2\pi\gamma_D^2}} \, F_I(k) \;=\; \frac{\pi}{\sqrt{2\pi\gamma_D^2}} \; e^{-(k^2\Delta\omega^2/2\gamma_D^2)} \tag{2.56}$$

Combining this expression with (2.27), and using identical arguments as in Section C, one finds:

$$\frac{1}{\sqrt{2\pi\gamma_D^2}} \; \sum_k \, G(k)F_I(k) \;=\; \frac{\sqrt{2\pi}}{\delta} \tag{2.57}$$

This result is identical to that of the pressure broadened case (2.54), and thus $W^{(2)}$ is given by (2.55).

<u>Remarks</u>

As for the efficiency expressions in Section C, the inverse linear dependence of the two-photon absorption rate on laser linewidth can be found using simple arguments. Assume again that the incident field consists of N independent modes of equal amplitude E. The time averaged absorption rate $\langle \dot{P}E \rangle$ for one pair of modes (m,n) is proportional to $E^3/\gamma \times E = E^4/\gamma$. Because of the independence of the phases, the total absorption is simply found by multiplying the absorption due to one pair of modes by the number of pairs such that their sum frequency is under the atomic linewidth. We derived in Section C

- 53 -

that this number is $\gamma/\Delta\omega \times N$ if $\Delta\omega < \gamma < \delta$. Hence:

$$W^{(2)} \propto \frac{E^4}{\gamma} \times \frac{\gamma}{\Delta\omega} \times N$$

or, in terms of $I_{av} \propto NE^2$:

$$W^{(2)} \propto \frac{I_{av}^2}{\delta}$$

independent of the atomic linewidth. In the Doppler broadened regime, since absorption is an "individual atom" phenomenon, the above expression is clearly unchanged if the laser is much wider than the Doppler width, such that all atoms are driven equally hard. If, in the Doppler regime, the mode spacing is larger than the linewidth of individual atoms, a non-homogeneous situation arises. One should check in that case whether the atoms which are driven hardest are not being bleached.

If the laser spectrum consists of only a few modes, (2.52) must be looked at as an ensemble average.

2. Time-Bandwidth-Limited Pulses

We assume an electric field of the form (2.38). The back-polarization is then given by an expression similar to (2.44), but with K_1 replaced by K_2 , and $3\omega_0$ replaced by ω_0 :

$$P^{(3)}(t) = -2K_2E_0^3 e^{-t^2/\tau^2} [C_R(t) \sin \omega_0 t + C_I(t) \cos \omega_0 t] \qquad (2.58)$$

- 54 -

After differentiation and multiplication by the incident field, we find, keeping only slowly varying quantities:

$$\dot{PE} = -K_2 \omega_0 E_0^1 e^{-2t^2/\tau^2} C_R(t) \tag{2.59}$$

The total probability for absorption during the pulse is found by substituting this expression in (2.9). The result is:

$$\int_{-\infty}^{\infty} W^{(2)} dt = \frac{4\eta_0^2 D_2 K_2 (J/A)^2}{\pi \hbar N}$$

where

$$D_2 = \frac{1}{\tau} \int_{-\infty}^{\infty} dv \, e^{-2v^2} C_R(\tau v) \tag{2.60}$$

The quantity D_2 is a dimensionless quantity, while J/A is the energy density in the pulse. On resonance, for the usual case where the pulselength is much shorter than the atomic dephasing time, one finds numerically $D_2 = 0.8$. Substituting this value into (2.60), together with the expression for K_2 (2.58), we find for the total absorption probability on resonance:

$$\int_{-\infty}^{\infty} W^{(2)} dt = \frac{0.52 \, \eta_0^2 \mu_{01}^2 \mu_{12}^2 \, (J/A)^2}{\hbar^4 \, (\omega_{10} - \omega_0)^2} \tag{2.61}$$

Note that this expression is <u>independent of the atomic linewidth</u>. In the derivation Doppler broadening was not considered, but as in Section C it is clear that the result (2.60) will also be correct in the Doppler broadened regime, if the laser bandwidth is much wider than the Doppler width such that all atoms are driven equally hard.

Remarks:

The dependence of (2.61) on J/A can easily be understood as follows. As explained in Section C, the back-polarization is proportional to $E_0^3 \tau$. Hence

$$W^{(2)} \quad \propto \quad \dot{P}E \quad \propto \quad E_0^4 \tau$$

and the integrated absorption probability will be proportional to:

$$\int_{-\infty}^{\infty} W^{(2)} \, dt \quad \propto \quad (E_0^4 \tau)\tau \quad \propto \quad (J/A)^2$$

E.   QUADRATIC KERR EFFECT

1.   Electric Field With a Discrete Spectrum of Independent Modes

We will calculate the Kerr contribution to the index of refraction using (2.10) and (2.11). Consider a mode with frequency $\omega_0 + m\Delta\omega$. The third order back-polarization at this frequency, due to the mode itself and all the other modes is given by an expression similar to

(2.58), but with $p \equiv n$, i.e.:

$$P^{(3)}(t;\omega_0 + m\Delta\omega) = -\frac{K_2 E_m}{\sqrt{2\pi\gamma_D^2}} \times \sum_n E_n^2$$

$$\times \left\{ F_R(k) \cos [(\omega_0 + m\Delta\omega)t - \varphi_m] \right.$$

$$\left. + F_I(k) \sin [(\omega_0 + m\Delta\omega)t - \varphi_m] \right\} \qquad (2.62)$$

The component in phase with the incident field can be written as:

$$P^{(3)}_{\text{in phase}} = -K_2 \times \sum_n E_n^2 \frac{F_R(m+n)}{\sqrt{2\pi\gamma_D^2}} \times E_m(t) \qquad (2.63)$$

Combining this expression with (2.10) and (2.11), we find:

$$\boxed{(n-1)_{\text{Kerr}} = -\frac{K_2}{2\epsilon_0} \sum_n E_n^2 \frac{F_R(m+n)}{\sqrt{2\pi\gamma_D^2}}} \qquad (2.64)$$

a. <u>Pressure broadened regime,</u> $\Delta\omega < \gamma < \delta$

On resonance:

$$\frac{F_R(m+n)}{\sqrt{2\pi\gamma_D^2}} = \frac{-(m+n)\Delta\omega}{[(m+n)\Delta\omega]^2 + (\gamma/2)^2} \qquad (2.65)$$

If we substitute this expression together with the definition of E_n^2 (2.26) into (2.64), we find:

$$(n - 1)_{Kerr} = \frac{K_2 E_0^2}{2\epsilon_0} \sum_n \frac{(m+n)\Delta\omega \; e^{-4n^2\Delta\omega^2/\delta^2}}{[(m+n)\Delta\omega]^2 + (\gamma/2)^2} \qquad (2.66)$$

If we let:

$$n\Delta\omega = -x$$

$$\delta'^2 = \delta^2/8$$

and assume that the mode spacing is much less than the atomic linewidth such that the sum can be approximated by an integral, this can be re-written as:

$$(n - 1)_{Kerr} = \frac{K_2 E_0^2 F_R(m, \delta')}{2\epsilon_0 \Delta\omega}$$

where

$$F_R(m, \delta') = \int_{-\infty}^{\infty} \frac{(x - m\Delta\omega) \; e^{-x^2/2\delta'^2}}{(x - m\Delta\omega)^2 + (\gamma/2)^2} \, dx \qquad (2.67)$$

If the laser bandwidth is much wider than the atomic linewidth, we can use the asymptotic form of $F_R(m, \delta')$:

$$F_R(m, \delta') = \sqrt{2\pi\delta'^2} \; \frac{(-m\Delta\omega)}{(m\Delta\omega)^2 + (\gamma/2)^2} \qquad (2.68)$$

Combination of (2.67) and (2.68) yields, in terms of the average intensity of the incident field:

$$(n - 1)_{Kerr} = - \frac{\eta_0 K_2 I_{av}}{\epsilon_0} \times \frac{m\Delta\omega}{(m\Delta\omega)^2 + (\gamma/2)^2}$$

where

$$I_{av} = \frac{\sqrt{\pi}}{4} \times \frac{E_0^2 \delta}{\eta_0 \Delta\omega} \qquad (2.69)$$

Finally, substituting the definition of K_2 (2.58):

$$(n - 1)_{Kerr} = - \frac{\eta_0 N \mu_{01}^2 \mu_{12}^2 I_{av}}{2\epsilon_0 \hbar^3 (\omega_{10} - \omega_0)^2} \times \frac{m\Delta\omega}{(m\Delta\omega)^2 + (\gamma/2)^2} \qquad (2.70)$$

the absolute value of $(n - 1)$ is maximum when the detuning $n\Delta\omega = \pm \gamma/2$. At this detuning the last factor in (2.70) equals $1/\gamma$.

b. Doppler broadened regime

The limiting form of $F_R(m + n)$, on resonance, is given by (2.31). The summation over n in (2.64) can only be done numerically in this case, and we will not consider it in detail here.

2. Time-Bandwidth-Limited Pulses

The in-phase component of the back-polarization is given by (2.58):

$$P^{(3)}(t) = - 2K_2 E_0^2 C_I(t) E(t) \qquad (2.71)$$

- 59 -

To find the effect of this polarization on the propagation of the pulse through the nonlinear medium, one has to solve the T.W.E. (2.12). Note that right on resonance, the function $C_I(t)$ vanishes, and the effect is zero.

Although it is not rigorous for short pulses, one can, analogous to the infinite plane wave case, calculate an index of refraction from (2.71), using (2.10) and (2.11). The result is:

$$(n - 1)_{Kerr} = - \frac{4 \eta_0 K_2 \ (J/A) \ C_I(t)}{\sqrt{2\pi} \ \epsilon_0 \tau} \tag{2.72}$$

From the maximum value that this expression obtains during the pulse, one can calculate a maximum value for $\Delta k \times L$, which should give a good indication of the importance of the effect.

F.   MEASUREMENT OF THE LINEWIDTH OF ELECTRIC DIPOLE FORBIDDEN
     TRANSITIONS

Several methods are currently available to measure the linewidth of non-allowed transitions,[7-10] but the required laser sources are not often available. Using the results of Section C, it is possible to quickly and conveniently measure such linewidths, even when they are considerably narrower than the Doppler width. The method requires a laser source which can be several orders of magnitude wider than the atomic linewidth being measured.

We will first discuss the theory on which the method is based, and then give experimental results for the broadening of the $3s^2S - 3d^2D$ transition in Na.

1. Theory of the Measurement

Because of the dependence of the efficiency in the pressure broadened regime on the linewidth γ (2.30), one could conceivably measure this linewidth by measuring the efficiency in one coherence length versus the pressure of the nonlinear species (self-broadening), or the pressure of a foreign gas (foreign gas broadening). This would require however detailed knowledge of atomic parameters (matrix elements), and also, as the pressure is changed, the efficiency may be influenced by effects like molecular absorption, change of the coherence length L_c by the foreign gas, etc. The requirement to know the atomic parameters may be avoided, and those interfering effects normalized out by making efficiency measurements on-resonance and off-resonance, and taking a ratio. Off-resonance, the efficiency is independent of both the laser bandwidth and the atomic linewidth, but it will still be influenced by the other processes mentioned above. For sufficient detunings (several laser bandwidths), the efficiency is given by (2.25):

$$\mathcal{E} = \frac{4(3\omega_0)^2 \eta_0^4 K_1^2 L_c^2 I_{av}^2}{\pi^2 (\omega_{20} - 2\omega_0)^2} \times \sin^2 (\Delta kL/2) \qquad (2.73)$$

The ratio of the efficiency on-resonance to the efficiency off-resonance is found by combining (2.30) and (2.73):

$$R = 2 \sqrt{2\pi} \ \frac{(\omega_{20} - 2\omega_0)^2}{\gamma\delta} \tag{2.74}$$

The detuning and the laser bandwidth in this expression can further be eliminated by normalizing to the low pressure limit of R which is found by combining (2.37) and (2.73). The result is:

$$\frac{R}{R_0} = \frac{4\pi}{\pi \sqrt{\pi} + 4 \sqrt{2}} \times \frac{\gamma_D}{\gamma} \tag{2.75}$$

One can thus determine the pressure broadened linewidth γ from the measured values of R and R_0 :

$$\boxed{\gamma = 1.12 \times \gamma_D \times \frac{R_0}{R}} \tag{2.76}$$

where γ_D is given by (2.16). This procedure does not require detailed knowledge of the laser spectral composition, but is only valid in the pressure broadened regime. Practically, this is usually the only region where values of γ are of interest, and extrapolation to lower pressures can usually be made with confidence.

A more general determination of γ , valid at all pressures, can be made using an exact (numerical) evaluation of the expression for the

efficiency (2.25). Using the fixed parameters γ_D , δ , and $\Delta\omega$, the ratio $R_c/R_{c0} = \mathcal{E}_c/\mathcal{E}_{c0}$ is computed as a function of γ and plotted (the subscript c refers to calculated values, m to measured values). The experimental procedure is identical to that explained above. Two sets of efficiency measurements (in one coherence length), on- and off-resonance, are made and the normalized ratio R_m/R_{m0} is plotted versus the pressure of the broadening agent. The normalized curves of measured and calculated efficiency are then used to determine γ from the relation $R_m(P)/R_{m0} = R_c(\gamma)/R_{c0}$. Thus for any pressure P , the linewidth γ may be read from the point on the calculated curve associated with the value $R_m(P)/R_{m0}$.

The two procedures are illustrated below.

2.   Measurement of the Broadening of the Na $3s^2S - 3d^2D$ Transition

The foreign gas broadening by He of the $3s^2S - 3d^2D$ transition in Na was measured using the above techniques.

A pumping wavelength of 6856 Å was obtained from an optical parametric oscillator, and the idler frequency at 2.37 μ was used as the input frequency ω to generate the observed lower sideband signal at $2\omega_0 - \omega$ (4006 Å). The pumping radiation had a bandwidth of 2 cm^{-1} and a mode spacing of 0.028 cm^{-1}. Both incident beams had a peak power of about 1 kW and were focused into a small Na heat pipe at a temperature of about 700°K, yielding a Doppler linewidth $\gamma_D = 0.049$ cm^{-1} , and a Na pressure of 0.75 torr $(1 \times 10^{16}$ cm$^{-3})$.

Efficiency measurements were made both on- and off-resonance while varying the He pressure from a few torr to two atmospheres. Figure 1 shows the ratio $R_m(P)/R_{m0}$ as a function of the He pressure, and Fig. 2 is a plot of the computed ratio $R_c(\gamma)/R_{c0}$ for this case. Figure 1 also shows the atomic linewidth γ as a function of pressure, both using the exact method and, for $P > 800$ torr, using the approximate method. Note that the two techniques are consistent, and that the numerical technique permits one to measure pressure broadened linewidths several times smaller than the Doppler width. The measured broadening coefficient is 0.3 cm^{-1} per atmosphere of He.

A similar procedure was used to determine the self-broadening of this transition by varying the Na density from 0.75 torr to 150 torr. Unfortunately, at these high Na densities, it was necessary to introduce 300 torr of He buffer gas to protect the cell windows, and the Na self-broadening was not observable above the 0.1 cm^{-1} He broadening. Thus we infer a self-broadening of less than 0.1 cm^{-1} at a density of 10^{18} cm^{-3}.

From a device point of view these results are very important. They indicate that a Na up-converter (operating around 9 μ) may be operated at pressures of about 100 torr without a significant reduction in efficiency due to broadening of the atomic linewidth, and second, that it is important to keep the buffer gas pressure as low as possible. Figure 1 shows, for example, that at a He buffer gas
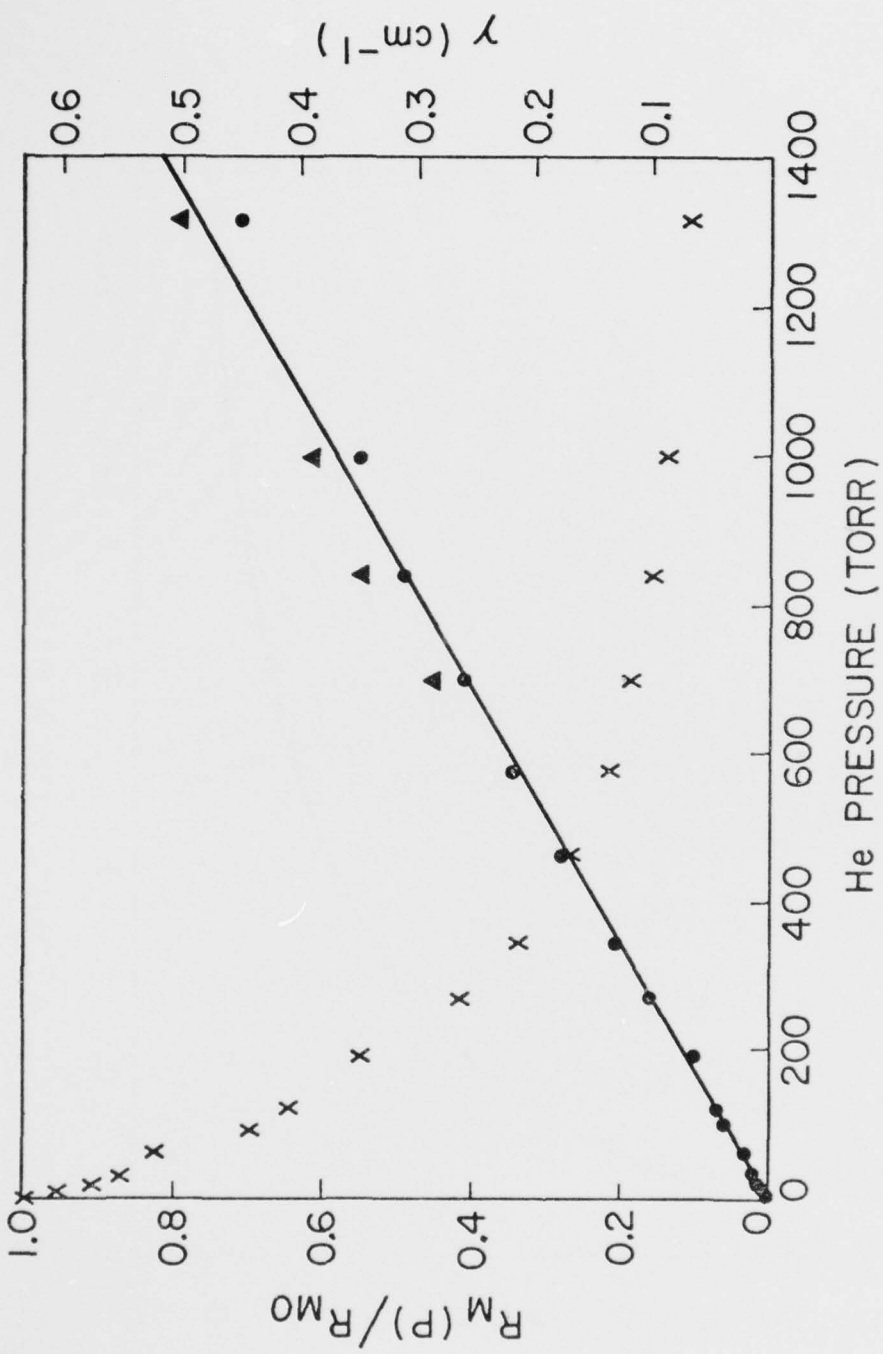
Fig. 1--Measured ratio R_m/R_{m0} ($\times$) and corresponding atomic linewidth γ of the Na $3s^2S - 3d^2D$ transition versus He pressure. Linewidths indicated by ($\triangle$) are from the simplified, high pressure procedure; those indicated by ($\cdot$) are found from the numerical technique.
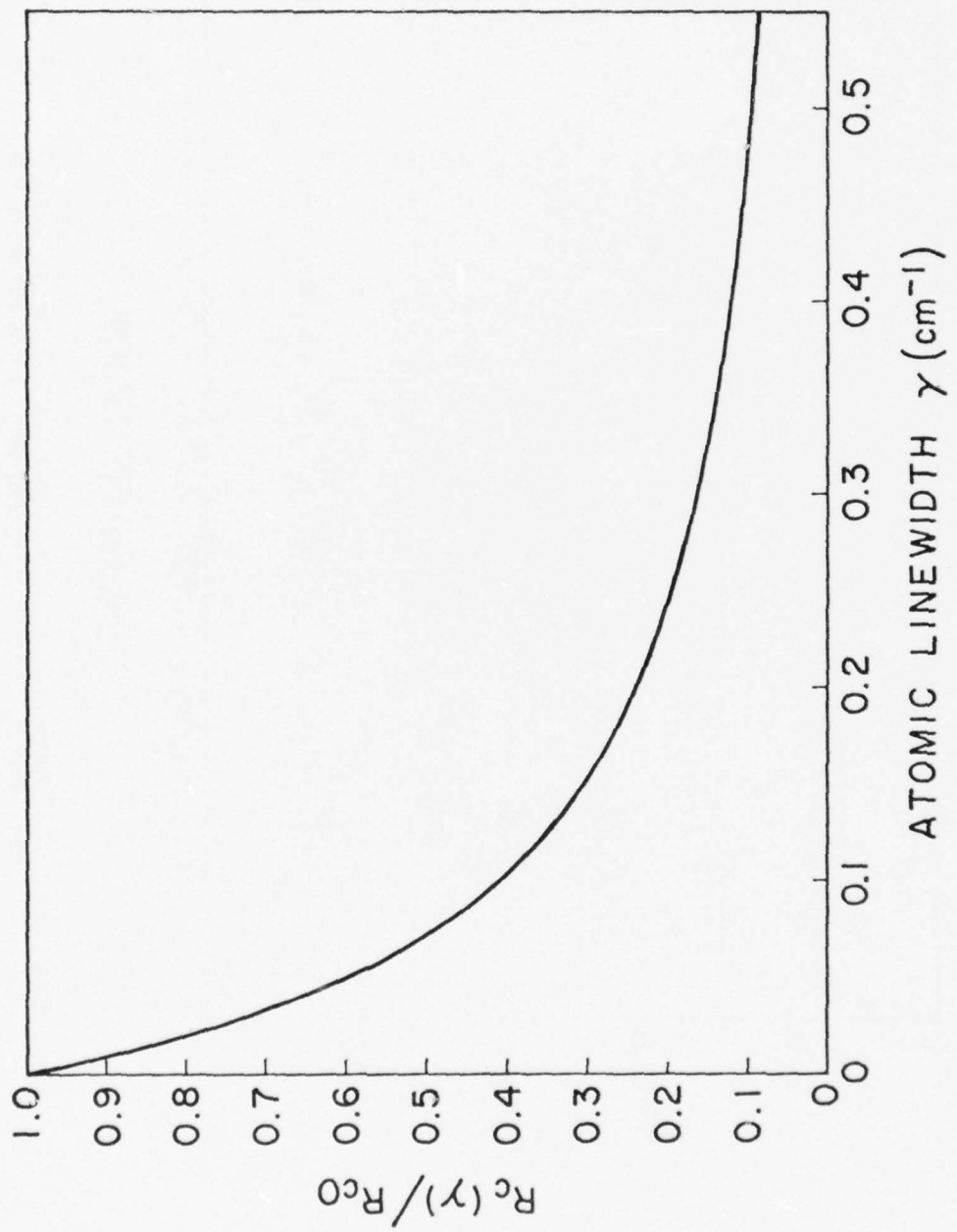
Fig. 2--Calculated ratio R_c/R_{cO} versus atomic linewidth.

pressure of about 300 torr, the efficiency is about a factor of three

less than the value with no He at all.

CHAPTER III

INFRARED IMAGE UP-CONVERSION IN ALKALI METAL VAPORS

A.   INTRODUCTION

The interest in frequency shifting radiation from the IR into the
visible or near UV stems mainly from two factors. First, there are now
available very efficient low-noise detectors of visible radiation such
as the human eye and photomultipliers, whereas most infrared detectors
are inefficient (and expensive) by comparison. A second attractive
feature of this method of detecting infrared is that the up-converter
and the visible detector following it can all operate at room tempera-
ture, whereas the competitive detectors in the infrared commonly oper-
ate between 4.2°K and 77°K.[15]

In this chapter, infrared imaging using two-photon-resonant fre-
quency converters is discussed in detail. Both passive and active
imaging are considered, but the emphasis is on active imaging. The
reason for this is that a recent study[16] has shown that active imaging
systems using such an up-converter look attractive when compared to
competing techniques using photoconductive detectors or quantum coun-
ters, but they compare rather poorly with these other techniques for
passive imaging of thermal radiation. The main reason behind this is

that the up-converters have to use a pulsed laser for a pump, resulting in a low duty factor. In the case of active imaging, the IR radiation itself is pulsed, and this duty factor problem is much less severe.

We will start with a brief discussion of the performance criteria for passive and active imaging systems. This will be followed by a description of the various optical systems that can be used with up-converters. The next section deals with field of view, resolution and bandwidth. Then follows the main section of this chapter, which is a detailed study of the efficiency of such up-converters, the physical processes limiting it, optimization procedures and a comparison with crystal up-converters. The last section is a discussion of the experimental results. It includes a description of the system that was used to obtain the first images, together with a comparison between measured and calculated efficiencies.

Whenever possible, theoretical results will be applied to the example of 2.94 μ up-conversion in cesium vapor, using the process 1.0790 μ + 1.0790 μ + 2.94 $\mu \rightarrow 4560$ $\overset{\circ}{A}$. The interest in this particular system stems from the fact that the high power Nd:BeL solid state laser at 1.0790 μ has an accidental two-photon-coincidence with the 6s-7s transition in cesium.

B.   INFRARED IMAGING SYSTEMS

1.   Performance Criteria for Imaging Systems

a.   Passive imaging

In passive imaging, an object is detected by the thermal radiation
it emits at any temperature above absolute zero. Different parts of
the object which are at slightly different temperatures emit different
amounts of radiation. The sensitivity of a detector or an imaging de-
vice is evidently related to the relative magnitudes of its response
to a change ΔT , and the random fluctuations in its response due to
various noise processes. Therefore, one (widely used) performance in-
dicator of a thermal detector is the noise-equivalent temperature dif-
ference (NETD), which may be defined as that effective temperature
difference that causes a response equal to the rms noise fluctuations
in the response of the detector, i.e., giving a signal-to-noise ratio
of unity. We will now derive an expression for the NETD.

The number of photons received per second by a detector with area
A and field of view $\Delta \Omega$, looking at an object of emissivity $\epsilon(\lambda)$
and temperature T , is given by:[17]

$$ N = A \times \Delta \Omega \times \int \frac{p\epsilon(\lambda)\ df}{e^{hf/kT} - 1} \tag{3.1}$$

In this expression p is a factor that takes into account the response
of the detector for orthogonal polarizations. If both polarizations are
up-converted with the same efficiency, p equals 2. If only one polar-
ization is up-converted, its value is 1. If both polarizations are up-
converted with different efficiencies, which is the case for two-photon-
resonant frequency converters making use of a s to d transition, one

- 70 -

has $1 < p < 2$. The dependence of third-order processes on polar-
ization is discussed in detail in Appendix E. Since the bandwidth
of up-converters is narrow compared to the center frequency of the
up-converted band, the integral in (3.1) can be approximated by the
product of the integrand, evaluated at this center frequency, and the
bandwidth. Thus

$$
N \simeq \frac{p\epsilon(\lambda_i) \, \Delta f}{e^{hc/\lambda_i kT} - 1} \times \frac{A\Delta\Omega}{\lambda_i^2} \tag{3.2}
$$

where λ_i is the wavelength at the center of the band, and Δf is
the bandwidth of the up-converter. The number of photons per resolu-
tion element is found by setting the solid angle in this expression
equal to the diffraction angle, i.e., $\Delta\Omega = \lambda_i^2/A$. Hence the number
of photons per resolution element is approximately given by

$$
n \simeq \frac{p\epsilon(\lambda_i) \, \Delta f}{e^{hc/\lambda_i kT} - 1} \tag{3.3}
$$

where the temperature T is the average temperature of that element.
Starting from this expression, we can derive an expression for the
NETD. The derivation presented here follows largely Falk and Tiffany.[17]
Adjacent resolution elements of the object have slightly different tem-
peratures, and the "signal" is given by the difference between the num-
ber of photons received from two adjacent spots with a temperature dif-
ference ΔT . Consider two such spots, emitting at average rates n_1
and n_2 . The signal received at the input of the up-converter, during

- 71 -

a time t , is then equal to:

$$S_{in} = (n_1 - n_2)t \qquad (3.4)$$

For Poisson noise, due to fluctuations in time of arrival, the noise is equal to the square root of the average number of received photons:

$$N_{in} = [(n_1 + n_2)t]^{\frac{1}{2}} \qquad (3.5)$$

From the expressions for the signal and noise at the input, the signal and noise at the output can be calculated. We assume up-conversion with photon efficiency $\mathcal{E}_{PH}$, followed by detection using a device with efficiency η , both processes being noisefree. Thus:

$$S_{out} = (n_1 - n_2) \times \mathcal{E}_{PH} \times \eta \times t$$

$$N_{out} = [(n_1 + n_2) \times \mathcal{E}_{PH} \times \eta \times t]^{\frac{1}{2}} \qquad (3.6)$$

and:

$$(S/N)_{out} = \frac{n_1 - n_2}{(n_1 + n_2)^{\frac{1}{2}}} \times (\mathcal{E}_{PH} \times \eta \times t)^{\frac{1}{2}} \qquad (3.7)$$

We will use this expression now to calculate the NETD, where the difference $n_1 - n_2$ is due to a temperature difference. One could also use this expression, however, to calculate the S/N ratio for detection

- 72 -

of a difference in reflectivity between adjacent spots (which could be used as a performance criterion for active imaging). Using for n_1 and n_2 expression (3.3), evaluated at temperature T and $T + \Delta T$, we find:

$$(S/N)_{out} = \frac{1}{\sqrt{2}} \left[\frac{p \epsilon (\lambda_i) \, \Delta f}{e^{hf_i/kT} - 1} \right]^{\frac{1}{2}} \left(\frac{hf_i}{kT} \right) \left(\frac{\Delta T}{T} \right) (\mathcal{E}_{PH} \times \eta \times t)^{\frac{1}{2}} \quad (3.8)$$

By definition, the NETD is a ΔT such that the resulting signal-to-noise ratio at the output of the imaging system equals unity. Hence:

$$NETD = \left\{ \frac{1}{\sqrt{2}} \left[\frac{p \epsilon (\lambda_i) \, \Delta f}{e^{hf_i/kT} - 1} \right]^{\frac{1}{2}} \left(\frac{hf_i}{kT} \right) \left(\frac{1}{T} \right) (\mathcal{E}_{PH} \times \eta \times t)^{\frac{1}{2}} \right\}^{-1} \quad (3.9)$$

Example:

We will use typical parameters for a Na up-converter, operating around $9 \, \mu$ in the $8 \, \mu \rightarrow 12 \, \mu$ atmospheric window.

$$\epsilon (\lambda_i) = 1$$
$$T = 300^{\circ}K$$
$$f_i = 1100 \text{ cm}^{-1}$$
$$\Delta f = 200 \text{ cm}^{-1}$$
$$\mathcal{E}_{PH} = 0.25$$
$$\eta = 0.3$$
$$p = 1.25$$
$$t = 1 \, \mu sec$$
$$\rightarrow NETD = 1.5^{\circ}K$$

b. Active imaging

For the case of active imaging, where the object is illuminated
using a high power laser and detected by the radiation it reflects to-
ward the up-converter, the NETD is clearly not a useful performance
criterion. One possible application of active imaging might be where
one is trying to detect an object with some finite reflectivity in a
non-reflecting ("dark") background. A reasonable performance crite-
rion for this case is the signal-to-noise ratio for the detection of
the difference between a spot in the "black" background, and a spot
on the reflecting object, e.g., spots 1 and 2 in Fig. 3. A "good"
S/N ratio would then permit one to tell the shape of the object. We
will use a constant reflectivity Ref for the entire object. If
this is not the case, one could use as one possible choice the mini-
mum value of Ref , in which case one would be able to see some de-
tail in the object.

The noise sources to be considered in this case are the shot
noise due to the signal itself, thermal radiation coming from the
object because it has a non-zero temperature, and dark-current noise
in the phototube following the up-converter. We will derive an ex-
pression for the signal-to-noise ratio, and we will also find a lower
limit for the power of the illuminating laser required in order to
make the reflected radiation stronger than the thermal radiation.
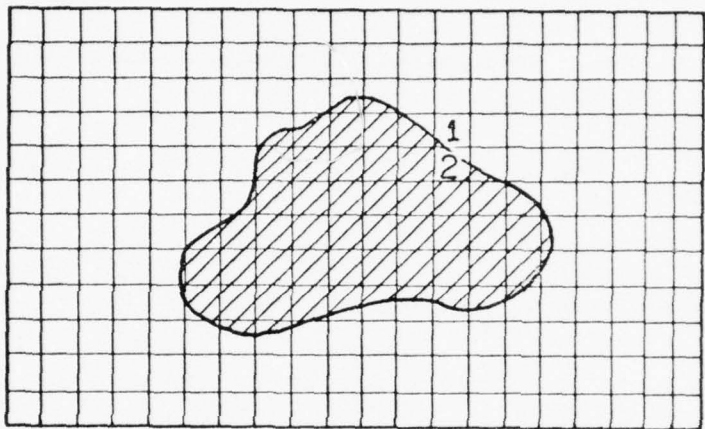
Fig. 3--Active imaging. Detection of reflecting
object in "dark" background.

The geometry for active imaging is shown in Fig. 4. We will assume:

$$\Omega_o < \Omega_{upc} \lesssim \Omega_L$$

If we call η the overall system efficiency, we have (Fig. 3)

$$S_{out} = (n_1 - n_2) \times \eta \times t = (n_s - 0) \times \eta \times t$$

$$N_{out} = \left[\left(n_1 + n_2 + n_b + 2\frac{i_d}{e} \right) \times \eta \times t \right]^{\frac{1}{2}}$$

$$= \left[\left(n_s + n_b + 2\frac{i_d}{e} \right) \times \eta \times t \right]^{\frac{1}{2}} \qquad (3.10)$$

and

$$(S/N)_{out} = \frac{n_s}{[n_s + n_b + 2(i_d/e)]^{\frac{1}{2}}} \times (\eta \times t)^{\frac{1}{2}} \qquad (3.11)$$

where

i_d = dark current

t = integration time

n_s = number of reflected photons per sec per resolution element on the object

n_b = number of thermal photons per sec per resolution element on the object

Fig. 4.--Geometry for active imaging.

UPCONVERTER
+L³TV

ILLUMINATOR

Ω_u

Ω_o

Ω_L

r
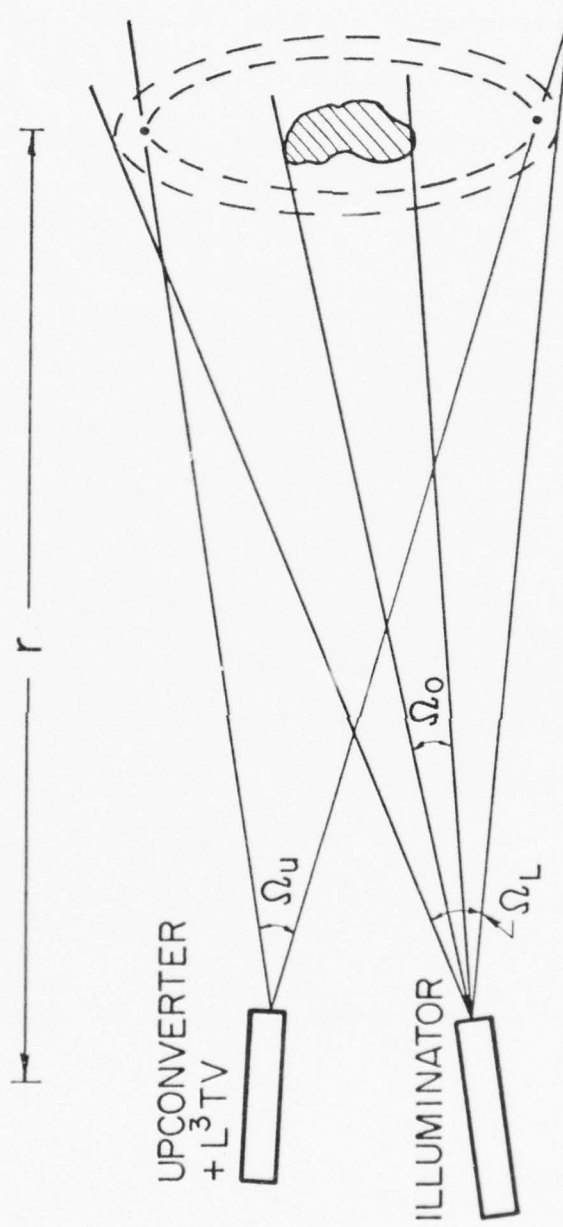
We will now calculate the number of photons reflected by the object per sec per resolution element, and also the number of thermal photons per sec per resolution element. If the illuminating laser emits N_L photons per second into a solid angle Ω_L, then the number of reflected photons received per second is:

$$N_s = N_L \times \frac{\Omega_o}{\Omega_L} \times \frac{Ref}{\pi} \times \frac{1}{r^2} \times \frac{\pi D^2}{4} \tag{3.12}$$

In this expression D is the diameter of the up-converter, and use was made of the fact that $\Omega_{upc} > \Omega_{obj}$. If the total number of resolution elements of the up-converter, corresponding to the full solid angle Ω_{upc}, is equal to R, then the number of resolution elements on the object, which spans a solid angle Ω_o, equals $R \times \Omega_o / \Omega_{upc}$. Hence the number of reflected photons per resolution element (on the object) is:

$$n_s = \frac{N_s}{R \times \Omega_o / \Omega_u} = N_L \times \frac{\Omega_u / R}{\Omega_L} \times \frac{Ref}{\pi} \times \frac{1}{r^2} \times \frac{\pi D^2}{4} \tag{3.13}$$

The total number of thermal photons emitted by the object at temperature T equals:

$$N_b = J_\lambda \times \Delta f \times (\Omega_o \times r^2) \times \frac{\pi D^2 / 4}{r^2} \tag{3.14}$$

where J_λ is the number of photons emitted per sec, per unit area,

per solid angle, per unit bandwidth. Using (3.2), J_λ is given by

$$J_\lambda = \frac{p\epsilon(\lambda_i)}{\lambda_i^2 (e^{hc/\lambda_i kT} - 1)} \qquad (3.15)$$

This radiation comes also from $R \times \Omega_o/\Omega_u$ resolution elements, and thus the number of photons per resolution element is equal to:

$$n_b = J_\lambda \times \Delta f \times \frac{\Omega_u}{R} \times \frac{\pi D^2}{4} \qquad (3.16)$$

By combining (3.13) and (3.16), we find the minimum number of laser photons per second required to make the reflected radiation dominate. The result is:

$$N_L > \frac{\pi \times J_\lambda \times \Delta f \times (\Omega_L r^2)}{Ref} \qquad (3.17)$$

If the laser power satisfies this condition, the detection is called signal-shot-noise-limited (neglecting the dark current). If we substitute (3.13) and (3.16) in the expression for the signal-to-noise ratio (3.11), and neglect the dark current contribution, we find in the signal-shot-noise-limited regime:

$$(S/N)_{out} = (n_s \times \eta \times t)^{\frac{1}{2}} = \frac{1}{2} D \sqrt{\frac{\Omega_u}{R}} \sqrt{\frac{Ref}{\Omega_L r^2}} \sqrt{\eta t} \sqrt{N_L} \qquad (3.18)$$

Example (Cs up-converter at 2.94μ):

$$\Omega_u = 1 \times 10^{-4}$$

$$D = 10 \text{ cm}$$

$$R = 10^4$$

$$\Omega_L = \Omega_u$$

$$\text{Ref} = 0.01$$

$$\eta = 0.1$$

$$t = 10 \text{ nsec}$$

$$r = 3 \text{ km}$$

$$\lambda_{ir} = 2.94 \mu$$

$$\Delta f = 100 \text{ cm}^{-1} \text{ (blue filter behind up-converter)}$$

$$\epsilon(\lambda_i) = 1$$

$$T = 300^{\circ}K$$

$$p = 2$$

one finds:

$$(S/N)_{out} = 5.3 \times 10^{-13} \times \sqrt{N_L}$$

To obtain a signal-to-noise ratio of unity, the required laser power is 230 kW. Using (3.17), for the reflected radiation to dominate, the

required power is about 200 times less, and thus we are indeed in the signal-shot-noise-limited regime.

2. Optical Systems for Up-Converters

We will only briefly discuss the various optical systems that can be used with image up-converters. For a more complete discussion, see Refs. 16 and 18. Three basically different types of optical systems for up-conversion have been discussed by Andrews;[18] they are illustrated in Fig. 5.

In a Type I optical system, the object is imaged in the up-converter, and the up-converted radiation is then imaged onto a detector. The image of a point on the IR object is formed in this case by a spherical wavefront converging on a point in the up-converter. Up-conversion employing a Type I optical system is also called up-conversion in image space.

In a Type II optical system, nearly plane waves from the IR object are up-converted, and the up-converted plane waves are imaged onto the detector.

In a Type III optical system, the object and the up-converter are placed respectively in the front and back focal plane of a lens. IR radiation from different object points gives plane waves with different directions in the up-converter. The up-converter and the detector are respectively in the front and back focal planes of a second lens, and this lens transforms every up-converted plane wave into a point in the
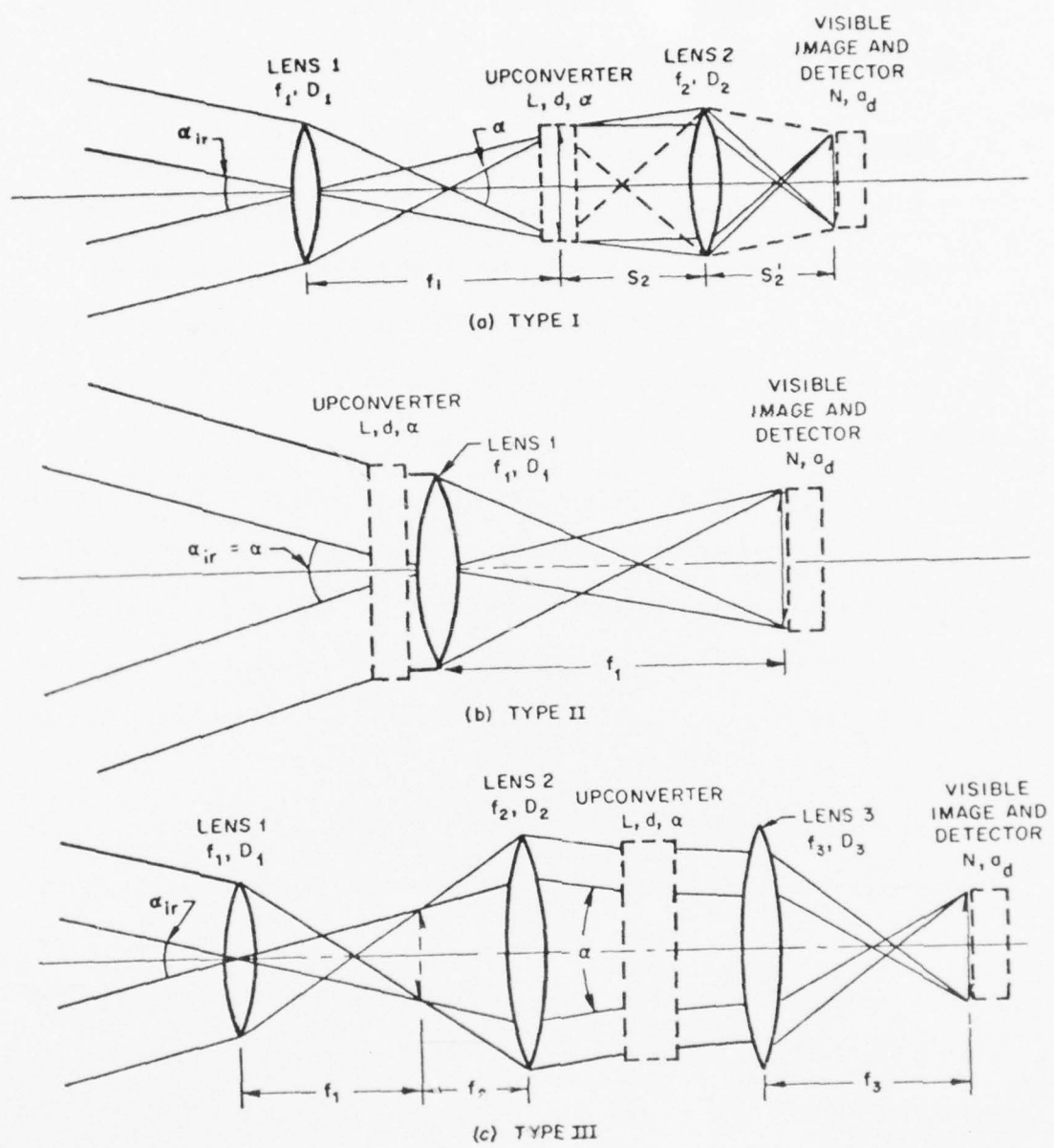
Fig. 5--Types of optical systems for IR up-conversion.

detector plane. Up-conversion employing a Type III optical system is also called up-conversion in Fourier space.

Because with a Type II system there is no freedom in matching the incident IR radiation to the area and field of view of the up-converter, this type is of very limited use. The resolution of a Type I system is limited below the diffraction limit by the length of the medium, while this is not the case for a Type III system.[18] In Appendix B it is shown in detail that the resolution of a Type III system is only limited by diffraction, assuming monochromatic light. The magnification of a Type III system is also derived there. All types suffer from chromatic aberration. For a Type III system this is discussed in Appendix C. According to Ref. 16, this aberration might in principle be corrected for in a Type III system, which would probably be required in the case of broadband thermal up-conversion. For active imaging chromatic aberration is of little importance since the radiation is very narrowband. In a Type I system, the output is the product of the IR image and the square of the pump profile. This poses very severe uniformity problems on the pump beam for the case of low-contrast imaging (thermal imaging). In a Type III system, on the other hand, each point of the object gives rise to a plane wave which is up-converted by the entire pump beam, and as a result the pump beam quality is much less important. For all these reasons a Type III system is usually optimal.[16]

C. FIELD OF VIEW, RESOLUTION, AND BANDWIDTH. APPLICATION TO THE
2.94 μ CESIUM UP-CONVERTER

1. Active Imaging

a. Field of view

Infrared rays incident on an up-converter at different angles are
up-converted with a different k-vector mismatch, resulting in an angle-
dependent efficiency. Clearly this response should be a "smooth" func-
tion, without any zeros. There are two possible ways for obtaining a
ripple-free response versus IR angle. A first possibility is to use a
cell that is less than one coherence length long. At the high pres-
sures where one wants to operate the up-converters, this length is very
short, however, typically being only a small fraction of a millimeter.
This is usually impractical, both because of the mechanical problems of
building such a short cell, and because the resulting field of view is
so large that it becomes hard to design a cell with a large enough
"physical" field of view. The second possibility is to make the medium
reasonably long (there are also limitations there, as explained in Sec-
tion D), and phasematch over its entire length. We will discuss only
the second case.

The k-vector mismatch caused by the angle between the IR rays and
the direction of the sum of the two pump vectors is given by:

$$\Delta k(\theta) = \frac{k_i \theta^2}{2} \qquad (3.19)$$

The efficiency varies versus angle according to:

$$\mathcal{E} \propto \text{sinc}^2 \left(\frac{\Delta k L}{2} \right) = \text{sinc}^2 \left(\frac{k_i \theta^2 L}{4} \right) \tag{3.20}$$

and thus the solid angle of the up-converter (40% points) is given by:

$$\Delta \Omega_u = \frac{\pi \lambda_i}{L} \tag{3.21}$$

Note that this solid angle is exactly equal to the maximum solid angle as allowed by the difference in curvature between the IR and visible wavefronts in the up-converter, as discussed in Appendix B. By using off-angle phasematching,[15] where a mismatch $\Delta k L = -\pi$ is allowed for zero IR angle, the field of view can be increased by a factor of two, but in view of the results of Appendix B this may be unacceptable.

b.   Methods of phasematching

Three possible techniques for phasematching the up-conversion process will be discussed. They are inert gas phasematching, self-phasematching, and phasematching by angle. We will now discuss each of these techniques in detail.

Phasematching by adding an inert gas[19] is probably not a useful technique. The reason is that because of the high pressure ratios required, the inert gas pressure becomes excessively high at the metal vapor pressures where one wants to operate the up-converter (on the

order of 10 atmospheres). This leads to a large broadening of the linewidth of the two-photon transition, not to mention the practical problems.

The second method is to select the IR wavelength such that the medium is self-phasematched. This method is the simplest one, but it requires an illuminating laser that can be tuned to the phasematching frequency. We will now derive an expression for the detuning from the upper level where the process is phasematched, by setting Δk equal to zero. For colinear waves, the expression for the k-vector mismatch is:

$$\Delta k = k_s - (2k_p + k_i)$$

$$= (n_s - 1) \frac{\omega_s}{c} - (n_p - 1) \frac{2\omega_p}{c} - (n_i - 1) \frac{\omega_i}{c} \qquad (3.22)$$

The factors $(n - 1)$ in this expression can be evaluated using Sellmeier's equation.[19] Assuming no population in the 7s level, the result for the cesium up-converter is:

$$\Delta k = \frac{N}{2\epsilon_0 c \hbar} \left(\frac{1.4 \times 10^{-55}}{\Delta v_3} - 8.7 \times 10^{-57} \right) \qquad (3.23)$$

where Δv_3 is in wavenumbers, and only the 6p and 7p doublets were used in the calculation. If, because of two-photon absorption, there is some population in the two-photon-resonant level, it will have only a small effect on the index of refraction at the pump and the sum

frequencies, but it will considerably affect the index at the IR, since the IR frequency has only a small detuning for the transition from the resonant level to the upper level (7s-7p in cesium). The expression for the mismatch, including this contribution, is, for the cesium up-converter:

$$\Delta k = \frac{N_{6s}}{2\epsilon_0 c \hbar} \left(\frac{1.4 \times 10^{-55} - 8.4 \times 10^{-56} \times f}{\Delta \omega_3} - 8.7 \times 10^{-57} \right)$$

where

$$f = 100 \times \frac{N_{7s}}{N_{6s}} = \begin{array}{l} \text{percentage population} \\ \text{in the 7s level} \end{array} \qquad (3.24)$$

The self-phasematching frequency is found by setting Δk equal to zero. For the cesium up-converter, the result is:

$$\boxed{\Delta \omega_{3_{\text{Ph.match}}} = 16.3 - 9.7 \times f \quad [\text{cm}^{-1}]} \qquad (3.25)$$

This result says that, as the population of the 7s level is increased, the phasematching IR frequency will originally increase such that the detuning from the upper level becomes smaller. At a smaller detuning the efficiency is higher, but absorption both at the IR and the sum frequency has to be checked (see Section D). As the fraction f is increased further, the process will eventually phasematch for negative detunings, i.e., above the upper level.

- 87 -

The third technique is more general than the second one in that it can be used for a range of IR frequencies, but it requires a more complicated system. It can easily be understood from the diagrams shown in Fig. 6. If the sum frequency does not come very close to the upper atomic level, the dominant contribution to the k-vector mismatch is due to the pump. Since the frequency of the pump is below the first doublet of the metal vapor, it sees an index of refraction larger than 1, and thus the vector $2\bar{k}_p + \bar{k}_i$ is longer than the vector $\bar{k}_s$. By splitting the pump beam in two beams and recombining them under a small angle, the mismatch Δk can be made zero. For small angles φ, the mismatch caused by the small angle (2φ) between the pump beams equals:

$$\Delta k(\varphi) = \frac{2\omega_p}{c} \times \frac{\varphi^2}{2} \tag{3.26}$$

By adding this term to the expression (3.24), the total mismatch for the cesium up-converter becomes:

$$\Delta k = \frac{N}{2\epsilon_0 c\hbar} \left(\frac{1.4 \times 10^{-55} - 8.4 \times 10^{-56} \, f}{\Delta\omega_3} - 8.7 \times 10^{-57} \right) + \frac{\omega_p}{c} \varphi^2 \tag{3.27}$$

For a given IR frequency or, equivalently, a given detuning $\Delta\omega_3$, the angle φ can be found which makes this expression zero. The
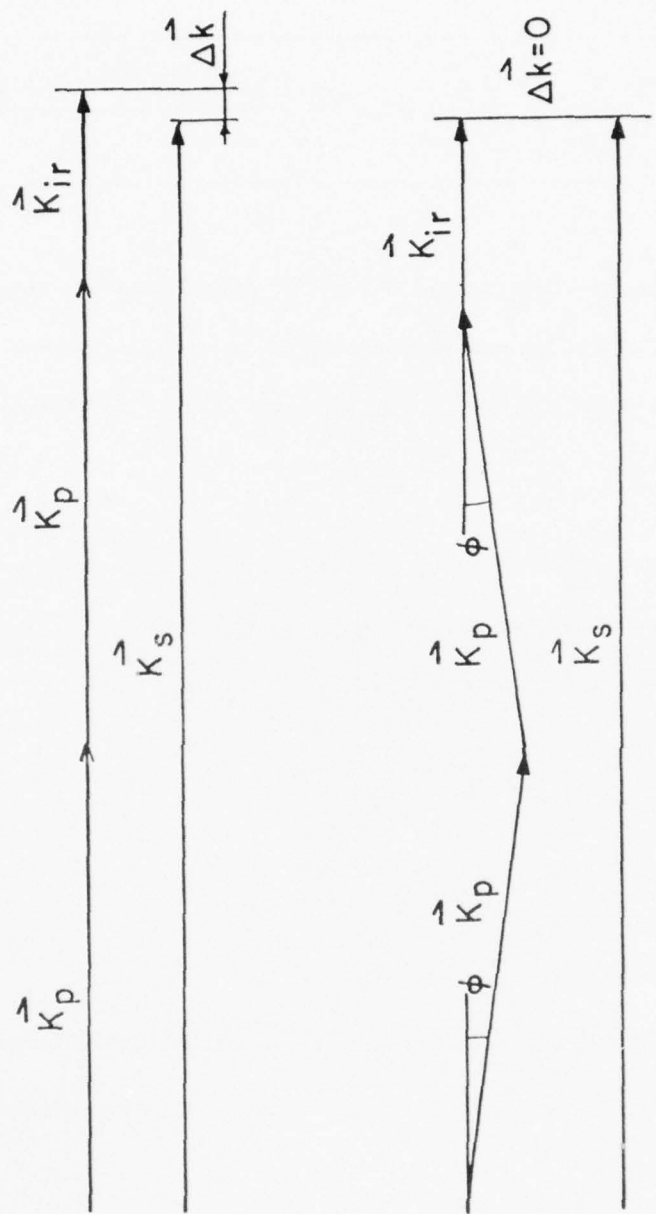
PHASE MATCHING BY ANGLE

Fig. 6--Phasematching by angle.

result is:

$$\varphi_{Ph.match} = \left(\frac{N}{2\epsilon_0 \hbar \omega_p}\right)^{\frac{1}{2}} \left(8.7 \times 10^{-57} - \frac{1.4 \times 10^{-55} - 8.4 \times 10^{-56} f}{\Delta\omega_3}\right)^{\frac{1}{2}}$$

(3.28)

For large detunings $\Delta\omega_3$, the angle φ approaches an asymptotic value. In Fig. 7 the phasematching angle is plotted versus detuning, for a number density of 10^{18} cm^{-3}, and for various fractions f .

c.   Resolution

The general expression for the resolution of an up-converter using a Type III optical system is derived in Appendix B. If we substitute for the solid angle the result (3.21), we obtain:

$$R = \frac{\pi A_p}{2\lambda_i L}$$

(3.29)

d.   Relation between efficiency, resolution, and number density

The efficiency in the phasematched case is proportional to:

$$\mathcal{E} \propto \frac{N^2 L^2 P^2}{A^2}$$
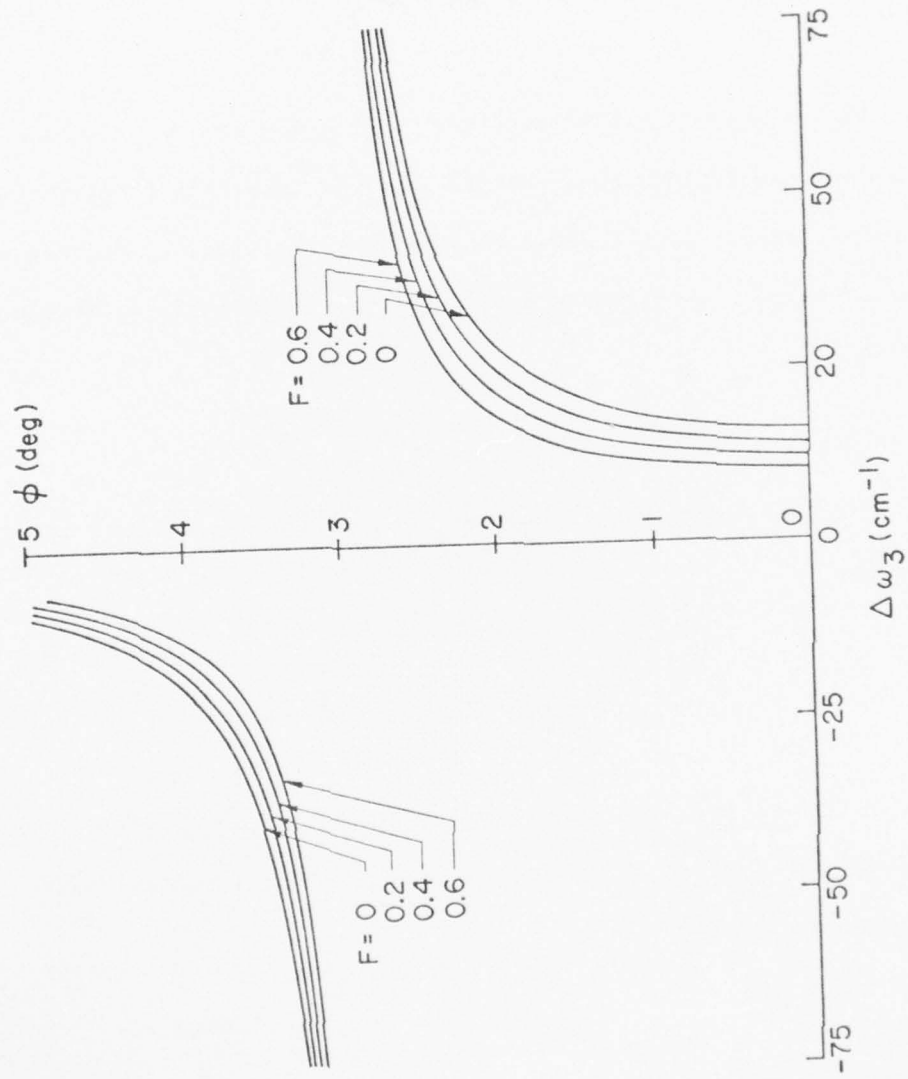
Fig. 7--Phasematching angle φ versus $\Delta\omega_3$ for cesium up-converter, for various populations in the 7s level.

Using (3.29), this can be written in terms of the number of resolution elements, as:

$$\boxed{\mathcal{E} \times R^2 \ \propto \ N^2 \times P^2} \tag{3.30}$$

This is a key relation for up-converters. It says that, for a given efficiency and resolution, the required power is inversely proportional to the number density of the metal vapor. Thus one wants to operate an up-converter at <u>as high a pressure as possible</u> (see Section D for lim-iting effects).

e.   <u>Bandwidth</u>

The efficiency depends on the detuning from the upper level in the following way:

$$\mathcal{E} \ \propto \ \frac{1}{\Delta\omega_3^2} \, \mathrm{sinc}^2 \left(\frac{\Delta k L}{2} \right) \tag{3.31}$$

where Δk is given by (3.27), and also depends on $\Delta\omega_3$. If the de-tuning is changed by a small amount $\delta(\Delta\omega_3)$ from its original value $\Delta\omega_3$, the resulting mismatch is:

$$\frac{\Delta k L}{2} \ = \ - \frac{NL}{4\epsilon_0 c\hbar} \ (1.4 \times 10^{-55} - 8.4 \times 10^{-56} \ f) \ \frac{\delta(\Delta\omega_3)}{\Delta\omega_3^2} \tag{3.32}$$

- 98 -

MICROCOPY RESOLUTION TEST CHART
NATIONAL BUREAU OF STANDARDS-1963-A
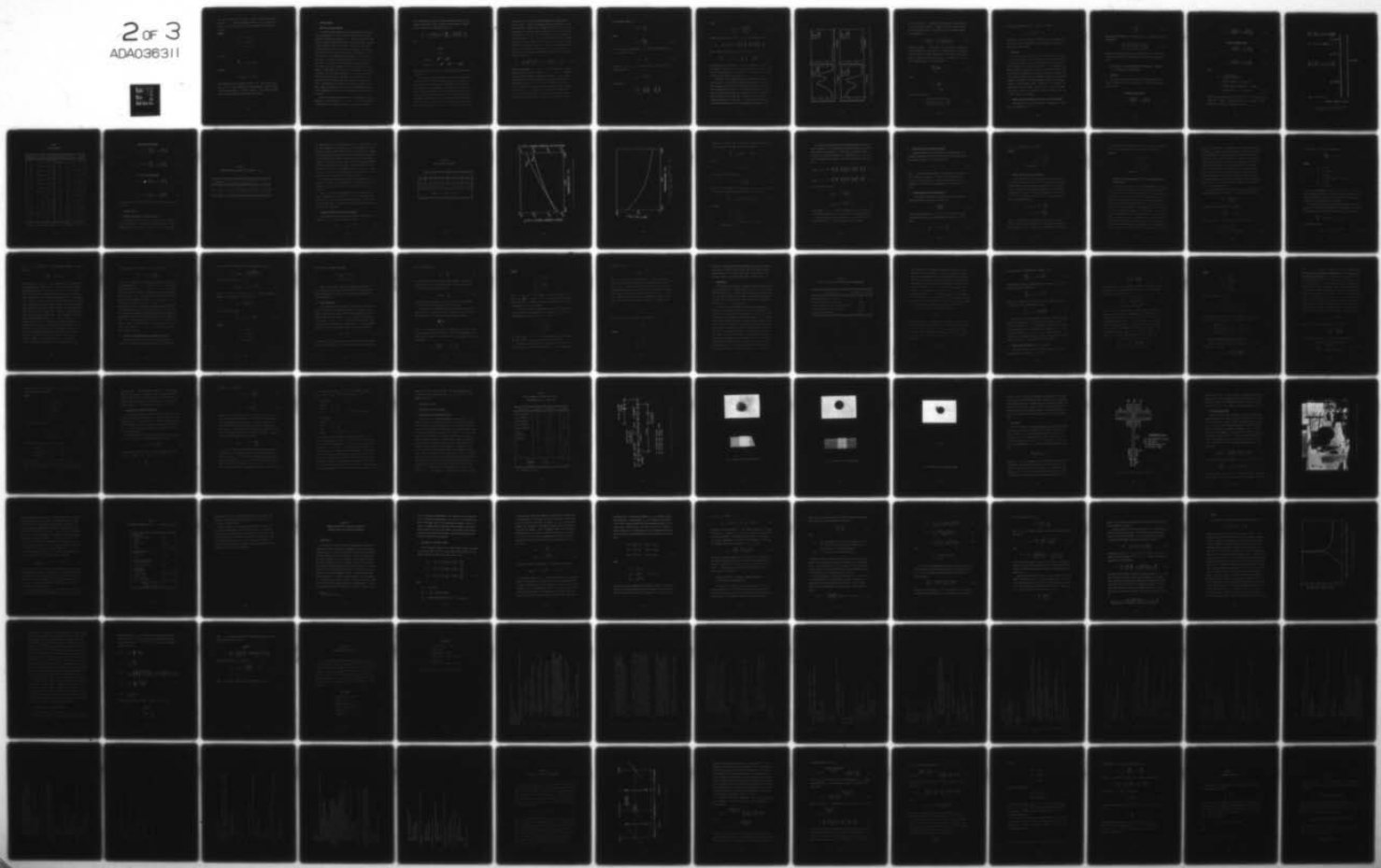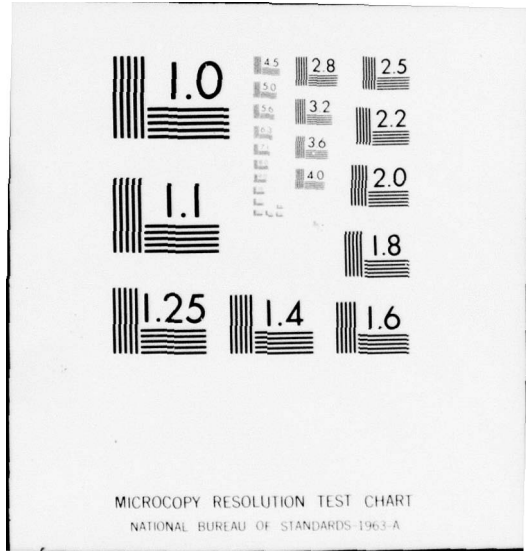
The sinc^2 factor in the efficiency is down to 40% of its peak value
when $\Delta kL = \pi$. From this a maximum value for $\delta(\Delta\nu_3)$ can be cal-
culated. We will illustrate this with an example for the cesium up-
converter.

Example:

$$N = 10^{24} \text{ m}^{-3}$$

$$\Delta\nu_3 = 20 \text{ cm}^{-1}$$

$$L = 2 \times 10^{-3} \text{ m}$$

$$f = 0$$

We find:

$$\frac{\Delta kL}{2} = -0.63 \times \delta(\Delta\nu_3)$$

and thus

$$[\delta(\Delta\nu_3)]_{max} \simeq 2.5 \text{ cm}^{-1}$$

So the bandwidth in this example is about 5 cm^{-1}. Note that the fac-
tor $1/(\Delta\nu_3)^2$ in the expression for the efficiency is nearly constant
over this narrow width. In general, however, it also affects the band-
width, and both factors should be taken into account.

2.   Passive Imaging

a.   Field of view and bandwidth

For passive imaging applications, an up-converter should have a large IR bandwidth, as is clear from the expression for the noise equivalent temperature difference (3.9). Because of the large bandwidth requirement, phasematching cannot be used as a means of getting a smooth angular response in this case. If a cell is used that is several coherence lengths long, at some IR frequency, the response versus angle will be oscillatory with zeros at certain angles. However, because of the dependence of the mismatch on the detuning $\Delta\omega_3$, the peaks and zeros for different IR frequencies do not occur at the same angles. As a result, a smooth frequency integrated response versus angle can still be obtained by using a cell that is several coherence lengths long for all or most of the frequencies in the band considered. As in the active imaging case, one has the possibility of splitting the pump beam in two beams at a small angle, in which case one has a free variable that can be chosen for an optimum response. The problem just described is sufficiently complex to warrant a numerical solution. We will derive now the general expression for the efficiency to be used in this computation, and then discuss the results.

Because the up-conversion process can be phasematched at certain combinations of the variables $\Delta\omega_3$, θ, and φ, one must start from an expression for the efficiency that takes into account saturation.

Such an expression can easily be found by analogy with the case of crystal up-converters, where a second order nonlinearity is used.[17] For metal vapors, the corresponding result is:

$$\mathcal{E}_{PH} = \frac{\kappa_i \kappa_s}{\kappa_i \kappa_s + (\Delta k/2)^2} \sin^2 \left\{ \left[\kappa_i \kappa_s + \left(\frac{\Delta k}{2} \right)^2 \right]^{\frac{1}{2}} L \right\}$$

where

$$\kappa_s = \omega_s \eta_0 dE_p^2/2$$

$$\kappa_i = (\omega_i/\omega_s) \kappa_s$$

$$d_{press.br.} = \sqrt{8\pi} \ K_1/ \sqrt{\gamma \delta}$$

$$d_{Doppl.br.} = [2(\pi \sqrt{\pi} + 4 \sqrt{2})]^{\frac{1}{2}} \ K_1/ \sqrt{\gamma_D \delta} \qquad (3.33)$$

The expression for the mismatch Δk is the same as for the active imaging case.

As an example, we will calculate the response versus angle for a cesium up-converter using the upper level of the 7p doublet. In the calculation, we will neglect the contribution, both to the efficiency and the k-vector mismatch, of the lower level of the 7p doublet. Since the upper level of the doublet has two-thirds of the oscillation strength, this should result in only a small error for detunings from the upper level less than about half the spacing between the two levels, which is 181 cm^{-1} for the case of that transition. So for bandwidths up to about 200 cm^{-1} (100 cm^{-1} on each side

of the level), the error introduced by making this simplification should be small. Because of absorption at the sum frequency for very small detunings, a small band of frequencies has to be excluded in the integration over frequency. For the case of the cesium up-converter, for a density of 10^{18} cm^{-3} and a cell length of 1 mm. the width of this band is about 20 cm^{-1}. This is small compared to the total band-width, and its exact value has little effect on the frequency averaged efficiency. We will also neglect the effect of a small population in the 7s level. When these approximations are made, the complete expression for the mismatch, including the contribution due to the angle of the IR vector is:

$$\Delta k = \frac{N}{2\epsilon_0 c\hbar} \left(\frac{1.4 \times 10^{-55}}{\Delta v_3} - 8.7 \times 10^{-57} \right) + \frac{\omega_p}{c} \varphi^2 + \frac{\omega_i}{2c} \theta^2 \qquad (3.34)$$

Using the expressions (3.33) and (3.34), the efficiency can be calculated for every set of the variables Δv_3 , θ , and φ , and from this a frequency integrated response versus angle θ can be found. The expression for the efficiency involves a very large number of parameters, however, and it is convenient to rewrite it in a form that only contains a small number of key variables. We will rewrite the expression (3.33) in terms of the calculated or measured efficiency in one coherence length. for the special case where the sum frequency comes close enough to the upper level such that it sets

the coherence length, i.e.:

$$\Delta k = \frac{\alpha}{\Delta \omega_3}$$

where

$$\alpha = \frac{N\mu_{03}^2 \omega_s}{2\epsilon_0 c\hbar} \tag{3.35}$$

We start by writing the quantity $\kappa_i \kappa_s$ such that the dependence on $\Delta \omega_3$ is explicitly shown:

$$\kappa_i \kappa_s = \frac{\beta}{\Delta \omega_3^2} \tag{3.36}$$

Using (3.35) and (3.36), the efficiency in one coherence length can then be written as:

$$\mathcal{E}_{L_c} = \frac{\beta}{\beta + (\alpha/2)^2} \tag{3.37}$$

Solving for β :

$$\beta = \frac{\mathcal{E}_{L_c}}{1 - \mathcal{E}_{L_c}} \times \left(\frac{\alpha}{2}\right)^2 \equiv \eta \left(\frac{\alpha}{2}\right)^2$$

where

$$\eta = \frac{\mathcal{E}_{L_c}}{1 - \mathcal{E}_{L_c}} = \frac{\omega_i \omega_s \eta_0^4 d^2 I^2}{(\alpha/\Delta\omega_3)^2} \qquad (3.38)$$

Substituting the expression for β in (3.33), we finally find:

$$\mathcal{E}_{PH} = \frac{\eta}{\eta + (\Delta k \Delta\omega_3/\alpha)^2} \sin^2 \left\{ \frac{\alpha L}{2\Delta\omega_3} \left[\eta + \left(\frac{\Delta k \Delta\omega_3}{\alpha}\right)^2 \right]^{\frac{1}{2}} L \right\}$$

where, using the parameters of the Cs up-converter:

$$\frac{\Delta k \Delta\omega_3}{\alpha} = 1 - 0.061 \, \Delta\omega_3 + \left(\varphi^2 \, \frac{\omega_p}{c} + \theta^2 \, \frac{\omega_i}{2c} \right) \frac{\Delta\omega_3}{\alpha} \qquad (3.39)$$

As is clear from its definition, η is the unsaturated efficiency in one coherence length, for an IR frequency such that the coherence length is set by the upper level. For a given η, the intensity required to obtain that efficiency is found from (3.38).

The results of the computation for the cesium up-converter are shown in Fig. 8, for the sets of parameters shown there. Frequencies with detunings of less than 15 cm^{-1} were excluded from the integration. If the computations are done for a different IR bandwidth, one finds that the resulting solid angle is such that the product of bandwidth and solid angle is nearly the same. Changing the number density changes this product proportionally. This proportionality can also be derived analytically, if some approximations and assumptions are
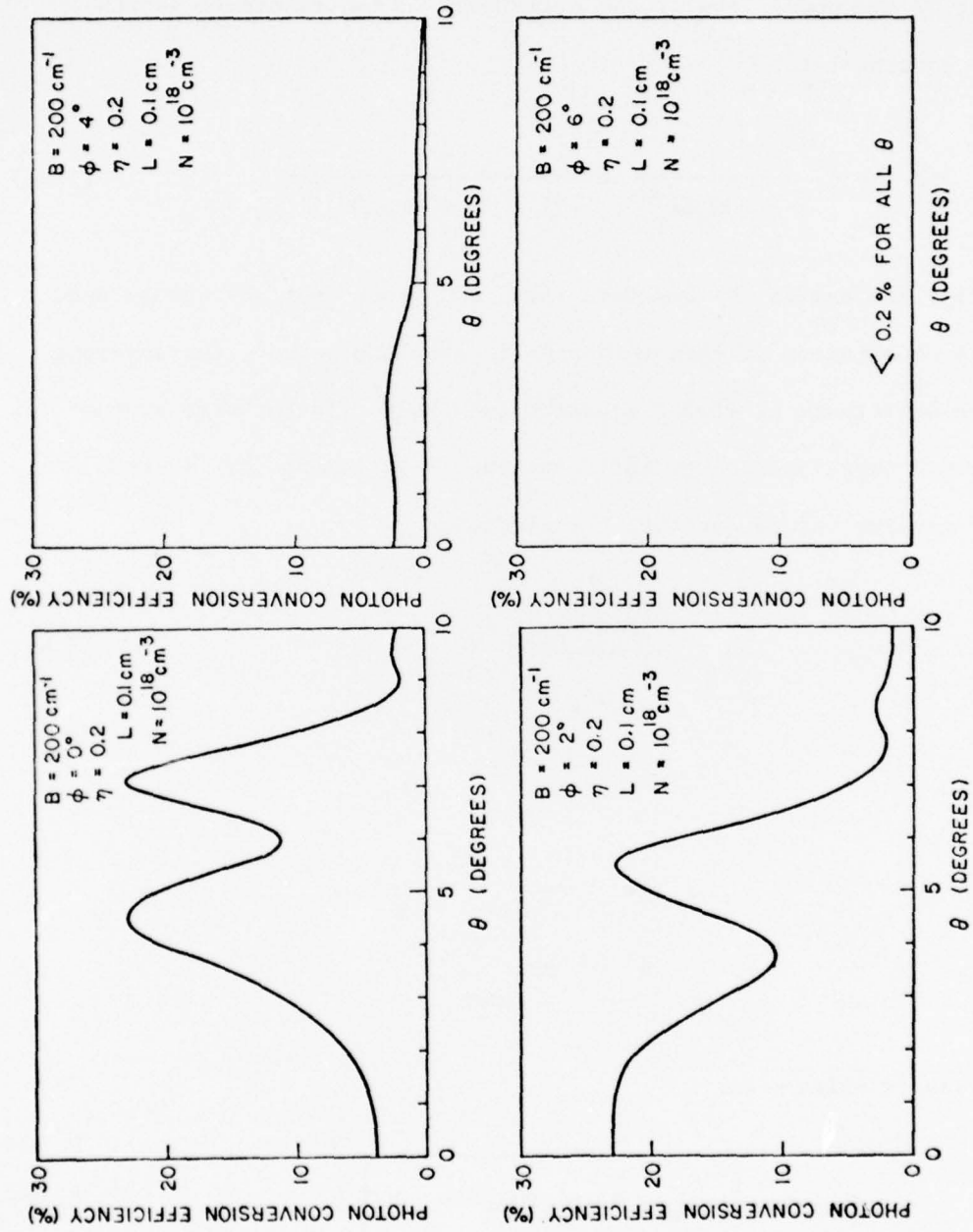
Fig. 8--Photon conversion efficiency of cesium up-converter as a function of IR incidence angle and pump phasematching angle, for given bandwidth.

made. If the angle φ is chosen such that only the term containing $\Delta\omega_3$ and the term containing θ remain (i.e., the coherence length is set by the upper level), the efficiency in one coherence length is proportional to:

$$\mathcal{E} \propto \frac{1}{(\Delta\omega_3 \Delta k)^2} \propto \frac{1}{[1 + (k_i \theta^2 \Delta\omega_3/2\alpha)]^2} \qquad (3.40)$$

Clearly, for angles θ and detunings $\Delta\omega_3$ such that the second term in the denominator is less than one (in absolute value), the envelope of the efficiency is almost constant (the $\sin^2$ factor with average value 0.5 oscillates under this envelope). By taking for θ and $\Delta\omega_3$ their maximum values, we find the condition:

$$\frac{\pi\theta_{max}^2 \Delta\omega_{3_{max}}}{\alpha\lambda_i} \lesssim 1 \qquad (3.41)$$

Since

$$\Delta\Omega = \pi\theta_{max}^2$$

$$B = 2\Delta\omega_{3_{max}}$$

this can be written as

$$\boxed{\Delta\Omega_u \times B \simeq 2\alpha\lambda_i \propto N} \qquad (3.42)$$

- 100 -

For the cesium example, with $N = 10^{18}$ cm^{-3} , we find:

$$\Delta\Omega_u \times B \ [\text{cm}^{-1}] \simeq 1.5$$

The numerical value of the product obtained this way is somewhat low. The general behavior predicted by it is also observed in the exact numerical solution, however.

b. Resolution

The general expression for the resolution is derived in Appendix B. For the solid angle in this expression one uses the value found in the preceding section. For the cesium example this angle is larger than the maximum value allowed by condition (B.8) in Appendix B. One should remember, however, that, except for a few IR frequencies where the process is phasematched, the generation happens in a length (the last coherence length) which is considerably shorter than the physical length of the medium. For the same example as above, the coherence length for large detunings equals 0.2 mm [from (3.34)], which is five times shorter than the length of the vapor zone. It is this length that should be used in the condition on the solid angle, and if this is done, there is no violation.

c. Relation between efficiency, resolution, and number density

The efficiency in one coherence length is proportional to (since NL_c is independent of N):

$$\mathcal{E} \propto \frac{P^2}{A^2} \tag{3.43}$$

Multiplying both sides by R^2, and using (3.42), we find, for a given IR bandwidth

$$\boxed{\mathcal{E} \times R^2 \propto P^2 \Delta \Omega_u^2 \propto P^2 N^2} \tag{3.44}$$

which is the same result as for the active imaging case. It says that one wants to operate at the maximum pressure allowed by limiting effects.

D. PHENOMENOLOGY OF TWO-PHOTON-RESONANT UP-CONVERTERS. EXAMPLE OF

   2.94 μ UP-CONVERSION IN CESIUM VAPOR

1. Efficiency

The expressions for the efficiency of two-photon-resonant frequency converters were derived in Chapter II. They are repeated here for convenience:

Doppler broadened regime

$$\mathcal{E} = 1.8 \times \frac{\omega_s^2 \eta_0^4 K^2 L_c^2 I^2}{\gamma_D^5} \times \sin^2\left(\frac{\Delta k L}{2}\right) \tag{2.37}$$

or

$$\mathcal{E} = 4.4 \times \frac{\omega_s^2 \eta_0^4 K_1^2 L^2 I^2}{\gamma_D \delta} \times \text{sinc}^2 \left(\frac{\Delta kL}{2} \right) \tag{3.45}$$

Pressure broadened regime

$$\mathcal{E} = 2.0 \times \frac{\omega_s^2 \eta_0^4 K_1^2 L^2 I_c^2}{\gamma \delta} \times \sin^2 \left(\frac{\Delta kL}{2} \right) \tag{2.30}$$

or

$$\mathcal{E} = 4.9 \times \frac{\omega_s^2 \eta_0^4 K_1^2 L^2 I^2}{\gamma \delta} \times \text{sinc}^2 \left(\frac{\Delta kL}{2} \right) \tag{3.46}$$

where

$$K_1 = \frac{N \mu_{01} \mu_{12} \mu_{23} \mu_{30}}{4\hbar^3 (\omega_{10} - \omega_0)(\omega_{30} - \omega_s)}$$

γ_D = Doppler linewidth $\equiv$ F.W.H.M./2.35

γ = pressure broadened linewidth $\equiv$ F.W.H.M.

δ = laser bandwidth $\equiv 1.2 \times$ F.W.H.M. $\tag{2.15}$

We will apply these expressions to the case of $2.94 \, \mu$ up-conversion in cesium vapor. Figure 9 shows the energy levels of cesium. The relevant atomic parameters are tabulated in Table I.

- 103 -

7p : j = 3/2 ――――――― 21 947
7p : j = 1/2 ――――――― 21 766

$\lambda_{ir} \simeq 2.93\mu$

7S ―――――― 18535.5 ― ― ― ― ―

$\lambda_p = 1.0790\mu$

$\lambda_s \simeq 0.4556\mu$

6p : j = 3/2 ――――― 11732
6p : j = 1/2 ――――― 11178

$\lambda_p = 1.0790\mu$

6S ――――― 0

CESIUM ENERGY LEVELS
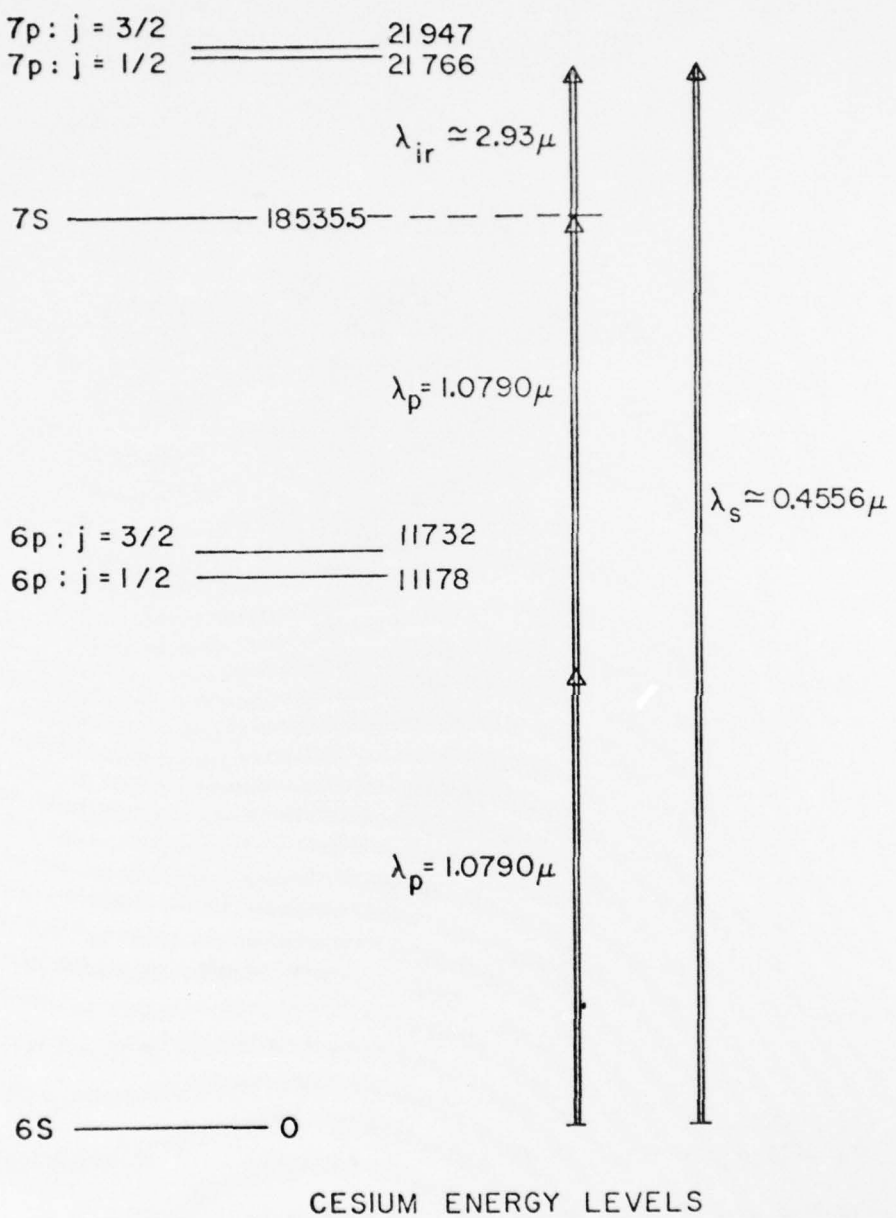
Fig. 9--Energy levels of cesium and relevant
wavelengths for IR up-converter.

TABLE I

CESIUM PARAMETERS[*]

Parameters	Value	Units	Parameters	Value	Units
ω_{10}^{ℓ}	11178.24	cm^{-1}	$\omega_{ir}^{u} \simeq \omega_{30}^{u} - \omega_{20}$	3411.15	cm^{-1}
ω_{10}^{u}	11732.35	cm^{-1}	λ_{ir}^{u}	2.93	μ
ω_{10}^{av}	11547.65	cm^{-1}	μ_{01}^{ℓ}	1.60×10^{-29}	C-m
ω_{20}	18535.51	cm^{-1}	μ_{01}^{u}	2.27×10^{-29}	C-m
ω_{30}^{ℓ}	21765.65	cm^{-1}	μ_{01}^{av}	2.78×10^{-29}	C-m
ω_{30}^{u}	21946.66	cm^{-1}	μ_{12}^{ℓ}	1.47×10^{-29}	C-m
ω_{30}^{av}	21886.32	cm^{-1}	μ_{12}^{u}	2.08×10^{-29}	C-m
ω_{0}	9267.75	cm^{-1}	μ_{12}^{av}	2.55×10^{-29}	C-m
λ_{0}	1.0790	μ	μ_{23}^{ℓ}	3.51×10^{-29}	C-m
$\Delta\omega_{1}^{\ell}$	1910.48	cm^{-1}	μ_{23}^{u}	4.97×10^{-29}	C-m
$\Delta\omega_{1}^{u}$	2464.59	cm^{-1}	μ_{23}^{av}	6.08×10^{-29}	C-m
$\Delta\omega_{1}^{av}$	2279.89	cm^{-1}	μ_{30}^{ℓ}	1.80×10^{-30}	C-m
$\omega_{ir}^{\ell} \simeq \omega_{30}^{\ell} - \omega_{20}$	3230.14	cm^{-1}	μ_{30}^{u}	2.54×10^{-30}	C-m
λ_{ir}^{ℓ}	3.09	μ	μ_{30}^{av}	3.11×10^{-30}	C-m

[*] Energy levels were taken from Ref. 46, matrix elements from Ref. 19.

Doppler broadened regime

$$\mathcal{E} = 1.02 \times 10^{-60} \times \frac{(NL_c I)^2}{\gamma_D \delta\Delta v_3^2} \times \sin^2 \left(\frac{\Delta kL}{2} \right) \qquad (3.47)$$

or

$$\mathcal{E} = 2.50 \times 10^{-60} \times \frac{(NLI)^2}{\gamma_D \delta\Delta v_3^2} \times \mathrm{sinc}^2 \left(\frac{\Delta kL}{2} \right) \qquad (3.48)$$

Pressure broadened regime

$$\mathcal{E} = 1.13 \times 10^{-60} \times \frac{(NL_c I)^2}{\gamma \delta\Delta v_3^2} \times \sin^2 \left(\frac{\Delta kL}{2} \right) \qquad (3.49)$$

or

$$\mathcal{E} = 2.78 \times 10^{-60} \times \frac{(NLI)^2}{\gamma \delta\Delta v_3^2} \times \mathrm{sinc}^2 \left(\frac{\Delta kL}{2} \right) \qquad (3.50)$$

All frequencies are in $[\mathrm{cm}^{-1}]$, lengths in $[\mathrm{m}]$, and the atomic density in $[\mathrm{m}^{-3}]$.

2. Limiting Effects

a. Molecular absorption at the pump frequency

The absorption cross section of Cs_2 dimers has been measured by Kostin and Khodovoi.[20] Their results are shown in Table II. The transmission through a length L equals $e^{-\sigma NL}$. As an example,

TABLE II

ABSORPTION CROSS SECTIONS OF Cs_2 DIMERS AT 1.079 μ

Temperature [^{O}C]	N_{Cs} [cm^{-3}]	N_{Cs_2} [cm^{-3}]	σ [cm^2]
320	5.9×10^{16}	4.7×10^{14}	4.2×10^{-17}
380	2.0×10^{17}	2.7×10^{15}	7.0×10^{-17}

at a temperature of 380°C, the transmission for a 2 mm long cell is 96%.
At higher temperatures, the cross section has unfortunately not been
measured. Workers at NRL[21] claim that the dimer absorption is reduced
by overheating the vapor using a side-arm cell, where the temperature
of the up-converting region can be much higher than the side-arm tem-
perature. Unfortunately, at the time of this writing, no quantitative
data were available yet on this effect. Kostin and Khodovoi[22] have
observed clarification of the absorption bands of Cs_2 at 1.06 μ inten-
sities of 10^7 W/cm^2 and up. Unfortunately, these intensities are con-
siderably higher than those used in the up-converters.

Additional measurements should be made on the absorption cross
section of Cs_2 dimers at high temperatures. They should be done in a
side-arm cell such that the effect of overheating the vapor can be
studied.

Table III gives the coefficients for the vapor pressure depen-
dence on temperature of Cs and Cs_2.[23] In Fig. 10, the number density
of Cs and Cs_2 are plotted versus temperature between 300°C and 500°C.
In Fig. 11 the ratio of the atomic to the molecular number density is
plotted versus temperature.

b.   Two-photon absorption of the pump radiation

The expression for the two-photon absorption rate was derived in
Chapter II (2.55). For the cesium up-converter:

$$W^{(2)} = 4.2 \times 10^{-14} \frac{I^2}{\delta} \tag{3.51}$$

TABLE III

VAPOR PRESSURE CONSTANTS

	A	B	C	D
Cs	8.22127	4006.048	- 0.00060194	- 0.19623
Cs$_2$	18.22054	6064.472	0.00009016	- 3.45395

$$\log p_{mm} = A - \frac{B}{T} + CT + D \log T$$
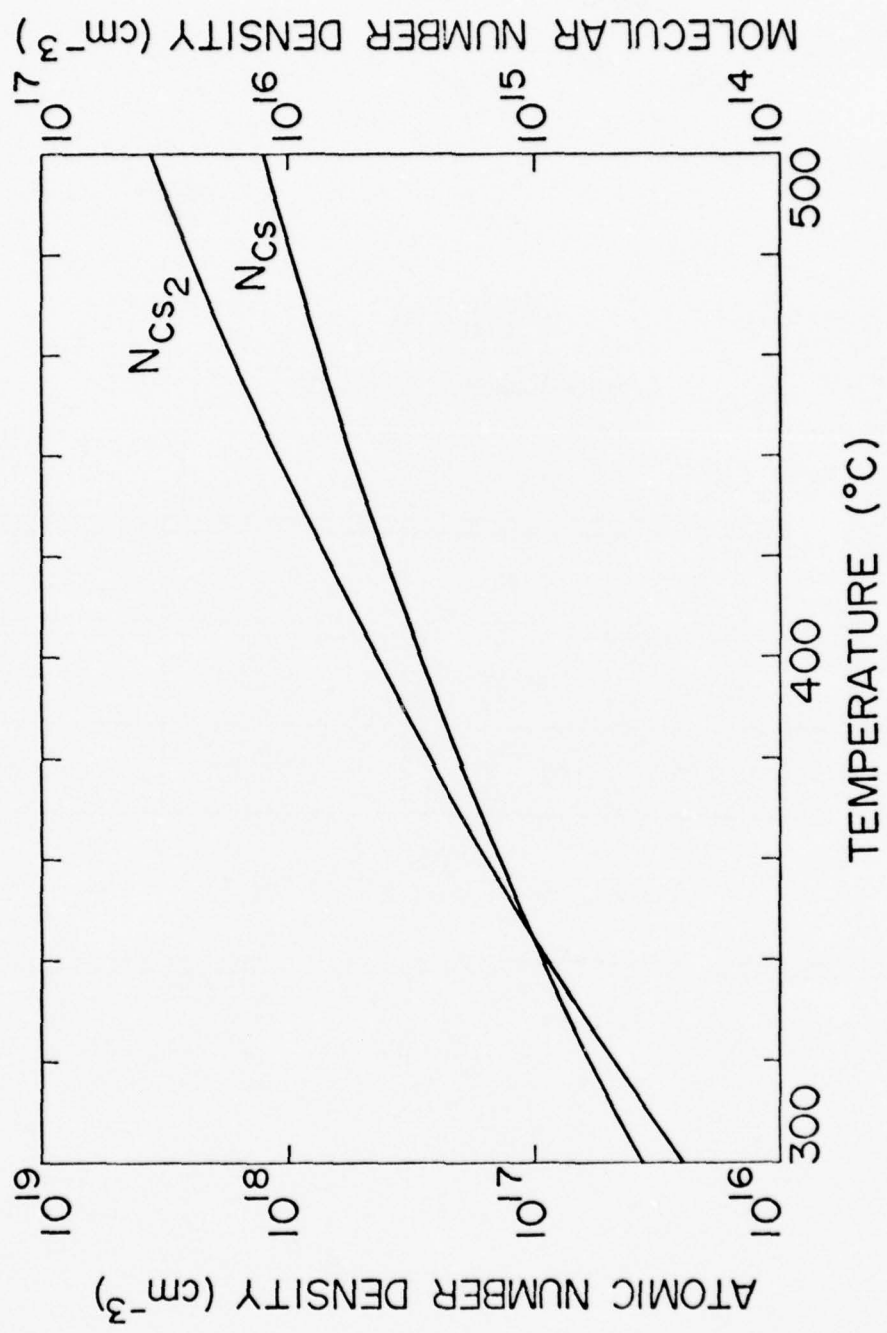
Fig. 10--Number density of Cs and Cs$_2$ versus temperature.
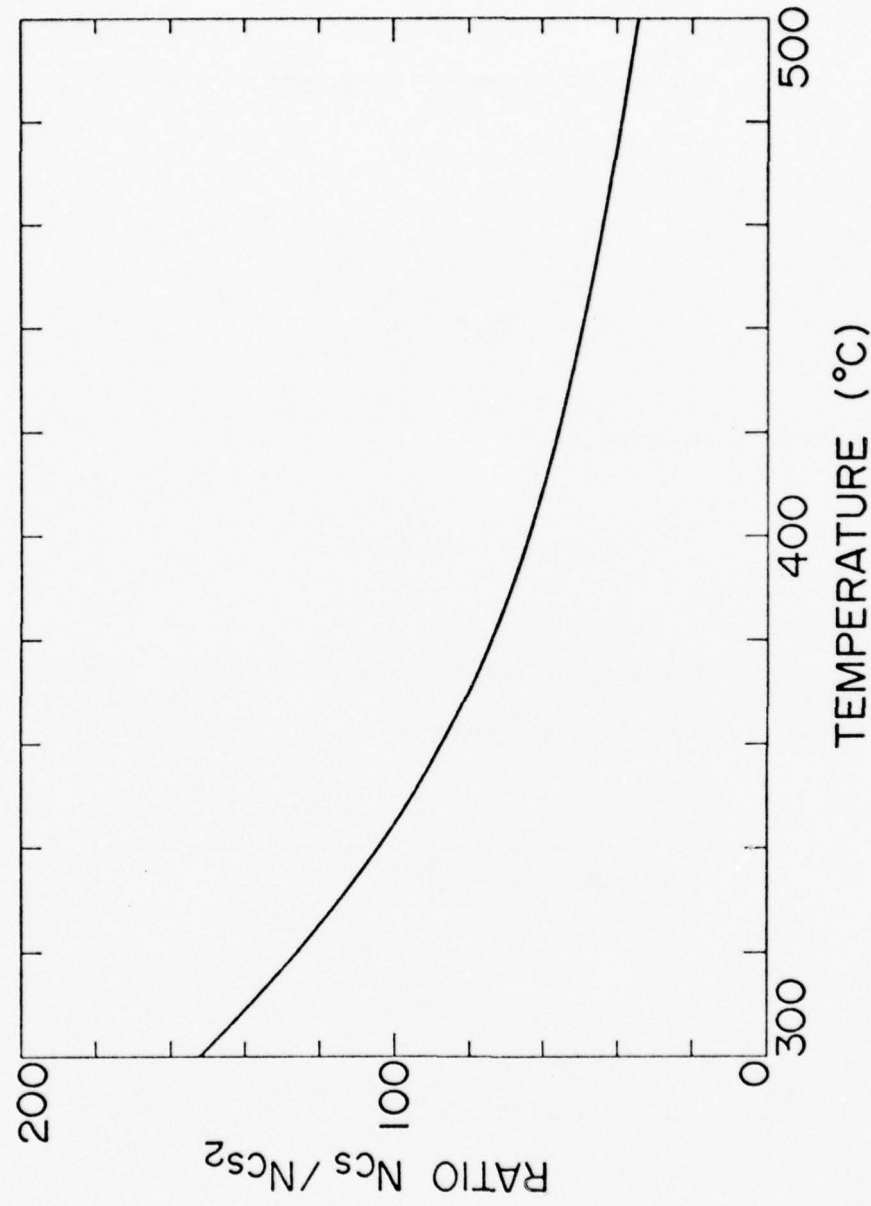
Fig. 11--Ratio of atomic to molecular number density of cesium versus temperature.

- 111 -

where I is in $[W/m^2]$ and δ is in $[cm^{-1}]$. Using this expression, the attenuation of the pump beam can be calculated:

$$\frac{dI}{dz} = -\hbar\omega_{20}NW^{(2)} \equiv -\alpha NI^2$$

where

$$\alpha = \hbar\omega_{20}W^{(2)}/I^2 \tag{3.52}$$

The solution to this equation is:

$$I(L) = \frac{I_0}{1 + \alpha NLI_0} \tag{3.53}$$

where I_0 is the intensity at the entrance of the cell. For the case of the cesium up-converter, the transmission of the cell is:

$$\frac{I(L)}{I_0} = \frac{1}{1 + 1.54 \times 10^{-32} \times NLI_0/\delta} \tag{3.54}$$

Example:

$$N = 10^{24} \, m^{-3}$$
$$L = 2 \times 10^{-3} \, m$$
$$I_0 = 10^9 \, W/m^2$$
$$\delta = 0.12 \, cm^{-1} \, (F.W.H.M. = 0.1 \, cm^{-1})$$
$$\rightarrow \text{transmission} = 80\%$$

- 112 -

By combining the expressions for the efficiency and for the two-photon attenuation of the pump beam, the maximum efficiency allowed by this effect can be calculated. We will limit the quantity αNLI_0 to a value of 0.5, which corresponds to a transmission of 67%. For the case of phasematched up-conversion, the resulting maximum efficiencies are:

$$\mathcal{E}_{Doppl.} \lesssim 1.1 \times 10^{-2} \times \left(\frac{\omega_s}{\omega_{20}}\right)^2 \times \left(\frac{\mu_{23}\mu_{30}}{\mu_{01}\mu_{12}}\right)^2 \times \left(\frac{\Delta\omega_1}{\Delta\omega_3}\right)^2 \times \left(\frac{\delta}{\gamma_D}\right) \qquad (3.55)$$

$$\mathcal{E}_{press.} \lesssim 1.2 \times 10^{-2} \times \left(\frac{\omega_s}{\omega_{20}}\right)^2 \times \left(\frac{\mu_{23}\mu_{30}}{\mu_{01}\mu_{12}}\right)^2 \times \left(\frac{\Delta\omega_1}{\Delta\omega_3}\right)^2 \times \left(\frac{\delta}{\gamma}\right) \qquad (3.56)$$

For the cesium up-converter:

$$\mathcal{E}_{Doppl.} \lesssim \frac{2.54 \times 10^3 \; \delta}{\gamma_D \Delta\omega_3^2} \qquad (3.57)$$

$$\mathcal{E}_{press.} \lesssim \frac{2.77 \times 10^3 \; \delta}{\gamma \Delta\omega_3^2} \qquad (3.58)$$

As an example, for $\delta = 0.12 \text{ cm}^{-1}$, a detuning of 20 cm^{-1} and a pressure broadened linewidth of 0.1 cm^{-1}, we find a maximum efficiency of 8.3, corresponding to a photon efficiency of 1.3. This means that a photon efficiency of 100% would be possible in this example.

- 113 -

c.   Saturation of the two-photon transition

The dipole moment at the sum frequency is proportional to the population difference between the ground level and the resonant level. The intensity thus has to be limited such that:

$$W^{(2)} \times \tau < 0.5 \tag{3.59}$$

where τ is either the pulselength or the lifetime of the resonant level, whichever is shorter. For the cesium up-converter, for $\delta = 0.12$ cm^{-1}, a pulselength of 100 nsec, and a lifetime of the 7s-6p transition of 52 nsec, we find a maximum allowed intensity of 5×10^5 W/cm^2.

d.   Atomic absorption at the sum frequency

For detunings larger than a few atomic linewidths, the single photon absorption cross section is given by:[19]

$$\sigma = \frac{\eta_0 \hbar \omega_s \gamma \mu_{03}^2}{2\hbar^2 \Delta \omega_3^2} \tag{3.60}$$

For the cesium up-converter, $\gamma = 3.27 \times 10^{-26} \times N$ [cm^{-1}] for the transition $6s^2 S - 7p^2 P_{3/2}$. The transmission of the cell is $e^{-\sigma NL}$, where:

$$\sigma NL = 8.3 \times 10^{-45} \frac{N^2 L}{\Delta \omega_3^2} \tag{3.61}$$

- 114 -

with Δv_3 in $[cm^{-1}]$ and N in $[m^{-3}]$.

Example:

$$N = 10^{24} \ m^{-3}$$

$$L = 2 \times 10^{-3} \ m$$

$$\Delta v_3 = 20 \ cm^{-1}$$

$$\rightarrow transmission = 96\%$$

e. Atomic absorption at the IR frequency

Even a small population in the resonant level will result in a considerable attenuation of the IR field, since this field is almost resonant with the allowed transition from that level to the upper level. In Appendix D the pressure broadening of this transition is estimated for the case of the cesium up-converter. The result is $\gamma \simeq 6 \times 10^{-26} \times N \ [cm^{-1}]$, with N in $[m^{-3}]$. Using this, we find for the cesium up-converter:

$$\sigma NL \simeq 9.0 \times 10^{-45} \ \frac{N^2 Lf}{\Delta v_3^2}$$

$$\simeq 4 \times 10^{-56} \ \frac{N^2 L I^2 \tau}{\Delta v_3^2 \delta} \tag{3.62}$$

where f is the fraction of atoms in the 7s level, in percent. In deriving this result, use was made of the fact that the broadening is almost completely due to the atoms in the ground state, since only a

- 115 -

very small fraction is allowed in the 7s level, while the absorption

is done by the small fraction of atoms that is in that level.

Example:

$$N = 10^{24} \, m^{-3}$$

$$f = 1$$

$$L = 2 \times 10^{-3}$$

$$\Delta\nu_3 = 20 \, cm^{-1}$$

$$\rightarrow transmission = 96\%$$

f. Breaking of phasematching due to a non-zero population in the
    resonant level

If the up-conversion process is self-phasematched, and no popula-

tion is present in the resonant level, then it will be phasematched at

any number density since all the contributions to the mismatch are pro-

portional to this number density. This is not the case if the third

technique for phasematching is used, since in this case the angle φ

depends on the number density according to (3.28). In Section C, the

effect of a non-zero population in the resonant level on the mismatch

Δk and the phasematching frequency (3.25) and angle (3.28) was dis-

cussed in considerable detail. Since the population of the resonant

level is a function of time, a distinction has to be made between the

case where the pulselength is shorter than the decay time of the reso-

nant level, and the case where the pulselength is much longer than that

time, such that steady-state conditions are present during most of the

- 116 -

pulse. In the first case, the population of the resonant level has to be limited to a value such that at the end of the pulse the process is still phasematched. In the second case, a larger population can be tolerated because its effect can be offset. However, since this population (steady-state value) depends on the pump power, the effect of pulse-to-pulse fluctuations of the laser power must be considered. Also, in the second case the beam profile of the pump is important, since the population in the resonant level will spatially vary according to the square of the local intensity, such that the process is only phasematched over part of the pump beam, unless beam apodization is used. We will now study both these cases, for the example of the $2.94 \, \mu$ cesium up-converter.

For pulses shorter than the decay time of the resonant level, the phase mismatch has to be less than π at the end of the pulse, i.e.:

$$\Delta k L = \frac{N_{7s} L \mu_{23}^2 \omega_i}{2\epsilon_0 c \hbar \Delta \omega_3} < \pi \tag{3.63}$$

Substituting the Cs parameters, this requires:

$$\frac{N_{7s} L}{\Delta \omega_3} < 2.1 \times 10^{17} \tag{3.64}$$

with N in $[m^{-3}]$, L in $[m]$, and $\Delta \omega_3$ in $[cm^{-1}]$. Since

$$N_{7s} = W^{(2)} N \tau$$

$$W^{(2)} = 4.2 \times 10^{-14} \frac{I^2}{\delta} \tag{3.51}$$

- 117 -

the condition (3.64) can also be written as:

$$\frac{NLI^2 \tau}{\Delta \nu_3 \delta} < 5 \times 10^{30} \qquad (3.65)$$

Example:

$$N = 10^{24} \, m^{-3}$$

$$L = 2 \times 10^{-3} \, m$$

$$\tau = 30 \, nsec$$

$$\delta = 0.12 \, cm^{-1} \quad (F.W.H.M. = 0.1 \, cm^{-1})$$

$$\Delta \nu_3 = 20 \, cm^{-1}$$

$$\gamma = 0.05 \, cm^{-1}$$

For this set of parameters, we find $f = 0.2\%$, $I \lesssim 4.5 \times 10^4 \, W/cm^2$, and the maximum efficiency is 94% (power). Since the condition (3.65) limits the mismatch in the center of the beam, where it is largest, the profile of the pump beam is not important.

For pulses that are much longer than the decay time of the resonant level, steady-state conditions prevail during most of the pulse. The population of the resonant level varies in time according to:

$$\frac{dN_2}{dt} = W^{(2)}N - N_2/\tau_{21} \qquad N_2 \ll N \qquad (3.66)$$

which has the solution:

$$N_2(t) = W^{(2)}N\tau_{21}(1 - e^{-t/\tau_{21}}) \qquad (3.67)$$

- 118 -

For $t \gg \tau_{21}$, $N_2 \simeq W^{(2)} N \tau_{21}$. The steady-state fraction f is thus equal to:

$$f = 100 \; \frac{N_{7s}}{N} = 100 \; W^{(2)} \tau_{21} \qquad (3.68)$$

With this fraction of atoms f in the resonant level, the process will self-phasematch at a detuning given by (3.25) or, for a given detuning, the phasematching angle φ will be given by (3.28). In this case, a larger fraction can be allowed than in the previous case, resulting in higher efficiencies. As an example, when the fraction f is increased to 0.6 from its 0.2 value in the other case, the square of the intensity can be increased by a factor of three, resulting in an efficiency three times higher. The process will in this example be self-phasematched at a detuning of 10.5 cm^{-1} instead of 16.3 (resulting in an additional increase in the efficiency because of the $1/\Delta\omega_3^2$ dependence) or, in the case of angle phasematching with $\Delta\omega_3 = 20$ cm^{-1}, the angle φ will increase from 1.3° to 2.1°. Because the steady-state population is proportional to the square of the intensity, one has to watch in this case the pulse-to-pulse stability of the pump laser, and also the effect of a non-rectangular beam profile. The condition for the pump stability can be found as follows. If there is a change ΔN_{7s}, caused by a change ΔI, the condition $\Delta kL < \pi$ is the same as (3.63), except that the population N_{7s} is replaced by the change

in that population. In terms of ΔI , the condition is:

$$\frac{\Delta I}{I} < 2.5 \times 10^{30} \frac{\delta \Delta \nu_3}{NLI^2 \tau_{21}} \tag{3.69}$$

Using the same parameters as in the previous example, we find for the
self-phasematched case $(\Delta \nu_3 = 10.5 \text{ cm}^{-1})$ $\Delta I/I < 5\%$, and for the
angle phasematched case $(\Delta \nu_3 = 20 \text{ cm}^{-1})$ $\Delta I/I < 9.5\%$. These sta-
bilities are easily obtainable with present-day solid-state lasers.
Since $\Delta N_{7s}/N_{7s} = 2\Delta I/I$, we can also find the time after which the
process becomes phasematched, using (3.67). For $\Delta I/I = 10\%$, we
find that the mismatch is less than π after $t = 1.6 \times \tau_{21}$. For
the cesium up-converter, this means that the pulselength should be
considerably longer than 83 nsec. From the value of $\Delta I/I$, we can
also calculate the maximum radius at which the process will still be
phasematched in the case of a Gaussian pump beam. As an example, for
$\Delta I/I = 10\%$, the maximum radius is equal to $0.23 \, w_0$, while the ef-
ficiency, which is proportional to I^2 , only drops to 50% of its
value in the center for $r = 0.42 \, w_0$. In such a case one might
want to apodize the beam.

g. Breaking of phasematching due to quadratic Kerr effect

The change in the index of refraction at the pump frequency,
caused by the quadratic Kerr effect, was calculated in Chapter II.

It was found that the maximum value of this change is given by:

$$(n - 1)_{max} = \frac{\eta_0 \mu_{01}^2 \mu_{12}^2 NI}{2\epsilon_0 \hbar^3 (\omega_{10} - \omega_0)^2 \gamma} \qquad (2.70)$$

For the cesium up-converter:

$$(n - 1)_{max} = 2.7 \times 10^{-40} \frac{NI}{\gamma} \qquad (3.70)$$

where N is in $[m^{-3}]$, I in $[W/m^2]$, and γ in $[cm^{-1}]$. The phase mismatch over a distance L is then given by:

$$\Delta kL = \frac{2\omega_p (n - 1)L}{c}$$

For the cesium up-converter:

$$\Delta kL = 3.1 \times 10^{-33} \frac{NLI}{\gamma} \qquad (3.71)$$

Example:

$$N = 10^{24} \, m^{-3}$$

$$\gamma = 0.05 \, cm^{-1}$$

$$L = 2 \times 10^{-3} \, m$$

$$I = 10^9 \, W/m^2$$

- 121 -

For this set of parameters, we find:

$$(n - 1)_{max} = 5.4 \times 10^{-6}$$

$$\Delta kL \simeq 0.1 \ll \pi$$

Because the IR field is very weak in imaging applications, the Kerr effect at the sum frequency can be neglected. Ths would not be the case, however, if one would try to deplete the pump beam with a high power IR beam.

h.   Thermal defocusing

If the pump beam is not apodized, the population of the resonant level, which has the same spatial dependence as the square of the intensity, will create a lensing effect for the incident waves. This happens because for the IR waves $\Delta n \propto N_{7s}$, while for the pump and the sum waves $\Delta n \propto \Delta N_{6s} = - N_{7s}$. When the pump beam is split into two beams which then interfere at a small angle 2φ , the transversal variation of the total pump field will be sinusoidal, with period:

$$X_p = \frac{\lambda_p}{2\varphi} \tag{3.72}$$

The population of the resonant level, and thus the index of refraction will vary sinusoidally in this case, with a spatial period one-quarter

- 122 -

that of the pump field:

$$X_{N_{7s}} = \frac{\lambda_p}{8\varphi} \tag{3.73}$$

The incident waves thus see a periodic phase grating. The Kerr contribution to the index of refraction, which is proportional to the intensity, varies with a spatial period:

$$X_{p,Kerr} = \frac{\lambda_p}{4\varphi} \tag{3.74}$$

creating another phase grating. We will now estimate the importance of these effects for the example of the Cs up-converter.

The effect of the Gaussian profile of the population in the resonant level can be estimated as follows. According to Ref. 19, the condition that has to be satisfied to avoid thermal defocusing is:

$$\frac{\sqrt{2\Delta n'}\ L}{w_p} \ll 1 \tag{3.75}$$

where Δn is the change in the index of refraction caused by the atoms in the resonant level, and the factor 2 comes from the dependence on the square of the intensity. For the IR waves, for the example of the cesium up-converter:

$$\Delta n = \frac{\mu_{23}^2 N_{7s}}{2\epsilon_0 \hbar \Delta \omega_3} = 7 \times 10^{-26}\ \frac{Nf}{\Delta \omega_3} \tag{3.76}$$

- 123 -

Example:

$$N = 10^{24} \, m^{-3}$$

$$f = 0.2$$

$$\Delta\omega_3 = 20 \, cm^{-1}$$

$$\rightarrow \Delta n = 7 \times 10^{-4}$$

For $L = 0.2$ cm , $R = 10^5$, the radius w_p is on the order of 1 cm. This yields $\sqrt{2\Delta n} \times L/w_p \simeq 10^{-2} \ll 1$. For the pump and sum waves, the matrix element is smaller and/or the detuning larger, and as a result condition (3.75) is satisfied.

The effect of the Kerr contribution to the index of refraction at the pump can also be estimated using (3.75), where Δn is now due to the quadratic Kerr effect. Using (2.70), with

$$N = 10^{24} \, m^{-3}$$

$$I = 10^9 \, W/m^2$$

$$\gamma = 0.05 \, cm^{-1}$$

one finds $\Delta n_{Kerr} = 5 \times 10^{-6}$. Since this value is even much smaller than the value of Δn_{7s} , the effect should be negligible.

The problem of the diffraction of a plane wave by a sinusoidal phase grating is considered in detail in Ref. 24. In the Raman-Nath

regime, i.e., for

$$L \lesssim L_{max} = \frac{X^2}{4\lambda} \tag{3.77}$$

where X is the period of the grating and λ is the wavelength of the incident light, the diffraction into higher order modes is small when $\Delta kL \lesssim 1$. Note that this is the same condition as the one for breaking phasematching due to atoms in the resonant level. Since the length L_{max} is only a few microns for typical values of φ , we are in the Bragg regime. In this regime, considerable coupling to higher order modes only exists when a wave is incident at the Bragg angle, i.e.:

$$\theta \simeq \frac{\lambda}{2X} \tag{3.78}$$

For the IR waves, this condition can be written as:

$$\theta \simeq 2 \times \frac{\lambda_i}{\lambda_p} \times \varphi \tag{3.79}$$

Example:

$$\varphi = 3^{\circ}$$
$$\lambda_i = 3\,\mu$$
$$\lambda_p = 1\,\mu$$
$$\rightarrow \theta = 18^{\circ}$$

This angle is much larger than the acceptance angle of the up-converter, and rays incident at such a large angle can be stopped using a mechanical stop. Also, in the Bragg regime, the condition for significant scattering into higher order modes is again $\Delta kL \simeq 1$.

3.   Optimization

We will address the problem of finding the optimum values for the atomic number density N and the length of the cell L , for a given efficiency and resolution. Because active imaging looks much more promising than passive imaging, when compared with competing techniques,[16] only that case will be discussed. The procedure will be explained on the hand of the 2.9^4 μ Cs up-converter.

In Table IV the most important limiting effects are summarized, together with the quantity they bound. To solve the problem we need in addition the expressions for the efficiency [(3.48) and (3.50)] and the expression for the number of resolution elements (3.29). Because at high number densities the atomic linewidth becomes pressure broadened, such that the dependence of the efficiency on number density is linear instead of quadratic, the Doppler and the pressure broadened case have to be considered separately. The optimization procedure is very similar, however, for both cases. By limiting the molecular absorption and the population in the resonant level (to avoid breaking phasematching) a maximum value can be found for the quantity NP/R . By substituting this value in the expression for the efficiency, a solution to the problem is obtained for both cases. This solution is

TABLE IV

LIMITING EFFECTS FOR TWO-PHOTON-RESONANT UP-CONVERTERS

Limiting Effect	Quantity to be Bounded
Molecular absorption of the pump	NL
Two-photon absorption of the pump	NP/R
Atomic absorption of the generated radiation	$N^2 L$
Atomic absorption of the IR radiation	$N^2 P^2/LR^2$
Breaking of phasematching	NP^2/LR^2

then substituted in the remaining conditions of Table IV to check whether they are not violated. In view of the results on thermal de-focusing, in applying the condition on breaking of phasematching, we will limit the population in the resonant level to a value such that phasematching is not broken when the IR frequency is tuned to the phasematching value for $f = 0$, or, for given IR frequency, when the angle φ is adjusted to its value for $f = 0$. In the self-phasematched case $(\varphi = 0)$, a higher population can be tolerated in the resonant level if long pulses are used, but the power required to obtain a given efficiency will be found to vary only as the square root of the increase in population, making it a small effect.

To limit the molecular absorption, we require:

$$\sigma N_{mol} L \lesssim 0.25 \qquad\qquad (3.80)$$

which corresponds to 80% transmission of the pump. Since we are not interested in the molecular number density, we replace it by the product of the atomic number density and some proportionality constant, which can be done over a small temperature range (Fig. 11). Around 440°C, this ratio is about 50. The condition (3.80) can then be written as:

$$NL \lesssim \frac{12.5}{\sigma} \qquad\qquad (3.81)$$

To avoid breaking of phasematching, we require (3.65):

$$\frac{NLP^2}{A^2} \lesssim 5 \times 10^{30} \times \frac{\delta\Delta_{\nu_D}^3}{\tau} \qquad (3.82)$$

By combining this with the expression for the resolution (3.29), this condition can also be written as:

$$\frac{NP^2}{LR^2} \lesssim 1.75 \times 10^{19} \frac{\delta\Delta_{\nu_D}^3}{\tau} \qquad (3.83)$$

Finally, the combination of this result with the condition on molecular absorption yields the important relation:

$$\frac{NP}{R} \lesssim 1.5 \times 10^{10} \left(\frac{\delta\Delta_{\nu_D}^3}{\sigma\tau}\right)^{\frac{1}{2}} \qquad (3.84)$$

We now have to consider separately the cases of Doppler broadening and pressure broadening. The Doppler width (F.W.H.M.) for Cs is 0.03 cm^{-1} at a temperature of 440°C. In Appendix D the pressure broadening of the linewidth of the 6s-7s transition is estimated to be 0.03 cm^{-1} at a number density of 6×10^{17} cm^{-3}. Thus for densities below 6×10^{17} cm^{-3} we are in the Doppler broadened regime, while for densities higher than this value we are in the pressure broadened regime.

a.   Doppler broadened regime: $N < 6 \times 10^{17}$ cm^{-3}

Combination of the expression for the efficiency (3.48) and the expression for the resolution (3.29) yields:

- 129 -

$$\mathcal{E}_D = \frac{7.2 \times 10^{-49}}{\gamma_D \delta\Delta v_{\frac{3}{2}}^2} \times \left(\frac{NP}{R}\right)^2 \tag{3.85}$$

The second factor in this expression is exactly the square of the quantity for which we already found an upper bound (3.84). Substituting, we find the very important result:

$$\mathcal{E}_D = \frac{1.6 \times 10^{-28}}{\gamma_D \Delta v_{\frac{3}{2}} \sigma\tau} \tag{3.86}$$

It says that in the Doppler broadened regime, there is a maximum obtainable efficiency, which is independent of the resolution. The combination of this result with (3.84), (3.81), and (3.29) solves the optimization problem. From (3.84) it is clear that for a given resolution, we want to maximize N. Thus we want to use the maximum density allowed by the requirement that we are in the Doppler broadened regime. Using $N = N_{max} = 2.5 \times 10^{17}$ cm^{-3} (see Fig. 2), the relation (3.84) between power and resolution can be written as:

$$P = 6 \times 10^{-14} \times \left(\frac{\delta\Delta v_{\frac{3}{2}}}{\sigma\tau}\right)^{\frac{1}{2}} \times R \tag{3.87}$$

Example:

$$\Delta v_3 = 20 \text{ cm}^{-1}$$

$$\gamma_D = 0.013 \text{ cm}^{-1}$$

$$\sigma = 7 \times 10^{-21} \text{ m}^2$$

$$\tau = 50 \text{ nsec}$$

$$\delta = 0.12 \text{ cm}^{-1}$$

With these parameters, we find:

$$\mathcal{E}_D = 1.76$$

$$P = 5.0 \times R \text{ W}$$

$$L = 0.71 \text{ cm}$$

$$A = 1.3 \times 10^{-4} \times R \text{ cm}^2$$

The remaining limiting effects can now be checked. Since N and L are fixed, we find, independent of the resolution (Table IV):

Absorption at ω_s (3.61): $\quad \sigma NL = 0.01$

Absorption at ω_{ir} (3.62): $\quad \sigma NL = 0.003$

Absorption at ω_p (3.54): $\quad \alpha INL = 0.09$

b. Pressure broadened regime: $N \gtrsim 6 \times 10^{17} \text{ cm}^{-3}$

Combination of the expressions for the efficiency (3.50) and the resolution (3.29) yields:

$$\mathcal{E}_{pr} = \frac{8 \times 10^{-49}}{\gamma \delta \Delta v_3^2} \times \left(\frac{NP}{R} \right)^2 \qquad (3.88)$$

- 131 -

Since $\gamma > \gamma_D$, and NP/R is a constant, we can say immediately that the efficiency in the pressure broadened regime will be less than in the Doppler broadened regime. This does not imply, however, that the maximum pressure allowed by the condition $\gamma \lesssim \gamma_D$ is always the optimum operating condition. If the desired efficiency is less than the maximum value allowed in the Doppler regime, then the required power in the pressure broadened regime will go down proportionally to the efficiency decrease, since $\mathcal{E} \propto L/N$ and $P \propto R/N$, while in the Doppler regime it will only go down as the square root of this decrease (3.85). We will now derive a relation between number density and efficiency, which is valid in the pressure broadened regime but can only be used for efficiencies less than the maximum efficiency obtainable in the Doppler regime. In Appendix D, the linewidth γ is estimated to be:

$$\gamma \simeq 5 \times 10^{-26} \, N \quad [\text{cm}^{-1}] \tag{3.89}$$

where N is in $[\text{m}^3]$. Substitution in (3.89) yields:

$$\mathcal{E}_{pr} = \frac{1.6 \times 10^{-23}}{\Delta \omega_3^2 \delta N} \times \left(\frac{NP}{R}\right)^2 \tag{3.90}$$

After combining this with (3.84), we find the desired result:

$$\boxed{\mathcal{E}_{pr} = \frac{3.6 \times 10^{-3}}{\Delta \omega_3 \sigma \tau} \times \frac{1}{N} < \mathcal{E}_D} \tag{3.91}$$

- 132 -

The combination of this result with (3.84), (3.81), and (3.29) then solves the optimization problem.

Example:

$$\Delta\omega_3 = 20 \text{ cm}^{-1}$$
$$\sigma = 7 \times 10^{-21} \text{ cm}^2$$
$$\tau = 50 \text{ nsec}$$
$$\delta = 0.12 \text{ cm}^{-1}$$
$$\mathcal{E} = 1.0$$
$$R = 10^5$$

With these parameters, we find:

$$N = 5 \times 10^{17} \text{ cm}^{-3} \qquad (3.91)$$
$$P = 2.5 \times 10^5 \text{ W} \qquad (3.84)$$
$$L = 0.36 \text{ cm} \qquad (3.81)$$
$$A = 6.7 \text{ cm}^2 \qquad (3.29)$$

The remaining limiting effects can now be checked:

Absorption at ω_s (3.61): $\qquad \sigma NL = 0.02$

Absorption at ω_{ir} (3.62): $\qquad \sigma NL = 0.005$

Absorption at ω_p (3.54): $\qquad \alpha NLI = 0.09$

The number density of 5×10^{17} cm^{-3} corresponds to a temperature of about 430°C, where the molecular cross section is not exactly known. This density is only a factor of 2.5 higher though than the maximum

density at which σ has been measured (Table II). If, as a rough guess, the cross section is assumed to vary in about the same way between $380^{o}C$ and $430^{o}C$ as it does between $320^{o}C$ and $380^{o}C$, the resulting increase in power would be only about 25%. So a more reasonable value for P in the example above may be 3×10^{5} W.

4. Comparison With Crystal Up-Converters

We are now in a position to make a comparison between vapor up-converters and crystal up-converters. As a specific example, we will compare the Cs 2.94 μ up-converter with a LINbO$_3$ up-converter for the same wavelength. The Cs up-converter is pumped by the Nd:BeL laser at 1.0790 μ, while the LiNbO$_3$ up-converter is pumped by the 1.064 μ line of the Nd:YAG laser.

First we summarize the important relations for crystal up-converters. The efficiency of the LiNbO$_3$ up-converter is given by:[15,25]

$$\mathcal{E} = 1.9 \times 10^{-7} \times \frac{L^2 P}{A} \qquad (3.92)$$

The resolution is given by (B.9). Using the maximum allowed solid angle $\Delta\Omega_u = \pi n_i \lambda_i / L$ (B.8), with $n_i = 2.16$:[15] .

$$R = \frac{\pi n_i A}{\lambda_i L} = 2.3 \times 10^6 \times \frac{A}{L} \qquad (3.93)$$

Combining (3.77) and (3.78):

$$\mathcal{E} = 9.8 \times 10^5 \times \frac{A \times P}{R^2} \qquad (3.94)$$

or

$$\mathcal{E} = 0.44 \times \frac{L \times P}{R} \qquad (3.95)$$

Because of the L^2/A dependence of the efficiency, it is optimum to use as long a length as possible for low resolutions. As the resolution is increased, however, the area A will also increase, and at some "critical" resolution the area becomes equal to some maximum value A_{max}. If the resolution is increased beyond that, the length has to be decreased, and formula (3.94) must be used with $A = A_{max}$. Clearly the critical resolution is given by:

$$R_{crit} = 2.3 \times 10^6 \times \frac{A_{max}}{L_{max}} \qquad (3.96)$$

We will now make a general comparison between vapor and crystal up-converters. Two separate cases must be considered, depending on whether $R \gtrless R_{crit}$. We will start by comparing the up-converters at the maximum efficiency $\mathcal{E}_D$ (3.86) of the vapor up-converter. Afterwards we will make some comments for the case where $\mathcal{E} < \mathcal{E}_D$. For the cesium up-converter, the same parameters are used as in the section

-135-

on optimization, such that $\varepsilon_D = 1.76$. For LINbO$_3$, we assume

$L_{max} = 4$ cm and $A_{max} = 2$ cm^2 such that $R_{crit} = 1.1 \times 10^4$.

a. $\underline{R < R_{crit}}$

   Crystal: $P = 100\ R$

   Vapor: $P = 5\ R$

   Ratio: $2 \times 100/5 = 40$ (2 because of polarization)

b. $\underline{R > R_{crit}}$

   Crystal: $P = 9 \times 10^{-3} \times R^2$

   Vapor: $P = 5\ R$

   For $R = 10^5$,

   Ratio: $2 \times (9 \times 10^7/5 \times 10^5) = 360$

In both cases, if the efficiency is dropped by a factor of 2, the

power can be dropped by a factor of 2, but only if N is increased

by 2 for the vapor up-converter. If the efficiency is considerably

lower than ε_D , such that N would become unreasonably large, one

will have to keep N constant at some maximum value. In that case,

the power decreases proportionally to the decrease in efficiency for

the crystal up-converter, but only as the square root for the vapor

up-converter because of the dependence on the square of the power.

We will not discuss this problem here because it is of little interest

for imaging applications where the highest possible efficiency is needed

because of the small signals received. The design parameters for a crystal and a vapor up-converter, with $\mathcal{E} = \mathcal{E}_D$ and $R = 10^5$, are summarized in Table V.

E. EXPERIMENTAL RESULTS

1. Up-Conversion of 2.94μ Images

a. Discussion of the experimental set-up

The set-up for the imaging experiment is shown in Fig. 12. The Nd:BeL rod used in the Q-switched laser has a line which comes within about 1 Å of the two-photon-resonance, and it could easily be tuned on resonance with a Fabry-Perot etalon inside the cavity. The beam coming out of the laser was split into two parts. About 74% of the power was focused into a CDA doubler, the output of which was used to drive a LiNbO$_3$ parametric oscillator. The pump and the signal of the OPO were filtered out with a germanium filter, while the idler wave was sent through a spatial filter and then collimated to a diameter of about 3 cm. The plane wave idler radiation was then sent through a quartz slide on which the object was either taped (Figs. 13 and 14) or painted (Fig. 15). The up-conversion was done using a Type III optical system. The object and the center of the cell were in the two focal planes of a 20 cm quartz lens, while the cell and the film were in the two focal planes of a 50 cm quartz lens. The magnification was thus $M = \lambda_s / \lambda_i \times 50/20 \simeq 0.4$. The remaining 26% of the pump was blown up to an area

TABLE V

DESIGN EXAMPLES OF A CESIUM AND A LiNbO$_3$

UP-CONVERTER FOR 2.94 μ RADIATION

Parameter	LiNbO$_3$	Cesium	Units
Pump wavelength	1.06	1.0790	μ
IR wavelength	2.94	2.94	μ
Sum wavelength	7800	4560	Å
Pump bandwidth	$\simeq 1.0$	0.1	cm^{-1}
Pump pulselength	50	50	nsec
$\mathcal{E}_{photon}$	27.5	27.5	%
Resolution	10^5	10^5	--
Pump power	9×10^7	5.0×10^5	W
N	--	2.5×10^{17}	cm^{-3}
$\Delta\omega_3$	--	20	cm^{-1}
A	2	13	cm^2
L	0.46	0.71	cm
p*	1	2	--

$$\frac{P_{crystal}}{P_{vapor}} = 2 \times \frac{9 \times 10^7}{5 \times 10^5} = 360$$

*p = polarization factor

Nd:BeI LASER

ETALON

SPAT. FILTER
+
TELESCOPE

O.P.O.   F₁ DOUBLER

FILM F₃ CELL OBJECT

F₂

2.94μ

0.4558μ

1.079μ

TELESCOPE

F₁ : FILTER FOR 1.079μ
F₂ : FILTER FOR 0.54μ, 0.66μ
F₃ : FILTER FOR 1.079μ
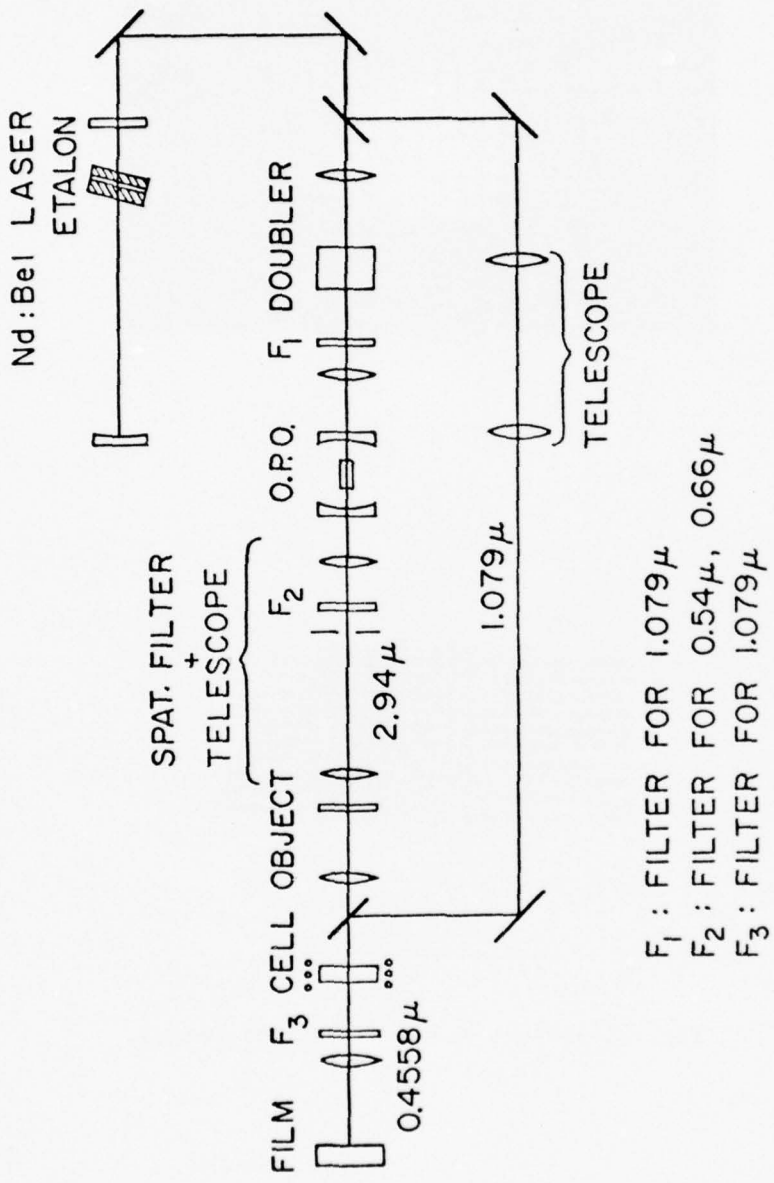
Fig. 12--Experimental set-up for IR up-conversion in cesium.
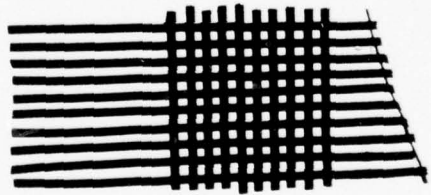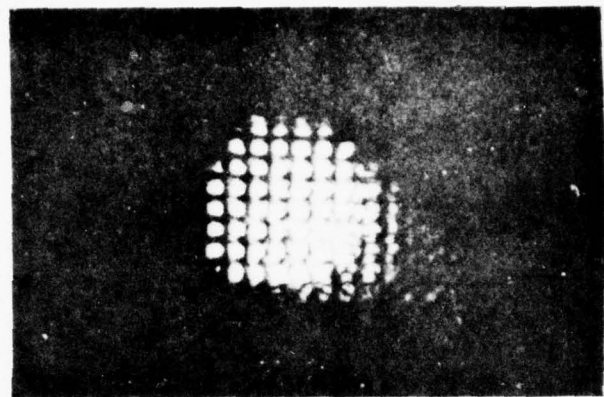
Fig. 13--Object and up-converted image.
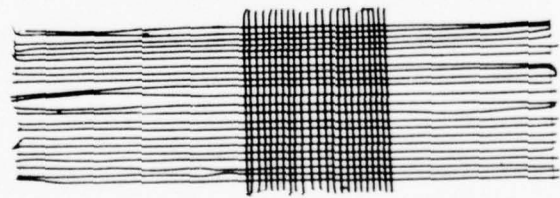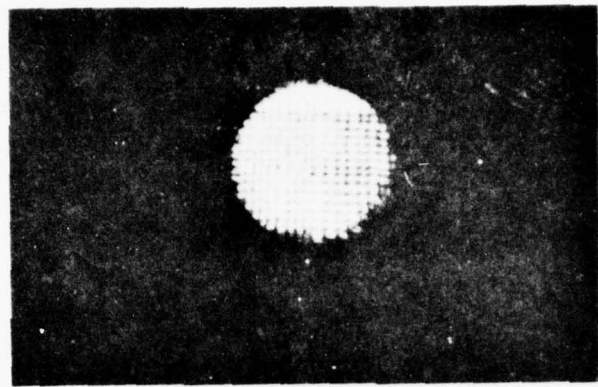
Fig. 14--Object and up-converted image.
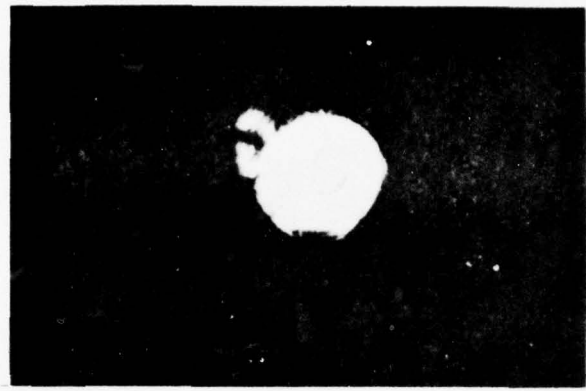
Fig. 15--Object and up-converted image.

of about 0.1 cm^2, and used as the pump of the up-converter. The pump

and IR beams were combined using a high reflector for 1.06 μ radiation.

High speed polaroid film (3000 ASA) was used to record the images. The

shutter of the camera was opened for 1/125 sec, and provided a short

circuit that was used to trigger the laser. A blue filter was put in

front of the camera to black out most of the light of the laser flash-

lamp.

b.   The images

The cell consisted of two sapphire windows (manufactured by EIMAC),

heli-arced inside two Varian flanges with a distance between them of

about 2 mm (Fig. 16). The corresponding solid angle given by $\pi\lambda_i/L$

is equal to 4.6×10^{-3} steradians, and the area of the object "seen"

by the up-converter, given by $\Delta\Omega_u \times f^2$, is equal to 1.85 cm^2. The

area of the pump beam was 0.1 cm^2, and thus the theoretical resolution

was:

$$R = \frac{A_p/2 \times \Delta\Omega_u}{\lambda_i^2} \simeq 2670$$

Figures 13 to 15 show photographs of three objects and the correspond-

ing images. Note that all the images are clearly resolved, also the

second one, which shows about 1000 rectangles. The uniformity of the

images is not very good, but this is most likely related to imperfect

filtering of the illuminating IR beam, and to imperfections in the

- 143 -
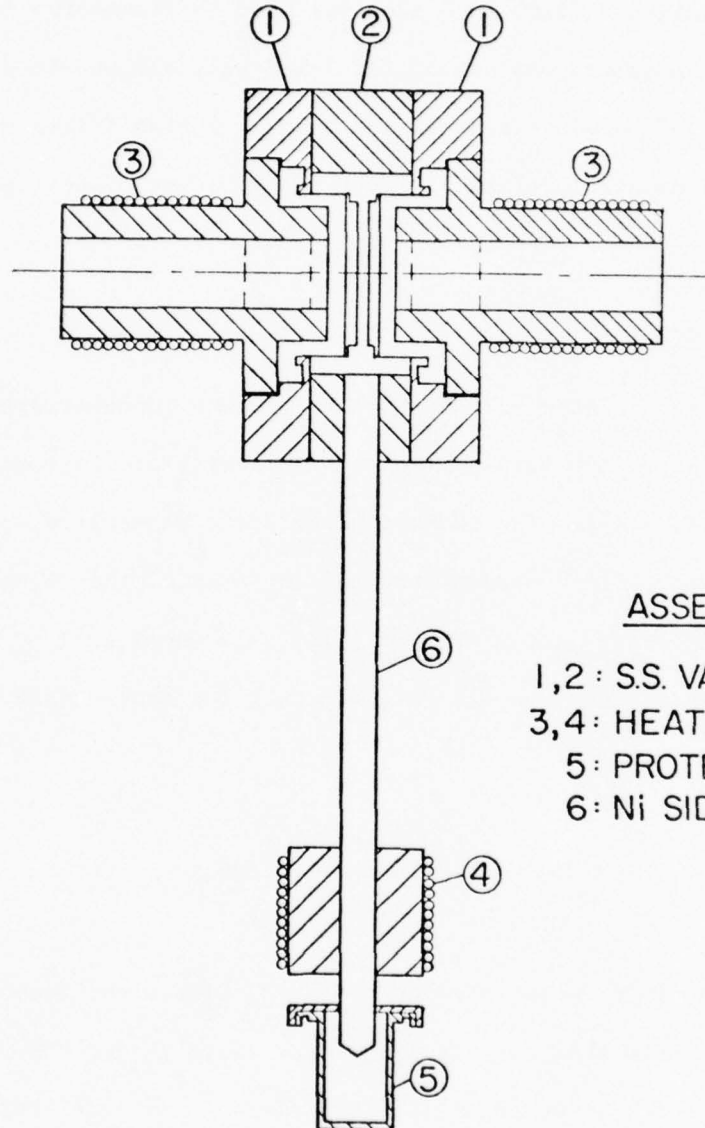
ASSEMBLED CELL

1,2 : S.S. VARIAN FLANGES
3,4 : HEATER
   5 : PROTECTION CAP
   6 : Ni SIDE – ARM

Fig. 16--Cell used for image up-conversion.

optics (filters, etc.). We were not able to measure the efficiency accurately during this experiment (see the next section), but it was roughly 20% (power), for a pump power of about 10 kW, and a number density of 1.4×10^{17} cm^{-3}. Figure 17 shows a photograph of the cell.

2. Efficiency Measurements

Because of problems with the imaging cell, the efficiency measurements were done in a small heat pipe. Since the cell was not used in the heat pipe mode, however, there is some uncertainty as to what N and L to use in the theoretical expression for the efficiency. Ideally, one would like to measure the quantity $\int N dz$, since the efficiency is proportional to the square of this quantity. What one can measure instead is $\int N^2 dz$. This can be done by shining a white light source through the cell and measuring the width of one of the lines of the 6p doublet. For a Lorentzian cross section, one can easily show:

$$(\text{F.W.H.M.})^2 = \left(\frac{4}{\ln 2}\right) \times \frac{\eta_0 \omega_{10} \mu_{01}^2}{2\hbar} \times \int \gamma N dz \qquad (3.97)$$

For the upper line of the 6p doublet, $\gamma = 2.86 \times 10^{-24} \times N$, [19] and:

$$\int N^2 dz = 5.6 \times 10^{39} \times (\text{F.W.H.M.})^2 \qquad (3.98)$$

where the F.W.H.M. is in [cm^{-1}]. If a rectangular profile is assumed for the number density, with a length equal to the length of the heater,

- 145 -
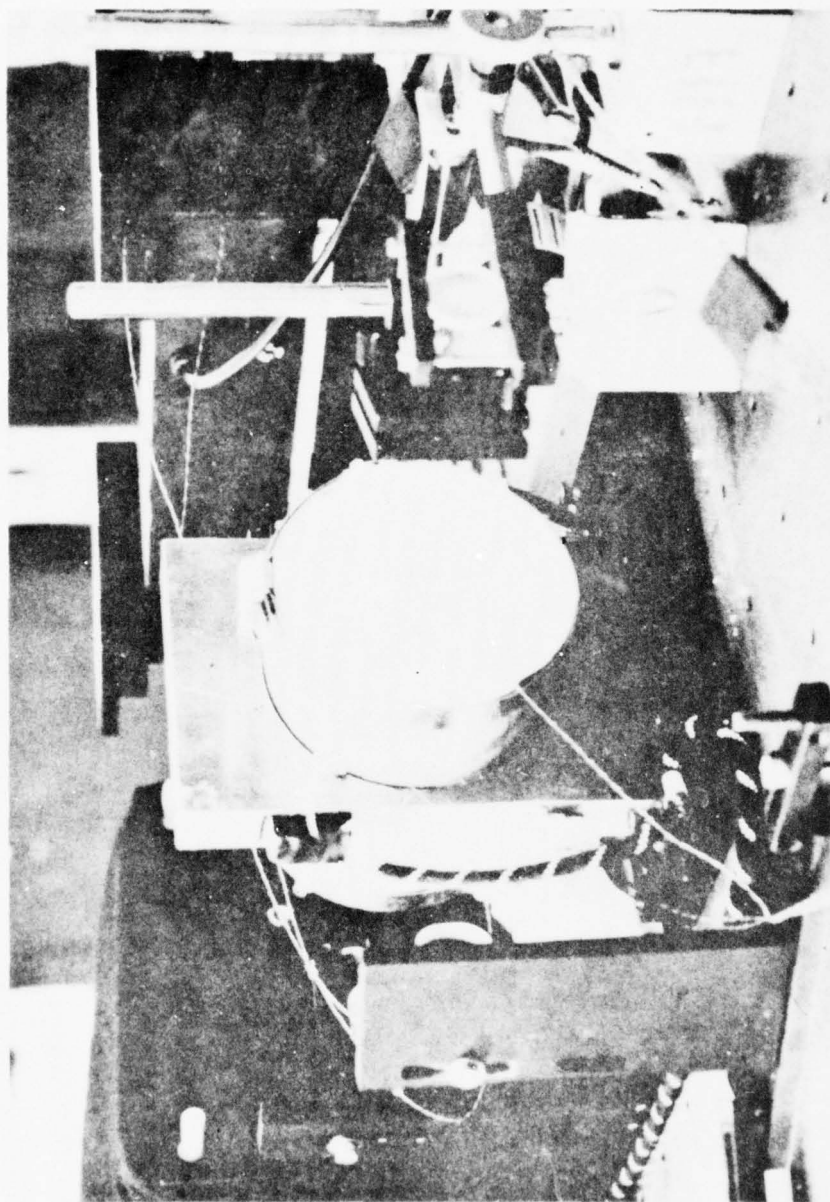
Fig. 17--Photograph of the cell used for the imaging experiments.

the number density found this way is consistent with the one found from
the temperature of the outside wall, if a temperature drop is assumed
across the wall of a little less than ten degrees. The zone is, of
course, not exactly rectangular, and probably somewhat shorter than
the length of the heater. The value of $\left(\int Ndz\right)^2$ was then approximated
by $L \times \int N^2 dz$. The wavelength of the up-converted radiation was mea-
sured with a 1 m Spex spectrometer. A detuning of about 9 cm^{-1} from
the $7p\,^2P_{3/2}$ level was found. Theoretically, with no atoms in the 7s
level, it should have been 16.3 cm^{-1}. If one calculates the fraction
f of atoms in the 7s level, one finds an average value $f_{av} \simeq 0.54$,
while at the end of the pulse $f \simeq 1.0$. Thus the measured detuning
is in good agreement with the predicted value, found from

$$\Delta\omega_{3_{Ph.match}} = 16.3 - 9.7 \times f \quad [cm^{-1}] \qquad (3.25)$$

An additional fact to remember in relation to this detuning is that the
IR wavelength was selected for maximum blue. As the IR moves away from
the phasematching value, closer to resonance, the efficiency will drop
because of the sinc dependence, but it will increase because of the
$\Delta\omega_3^2$ factor. One can check numerically, however, that this shift is
much smaller than the observed one.

The efficiency was measured using a pyroelectric detector. To mea-
sure the IR, the pump beam was blacked before entering the cell, and no

TABLE VI

EXPERIMENTAL PARAMETERS FOR $2.94\ \mu$ UP-CONVERSION IN CESIUM

Nd:BeL pump

Wavelength (vacuum)	$1.0790\ \mu$
Power	8 kW
Pulselength	100 nsec
Area	$0.1\ cm^2$
Intensity	$0.8 \times 10^5\ W/cm^2$

Infrared radiation

Wavelength	$2.94\ \mu$
Area	$0.01\ cm^2$

Up-Converted radiation

Wavelength (vacuum)	$4558.3\ \overset{o}{A}$
Detuning from $7p\ ^2P_{3/2}$	$9\ cm^{-1}$

Cell parameters

Temperature	290^oC
Number density	$2.9 \times 10^{16}\ cm^{-3}$
Length of zone	2 cm
$\int N^2 dz$ (absorption)	$9.2 \times 10^{42}\ m^{-5}$

Measured	$\mathcal{E}_{power}$	:	86%
Calculated	$\mathcal{E}_{power}$	:	250%

filters had to be used. To measure the generated blue, filters were inserted to remove the transmitted pump and the IR (H.R. at 1.06 μ, 1-58 and 5-61 Corning filters).

Table VI shows a set of experimental parameters, together with the corresponding measured and calculated efficiency. The agreement between theory and experiment can be considered to be very good. Part of the discrepancy could possibly be explained by an imperfect overlap of the pump and the IR beams, but even without that, the number of theoretical and experimental ingredients of this experiment was large enough to make such a factor acceptable.

CHAPTER IV

HARMONIC GENERATION AT HIGH FIELD STRENGTHS.

FREQUENCY SHIFTS AND SATURATION PHENOMENA[*]

A.   INTRODUCTION

It is known[26-29] that at high field strengths the resonances of
interactions between atoms and electromagnetic fields show intensity
dependent shifts. In two recent papers[30,31] Harris discussed harmonic
generation and mixing processes which may be used for the generation
of coherent radiation in the $100 \overset{\circ}{A}$ region. These processes require
quite high intensities and in this chapter we discuss how his results
are modified when frequency shifts are taken into account. We proceed
by solving the density matrix equations for a collection of atoms in-
teracting with two electromagnetic fields: a strong incident pump
field at frequency ω and a much weaker generated field at frequency
$n\omega$ (in what follows we limit ourselves to harmonic generation, exten-
sion of the results to mixing processes is straightforward). The rea-
son why frequency shifts will appear in our results is that we do not

_____

[*]Reproduced from Ref. 38.

- 150 -

solve the equations independently, as is usually done in the calcula-
tion of nonlinear susceptibilities (e.g., Ref. 32), but consider feed-
back of the higher orders in the perturbation sequence to the lower
orders. We demonstrate the technique with the example of third har-
monic generation in a four-level system. Generalized closed form ex-
pressions for generated dipole moment, absorption probabilities and
coherence length are also presented.

B. DERIVATION OF FREQUENCY SHIFTS

The off-diagonal elements of the density matrix between the ground
level and some other level, for a four-level system, satisfy the fol-
lowing equations (the levels are labeled from 0 to 3):

$$\dot{\rho}_{01} = i\omega_{10}\rho_{01} + \frac{i}{\hbar}(\rho_{00}H'_{01} + \rho_{02}H'_{21}) - \frac{\rho_{01}}{T_{01}}$$

$$\dot{\rho}_{02} = i\omega_{20}\rho_{02} + \frac{i}{\hbar}(\rho_{01}H'_{12} + \rho_{03}H'_{32}) - \frac{\rho_{02}}{T_{02}}$$

$$\dot{\rho}_{03} = i\omega_{30}\rho_{03} + \frac{i}{\hbar}(\rho_{02}H'_{23} + \rho_{00}H'_{03}) - \frac{\rho_{03}}{T_{03}} \qquad (4.1)$$

where

$$\omega_{i0} = (E_i - E_0)/\hbar$$

$$H'_{ij} = -\mu_{ij} \times (\text{electric field})$$

$$T_{0i} = \text{atomic dephasing time for the } 0 \to i \text{ transition}$$

- 151 -

We assume that the fields are limited to a value such that the change
of the population of the ground level due to absorption to other levels
during the time the fields are on is small, i.e., ρ_{00} is essentially
constant (this assumption is discussed in Section C for various kinds
of absorption processes). Other on-diagonal elements and off-diagonal
elements between levels neither of which is the ground level are left
out because for the processes considered they are usually far from
resonance and hence have little effect. The fields are taken to be
sinusoidal:

$$E(t;\omega) = E \frac{e^{i\omega t}}{2} + c.c.$$

$$E'(t;3\omega) = E' \frac{e^{i3\omega t}}{2} + c.c. \qquad (4.2)$$

The solution to the set of equations (4.1) can then be written as:

$$\rho_{0k}(t;k\omega) = \rho_{0k} e^{ik\omega t} \qquad k = 1,2,3 \qquad (4.3)$$

In the transient regime the ρ_{0k} are functions of time, slowly varying
compared to the period of the applied field. We are interested however
in interaction times which are long compared to the decay times of these
transients. If, as is explained in Section C, the power density is lim-
ited such that the change of the population of the ground state due to
absorption processes is small during the interaction time, then the set

- 152 -

of equations (4.1) can be solved treating ρ_{00} as a constant (quasi-static approach). The quantities ρ_{0k} will however be modulated by a very slowly varying envelope due to the changing occupation of the ground state. Substitution of (4.2) and (4.3) into (4.1) yields, by harmonic balance, the following system of linear algebraic equations for the case where the generated field is much smaller than the pump field:

$$(\Delta\omega_1 + i/T_{01})\ \rho_{01} = \alpha_{21}\rho_{02} + \alpha_{01}\rho_{00}$$

$$(\Delta\omega_2 + i/T_{02})\ \rho_{02} = \alpha_{12}\rho_{01} + \alpha_{32}\rho_{03}$$

$$(\Delta\omega_3 + i/T_{03})\ \rho_{03} = \alpha_{23}\rho_{02} + \alpha'_{03}\rho_{00} \qquad (4.4)$$

where

$$\Delta\omega_j = \omega_{j0} - j\omega$$

$$\alpha_{ij} = \mu_{ij}E/2\hbar \qquad i,j = 1,2,3$$

$$\alpha'_{ij} = \mu_{ij}E'/2\hbar$$

The solution of these equations is discussed in Section C. The resonances of this third-harmonic process are defined by setting the real part of the determinant of the set of equations (4.4) equal to zero,

i.e., $D_r = 0$, where

$$D_r = \Delta\omega_1 \Delta\omega_2 \Delta\omega_3 - |\alpha_{12}|^2 \Delta\omega_3 - |\alpha_{23}|^2 \Delta\omega_1 \qquad (4.5a)$$

The zeros of this polynomial in ω are intensity dependent. For small intensities D_r reduces to $D_r = \Delta\omega_1 \Delta\omega_2 \Delta\omega_3$, which is the well-known form of the denominator of the third order nonlinear susceptibility. The intensity dependence of the widths of the resonances is found from the imaginary part of the determinant, i.e., D_i , where

$$D_i = \frac{\Delta\omega_1 \Delta\omega_3}{T_{02}} + \frac{\Delta\omega_1 \Delta\omega_2 - |\alpha_{12}|^2}{T_{03}} \qquad (4.5b)$$

Although the intensity dependence of the widths of the resonances of the physical quantities studied in Section C could be calculated from the set of equations (4.4), we will not study it in detail in this chapter. This dependence was taken into account however in the example discussed in Section D.

C. CONVERSION EFFICIENCY OF HARMONIC GENERATION PROCESSES
    IN THE PRESENCE OF FREQUENCY SHIFTS

In earlier work[30] Harris has derived an expression for the conversion efficiency of a nth harmonic generation process where the generated frequency comes close to a single photon allowed transition. He shows that if the coherence length is dominated by the nearby

transition and if the pump power is limited by n-photon absorption to that level, the conversion efficiency is given by:

$$\mathcal{E} = \frac{2\hbar n\omega}{\sigma_{On}} \frac{1}{J_i/A} \tag{4.6}$$

where

σ_{On} = the single-photon cross section for absorption to the nth atomic level (this level is by definition the level closest to the generated frequency)

J_i/A = the energy density in the incident pulse

To obtain this result the pump power density is chosen such that the product of the absorption probability per second and the pulselength is 0.5, in which case about 70% of the atoms are still in the ground state at the end of the interaction (this limit is somewhat arbitrary, it is used here to be consistent with Refs. 30 and 31).

Using the solution of the system of equations (4.4), we find the following expressions for generated dipole moment at frequency 3ω, single-photon absorption probability per second to level 3, three-photon absorption probability per second to level 3, and coherence length:

$$\langle \mu(t;3\omega) \rangle = \frac{2\alpha_{01}\alpha_{12}\alpha_{23}\mu_{30}}{D_r^2 + D_i^2} (D_r \cos 3\omega t + D_i \sin 3\omega t) \tag{4.7}$$

- 155 -

$$W^{(1)} = \frac{2}{T_{03}} |\alpha'_{03}|^2 \left(\frac{\Delta w_1 \Delta w_2 - |\alpha_{12}|^2}{D_r} \right)^2 \qquad (4.8)$$

$$W^{(3)} = \frac{2}{T_{03}} \frac{|\alpha_{01}|^2 \, |\alpha_{12}|^2 \, |\alpha_{23}|^2}{D_r^2 + D_i^2} \qquad (4.9)$$

$$L_c = \frac{h}{3 w \eta_0 |\mu_{03}|^2 N} \cdot \frac{D_r}{\Delta w_1 \Delta w_2 - |\alpha_{12}|^2} \qquad (4.10)$$

where

$$N = \text{the density of atoms}$$
$$\eta_0 = 377 \text{ ohm}$$

For small field strengths these expressions reduce to those calculated without considering feedback effects. Substitution of (4.7) to (4.10) in the expression for the power density generated in one coherence length,

$$\frac{P(3w)}{A} = \frac{\eta_0 (3w)^2 \, |\langle \mu(3w) \rangle|^2 \, (NL_c)^2}{2\pi^2} \qquad (4.11)$$

together with the requirement $W^{(3)} \times (\text{pulselength}) = 0.5$, yields an expression for the efficiency of the process which is the same as

- 156 -

in the small field case, i.e.,

$$\mathcal{E} = \frac{2\hbar \cdot 3\omega}{\sigma_{03}} \cdot \frac{1}{J_i/A}$$

where σ_{03} is now defined, however, in terms of a modified detuning from level 3:

$$\sigma_{03} = \frac{3\omega\eta_0}{\hbar} \cdot \frac{|\mu_{03}|^2}{T_{03}} \cdot \left(\frac{1}{\Delta'\omega_3}\right)^2 \qquad (4.12)$$

where

$$\Delta'\omega_3 = \Delta\omega_3 - \frac{|\alpha_{23}|^2 \Delta\omega_1}{\Delta\omega_1 \Delta\omega_2 - |\alpha_{12}|^2} = \frac{D_r}{\Delta\omega_1 \Delta\omega_2 - |\alpha_{12}|^2}$$

So that the earlier result is correct if one replaces the detuning from the third level in the expression for the single photon cross section by a modified detuning which depends on the intensity of the applied field.

Harris has also shown[31] that the conversion efficiency of a nth harmonic generation process (or n-photon mixing), where $n - 1$ photons are resonant with a single-photon non-allowed transition to the ground state, such that the power density of the pump is limited by $(n - 1)$ photon absorption to that level, is given by:

$$\mathcal{E} = \frac{T_{02}}{T_1} \frac{|\mu_{n-1,n}|^2}{|\mu_{0,n}|^2} \qquad (4.13)$$

- 157 -

where T_1 is either the pulselength or the lifetime of the absorbing level, whichever is shorter.

Using the solution of the set of equations (4.4), and taking into account the fact that the sum of two pump photons can come close to level 2 such that the linewidth $2/T_{02}$ can no longer be neglected, the two-photon absorption probability per second is given by

$$W^{(2)} = \frac{2}{T_{02}} |\alpha_{01}|^2 |\alpha_{12}|^2 \frac{\Delta^2 \omega_3}{D_r^2 + D_i^2} \tag{4.14}$$

Substitution of Eqs. (4.7), (4.14), and (4.10) into Eq. (4.11), together with the requirement $W^{(2)} \times T_1 = 0.5$, yields the following expression for the efficiency:

$$\mathcal{E} = \frac{T_{02}}{T_1} \frac{|\mu_{23}|^2}{|\mu_{03}|^2} \left(1 - \frac{|\alpha_{23}|^2 \Delta \omega_1}{\Delta \omega_1 \Delta \omega_2 \Delta \omega_3 - |\alpha_{12}|^2 \Delta \omega_3} \right) \tag{4.15}$$

For small field strengths the factor in brackets reduces to 1. If one limits the shifts to values which are small compared to the atomic level spacings, the allowed power densities are usually smaller than those found from the limitation on multiphoton absorption. At such lower power densities the factor in brackets reduces to 1, but the efficienty of the process is reduced by another factor which is given by:

$$\left(\frac{\text{power density applied}}{\text{power density as limited by (n-1) photon absorption}} \right)^{n-1}$$

D.   EXAMPLE

As an example we consider a five-photon mixing process in Li^+:

$$4 \times 816 \text{ Å} + 6745 \text{ Å} \rightarrow 198 \text{ Å}$$
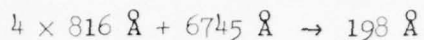
The path used is: $1s^2 \rightarrow 1s2p \rightarrow 1s^2 \rightarrow 1s2p \rightarrow 1s2s \rightarrow 1s2p$. Level
positions and oscillator strengths were taken respectively from Refs.
33 and 34. The pump frequencies were chosen such that the detuning
from the unshifted four-photon resonance was 1250 cm^{-1} (below the
resonance) while the detuning from the unshifted five-photon reso-
nance was 3750 cm^{-1} (above the resonance). The laser pulselength was
assumed to be 30 picoseconds and the linewidth 1 cm^{-1}. Figure 18 shows
how at a power density of 2×10^{14} W/cm^2 the system becomes four-photon
resonant and also how, at higher power densities, the efficiency satu-
rates; here the efficiency was defined consistent with Ref. 30 as the
ratio of the generated power and the power at 6745 Å. Figure 18 was
computer generated and takes into account the intensity dependent
widths. At the high intensities involved, five-photon ionization by
the pump field at 816 Å has to be considered. From Refs. 36 and 37
an approximate value for the ionization probability can be calculated.
If the expressions in Refs. 36 and 37 are adjusted for shifts, a lim-
iting intensity of about 2×10^{14} W/cm^2 is found, i.e., if a pulse
with this intensity is applied, then about 50% of the Li^+ ions will
be ionized during the pulse, and also the broadening of the four-photon
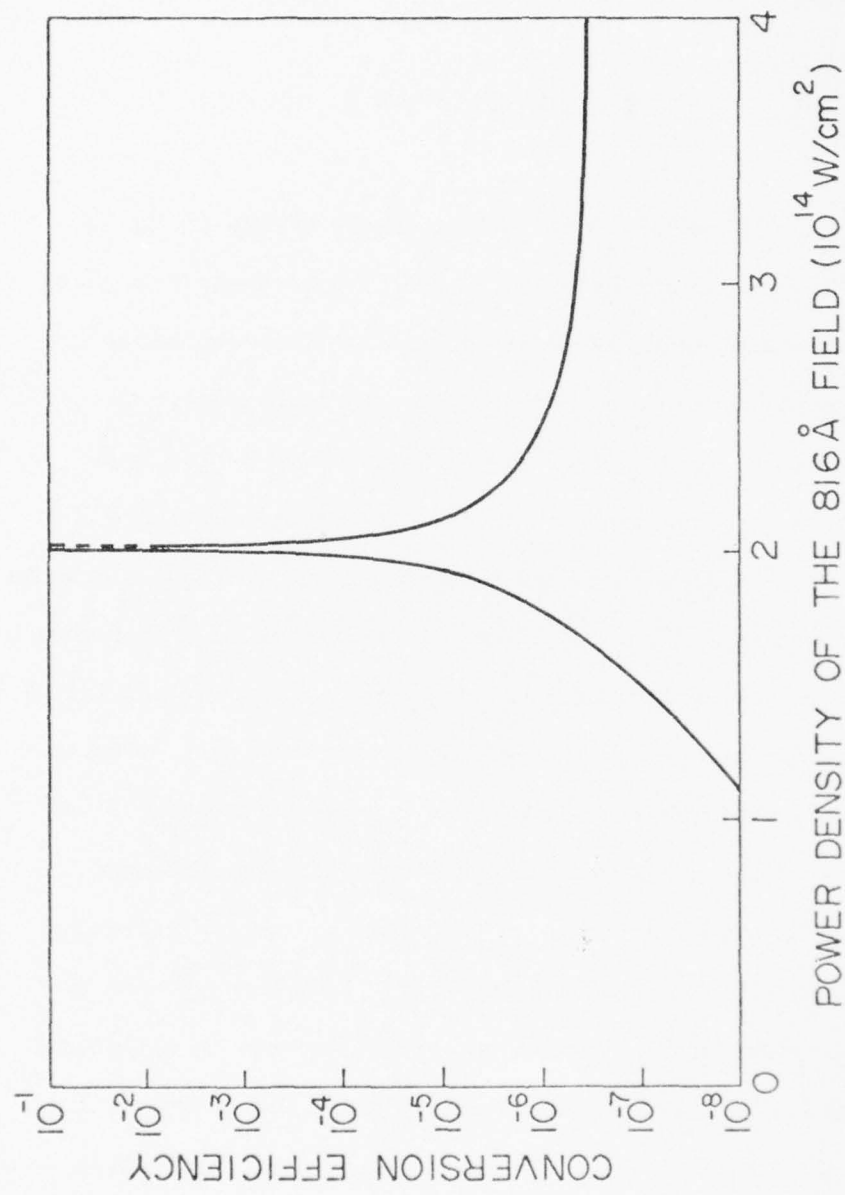
Fig. 18--Conversion efficiency for generation of 198 Å radiation using a five-photon mixing process.

resonance due to ionization will be comparable to the laser linewidth. It should be noted that if shifts were not taken into account, the limiting power density (as calculated by the formulae of Bebb and Gold in Ref. 36) would be about a factor of 17 higher. At the intensity of 2×10^{14} W/cm^2 the four-photon absorption is well below the maximum allowed value. To keep the coherence length short (about 1 cm at a pressure of a few torrs), the power density of the 6745 Å field has to be limited to about one part in ten thousand of the density of the 816 Å field. It is also indicated in Fig. 18 that in certain regions of the intensity the dispersion of the medium can change sign. This is important because harmonic generation with a focused Gaussian beam in an infinite positively dispersive medium is impossible.[35] It should also be noted that the width of the resonance in Fig. 18 is quite small, and hence a stable laser is required, typically around 1%.

We conclude that, taking into account frequency shifts, harmonic generation is a promising means of generating wavelengths in the VUV and soft x-ray spectral region. The most important consequences of frequency shifts are that the pump laser has to be tuned to a wavelength different from that required to bring the system into resonance at small field strengths, that the conversion efficiency may saturate, and that the dispersion of the medium may change sign.

E.   GENERALIZATION TO n^{th} ORDER PROCESSES

Using the technique explained in Section B it can be shown that for a nth harmonic process (or n-photon mixing), the generated dipole

moment at frequency $n\omega$, the single-photon absorption probability per second to the nth level, the multiphoton absorption probabilities per second to the $(n-1)^{th}$ and n^{th} level, and the coherence length, are given by:

$$\langle \mu(n\omega) \rangle = 2\mu_{n0} \prod_{k=1}^{n} \frac{\alpha_{k-1,k}}{D_k}$$

$$W^{(1)} = \frac{2}{T_{0n}} \frac{|\alpha'_{0n}|^2}{D_n^2}$$

$$W^{(n-1)} = \frac{2}{T_{0n-1}} \left(\prod_{k=1}^{n-2} \left| \frac{\alpha_{k-1,k}}{D_k} \right|^2 \right) \frac{|\alpha_{n-2,n-1}|^2}{\{D_{n-1} - [|\alpha_{n-1,n}|^2/(\omega_{n0} - n\omega)]\}^2}$$

$$W^{(n)} = \frac{2}{T_{0n}} \prod_{k=1}^{n} \frac{|\alpha_{k-1,k}|^2}{D_k^2}$$

$$NL_c = \frac{h}{n\omega\eta_0|\mu_{0n}|^2} D_n$$

The efficiencies for the processes discussed in Section C are:

$$\underline{\text{Case A:}}^{30}$$

$$\mathcal{E} = \frac{2\hbar n\omega}{\sigma_{0n}} \cdot \frac{1}{J_i/A}$$

where σ_{On} is defined in terms of the single-photon absorption probability per second to level n .

<div align="center"><u>Case B</u>:[31]</div>

$$\mathcal{E} = \frac{T_{On-1}}{T_1} \frac{|\mu_{n-1,n}|^2}{|\mu_{0,n}|^2} \left\{ 1 - \frac{[|\alpha_{n-1,n}|^2/(\omega_{nO} - n\omega)]}{D_{n-1}} \right\}$$

In these expressions D_k is defined by:

$$D_k = \omega_{kO} - k\omega - \frac{|\alpha_{k-1,k}|^2}{D_{k-1}} \qquad k \neq 1$$

$$D_1 = \omega_{10} - \omega$$

Note: in all these expressions the *linewidth* was neglected.

APPENDIX A

PROGRAMS SEATPR AND SEATPR2

These programs calculate respectively the efficiency of two-photon-resonant frequency converters versus detuning from the resonance, and the dependence of the on-resonance efficiency on the pressure broadened linewidth. They perform a numerical evaluation of (2.25), within an arbitrary constant. As they are, they assume a Gaussian power spectrum for the laser, but this could easily be generalized to any spectrum, at a point in the programs that is clearly indicated. The input data are:

For SEATPR

- laser linewidth (F.W.H.M.)

- mode spacing

- Doppler width (F.W.H.M.)

- atomic linewidth (F.W.H.M.)

- maximum detuning $(\omega_{20} - 2\omega_0)$

- increment of $(\omega_{20} - 2\omega_0)$

For SEATPR2

- laser linewidth (F.W.H.M.)

- mode spacing

- Doppler width (F.W.H.M.)

- maximum atomic linewidth (F.W.H.M.)

- detuning $(\omega_{20} - 2\omega_0)$

- increment of the atomic linewidth

The programs are listed on the following pages.

```
//SEATPR JOB 'N150,240,1.,1','STAPPAERTS'
**SERVICE CLASS=Q EXEC=S
// EXEC WATFIV
//GO.SYSIN DD *
$WATFIV
C************************* START OF COMERR ***************************************
      COMPLEX FUNCTION COMERR*16 (Z)
C
C     COMPUTES THE COMPLEX ERROR FUNCTION
C     W(Z) = EXP(- Z * Z) * ERFC( -I * Z),
C
C     FOR ARGUMENTS Z IN THE COMPLEX PLANE.
C     HERE ERFC (ZETA) = COMPLEMENTARY ERROR FUNCTION =
C            2 / SQRT(PI) * INTEGRAL (FROM ZETA TO INFINITY) OF
C            EXP(-T * T) DT.
C
C     AN EQUIVALENT FORMULATION (DAWSON'S INTEGRAL) IS
C            EXP(-Z*Z) * (1 + (2 I / SQRT(PI)) * INTEGRAL (FROM 0 TO Z)
C            EXP(T*T) DT.
C
C     STILL ANOTHER EQUIVALENT FORMULATION FOR IM(Z) > 0 IS
C            I / PI * INTEGRAL (FROM MINUS INFINITY TO INFINITY)
C            EXP (-T * T) / (Z - T) DT.
C
C     THIS FUNCTION IS VERY WIDELY USED IN A NUMBER OF FIELDS, E.G.,
C     PLASMA PHYSICS, WAVE PROPAGATION, ASTRONOMY, AND IT MASQUERADES
C     UNDER A VARIETY OF NAMES:  THE VOIGT FUNCTION, DAWSON'S
C     INTEGRAL, THE PLASMA DISPERSION FUNCTION, THE FRIED-CONTE
C     FUNCTION, THE HILBERT TRANSFORM OF THE GAUSSIAN, ETC.  THIS
C     PROGRAM IS A TRANSLATION OF GACH ALGORITHM 363 BY W. GAUTSCHI,
C     EXTENDED TO THE WHOLE COMPLEX PLANE.
C
C     SEPARATE SUBROUTINES ARE SUPPLIED BELOW FOR THE COMPLEX
C     COMPLEMENTARY ERROR FUNCTION, AND FOR THE PLASMA
C     DISPERSION FUNCTION.
C
C     DESCRIPTION OF PARAMETERS
C
C     Z     COMPLEX DOUBLE PRECISION ARGUMENT
C     COMERR  MUST BE TYPED COMPLEX*16 IN CALLING PROGRAM
```

```
C
C
C    SUBROUTINES REQUIRED
C
C      DABS, DCMPLX, DCOS, DEXP, DIMAG, DREAL, DSIN, DSQRT, WZERR.
C      PROBLEMS ARISE WITH DREAL AND DIMAG, SINCE THE ONLY IBM
C      COMPILER WHICH SUPPLIES THEM IS H EXTENDED.  ON CAMPUS, THESE
C      ARE DIRECTLY CALLABLE FROM FORTRAN G AND H.  FOR USERS OF
C      WATFIV WE HAVE SUPPLIED DREAL AND DIMAG SUBPROGRAMS.  USERS OF
C      G AND H MAY WISH TO REMOVE THE DREAL AND DIMAG CODE.
C      THE ERROR MONITORING ROUTINE WZERR IS SUPPLIED.
C
C    ERROR CONDITIONS
C
C      FOR ARGUMENTS Z = R*EXP(I THETA) IN THE FIRST TWO QUADRANTS,
C      THE FUNCTION IS ALWAYS EVALUATED SUCCESSFULLY.  HOWEVER, FOR
C      ARGUMENTS IN THE WEDGE   -3 PI/4 < THETA < -PI/4, EXPONENTIAL
C      OVERFLOW CAN OCCUR.  (FOR EXAMPLE, ON THE 360, Z = -14*I WILL
C      CAUSE IT).  PROBLEMS CAN ALSO OCCUR IN THE LOWER HALF PLANE
C      WHEN THE ARGUMENT OF SINE OR COSINE BECOMES TOO LARGE, BUT THIS
C      IS FAR LESS COMMON, AND REQUIRES THAT THE PRODUCT OF RE(Z) AND
C      IM(Z) BE OF THE ORDER OF 10 ** 15.  IN CASE OF SUCH ERRORS,
C      ROUTINE WZERR IS CALLED, WHICH PRINTS RE(Z), AND IM(Z) ON THE
C      STANDARD OUTPUT UNIT.  A FUNCTION VALUE IS RETURNED TO THE
C      CALLING PROGRAM, BUT IT WILL BE INCORRECT.
C
C    METHOD
C
C      THE COMPLEX PLANE IS DIVIDED INTO TWO REGIONS:   THE INTERIOR OF
C      THE RECTANGLE ABS(X) < 5.33, ABS(Y) < 4.29, AND ITS EXTERIOR.
C      IN THE EXTERIOR, GAUSS-HERMITE QUADRATURE (OF THE LAST
C      EQUIVALENT FUNCTIONAL FORM ABOVE), OR, EQUIVALENTLY, THE
C      LAPLACE CONTINUED FRACTION IS USED.  IN THE INTERIOR, FOR Z = X
C      + I Y IN THE FIRST QUADRANT, THE FUNCTION IS OBTAINED BY A
C      TAYLOR EXPANSION ABOUT X + I*(Y + H), WHERE H > 0 IS SUITABLY
C      CHOSEN.  FURTHER DETAILS CAN BE FOUND IN REF. (1).
C
C    FOR REFERENCE, SEE
C      1)  GAUTSCHI, WALTER, EFFICIENT COMPUTATION OF THE COMPLEX
C          ERROR FUNCTION, SIAM. J. NUM. ANAL. 7 (1970), PP. 187-
C          198.
C
```

```
C     2)  -----, ALGORITHM 363, COMPLEX ERROR FUNCTION W(Z), COMM.
C         ASSOC. COMP. MACH 12 (1969), P. 635.
C     3)  -----, ERROR FUNCTION AND FRESNEL INTEGRALS, IN
C         ABRAMOWITZ AND STEGUN, HANDBOOK OF MATHEMATICAL
C         FUNCTIONS, U.S. GOVT. PRTG. OFF., PP. 297-299.
C     4)  KOLBIG, K. S., CERTIFICATION OF ALGORITHM 363, COMM. ACM 15
C         (1972), 465-466.
C     5)  FRIED AND CONTE, THE PLASMA DISPERSION FUNCTION,
C         ACADEMIC PRESS, NEW YORK, 1961.
C     6)  FADDE'EVA AND TARENT'EV, TABLES OF THE PROBABILITY
C         INTEGRAL FOR COMPLEX ARGUMENT, PERGAMON PRESS, 1961.
C
C     TRANSLATED BY
C                      JOHN BOLSTAD
C                      COMPUTER SCIENCE DEPT., SERRA HOUSE
C                      STANFORD UNIVERSITY
C                      DEC. 21, 1974
C
C     . . . . . . . . . . . . . . . . . . . . . . . . . . . .
      COMPLEX*16 Z, DCMPLX
      DOUBLE PRECISION C, H, H2, LAMBDA, NP1, R1, R2, S, S1, S2,
     X  SINARG, T1, T2, TSOTPI, VR, VI, X, XABS, Y, YABS, EXPARG
      DOUBLE PRECISION DABS, DCOS, DEXP, DIMAG, DREAL, DSIN, DSQRT
      INTEGER CAPN, F, NU
      LOGICAL B
      DATA TSQTPI /1.12837916709551D0/, EXPARG /174.673D0/
      DATA SINARG /-3.537119D15/
C
C         TSOTPI = 2 / SQRT(PI)
C         EXPARG = LARGEST ARGUMENT ACCEPTED BY EXPONENTIAL FCN.
C         SINARG = SMALLEST NEGATIVE ARGUMENT ACCEPTED BY SIN AND
C                  COSINE FUNCTIONS.
C         T = T1 + I T2 IS USED REPEATEDLY AS A TEMPORARY VARIABLE
C                  THROUGHOUT.
C
      X = DREAL(Z)
      Y = DIMAG(Z)
      XABS = DABS(X)
      YABS = DABS(Y)
```

```
C
C
C        COMPUTE W(Z) FOR ARGUMENT IN FIRST QUADRANT

      IF (YABS .GE. 4.29D0 .OR. XABS .GE. 5.33D0) GO TO 3
         S = (1. - YABS/4.29D0) * DSQRT(1. - XABS*XABS/28.41D0)
         H = 1.6D0*S
         H2 = 2.0*H
         CAPN = 6.5D0 + 23.D0*S
         NU = 9.5D0 + 21.D0*S
         LAMBDA = H2 ** CAPN
         GO TO 5

3        H = 0.
         CAPN = 0
         NU = 8
         LAMBDA = 0.

C
C        IN THE FOLLOWING STATEMENT, LAMBDA = 0 COVERS THE UNDER-
C        FLOW CASE WHEN H > 0 IS VERY SMALL.

5     B = (H .EQ. 0.) .OR. (LAMBDA .EQ. 0.)
      R1 = 0.
      R2 = 0.
      S1 = 0.
      S2 = 0.
      S = YABS + H
      N = NU

C
C        FOR N = NU STEP - 1 UNTIL 0 DO
20       NP1 = N + 1
         T1 = S + NP1*R1
         T2 = XABS - NP1*R2
         C = 0.5D0 / (T1*T1 + T2*T2)
         R1 = C*T1
         R2 = C*T2
         IF (H .LE. 0. .OR. N .GT. CAPN) GO TO 25
            T1 = LAMBDA + S1
            S1 = R1*T1 - R2*S2
            S2 = R2*T1 + R1*S2
            LAMBDA = LAMBDA/H2
```

- 169 -

```
25    N = N - 1
      IF (N .GE. 0) GO TO 20
C
C     END OF LOOP;
C
      IF (B) GO TO 45
      T1 = S1
      T2 = S2
      GO TO 50
C
45    T1 = R1
      T2 = R2
C
50    VI = TSQTPI * T2
      IF (YABS .EQ. 0.) GO TO 60
      WR = TSQTPI * T1
      GO TO 65
C
60    WR = DEXP(-XABS*XABS)
C
C     USE SYMMETRY RELATIONS FOR QUADRANTS OTHER THAN THE
C     FIRST:   W(CONJG(Z)) = CONJG(W(-Z)) FOR SECOND QUADRANT,
C     W(-Z) = 2 EXP(-Z*Z) - W(Z) FOR THIRD QUADRANT, AND BOTH
C     RELATIONS FOR THE FOURTH QUADRANT.
C
65    IF (X .GE. 0. .AND. Y .GE. 0.) GO TO 95
      IF (X .LT. 0. .AND. Y .GE. 0.) GO TO 90
C
C     THIRD AND FOURTH QUADRANTS:   COMPUTE T = -Z*Z, AND
C     V = 2 * CEXP(T) - W
C
      T1 = YABS*YABS - XABS*XABS
      T2 = -2.0*XABS*YABS
C
C     ERROR FOR EXPONENTIAL TOO LARGE
C
      IF (T1 .LT. EXPARG) GO TO 70
      CALL WZERR(X, Y, -1)
      GO TO 95
C
C     ERROR - ABS(ARGUMENT) FOR SIN OR COS TOO LARGE
C
70    IF (T2 .GT. SINARG) GO TO 80
```

```
      CALL WZERR(X, Y, -2)
      GO TO 95
C
   80 T1 = 2.0 * DEXP(T1)
      WR = T1 * DCOS(T2) - WR
      WI = T1 * DSIN(T2) - WI
      IF (X .LE. 0.) GO TO 95
C
   90 WI = -WI
   95 COMERR = DCMPLX(WR, WI)
      RETURN
      END
C
C
      COMPLEX FUNCTION FRDCNT*16 (Z)
C
C     COMPUTES THE (FRIED-CONTE) PLASMA DISPERSION FUNCTION
C     F(Z) = 1/ SQRT(PI) * INTEGRAL (FROM -INFINITY TO INFINITY)
C     EXP(- T*T) / (T - Z) DT.
C
C     (THIS FORMULATION, WHICH IS CORRECT FOR IM(Z) > 0, MUST BE
C     MODIFIED FOR IM(Z) < 0.  HOWEVER, THE PROGRAM ACCEPTS ANY
C     ARGUMENT IN THE COMPLEX PLANE.)
C
C     THE METHOD IS TO COMPUTE SQRT(PI) * I * W(Z), WHERE
C     W(Z) = EXP(- Z*Z) * ERFC(-I * Z).  FOR DETAILS, REFER TO
C     SUBROUTINE COMERR, WHICH COMPUTES W(Z).
C
C     DESCRIPTION OF PARAMETERS
C
C     Z     COMPLEX DOUBLE PRECISION ARGUMENT
C     FRDCNT MUST BE TYPED COMPLEX*16 IN CALLING PROGRAM
C
C     SUBROUTINES REQUIRED
C
C     COMERR, DABS, DCMPLX, DCOS, DEXP, DIMAG, DREAL, DSIN, DSQRT,
C     AND WZERR (WHICH IS SUPPLIED).
C
C     ERROR CONDITIONS
```

```fortran
C     SEE DISCUSSION IN SUBROUTINE COMERR
C
C     . . . . . . . . . . . . . . . . . . . . . . . . . . . . . . . . . . . . .
C
      COMPLEX*16 Z, F, COMERR
      COMPLEX*16 DCMPLX
      DOUBLE PRECISION SQRTPI, DIMAG, DREAL
      DATA SQRTPI /1.7724538509055160D0/
C
      F = COMERR(Z)
      FRDCNT = DCMPLX(-SQRTPI * DIMAG(F), SQRTPI * DREAL(F))
      RETURN
      END
C
C
      COMPLEX FUNCTION CDERFC*16 (Z)
C
C     COMPUTES THE COMPLEX COMPLEMENTARY ERROR FUNCTION
C       ERFC(Z) = 2 / SQRT(PI) * INTEGRAL (FROM Z TO INFINITY) OF
C       EXP (-T*T) DT.
C
C     THE METHOD IS TO COMPUTE EXP(-Z*Z) * W(I*Z), WHERE
C       W(ZETA) = EXP(- ZETA*ZETA) * ERFC(-I * ZETA).  FOR DETAILS,
C       REFER TO SUBROUTINE COMERR, WHICH COMPUTES W(ZETA).
C
C     TO COMPUTE ERF(Z):
C
C       TO COMPUTE THE COMPLEX ERROR FUNCTION ERF(Z), SIMPLY
C       COMPUTE 1 - ERFC(Z).
C
C     DESCRIPTION OF PARAMETERS
C
C       Z     COMPLEX DOUBLE PRECISION ARGUMENT
C       CDERFC  MUST BE TYPED COMPLEX*16 IN CALLING PROGRAM
C
C     SUBROUTINES REQUIRED
C
C       COMERR, DABS, DCMPLX, DCOS, DEXP, DIMAG, DREAL, DSIN, DSQRT,
```

```
C      AND VZERR (WHICH IS SUPPLIED).
C
C      ERROR CONDITIONS
C
C         SEE DISCUSSION IN SUBROUTINE COMERR.
C
C      . . . . . . . . . . . . . . . . . . . . . . . . . . . . . . . . .
C
       COMPLEX*16 Z, F, COMERR
       COMPLEX*16 DCMPLX, CDEXP
       DOUBLE PRECISION X, Y, DIMAG, DREAL
C
       F = COMERR(DCMPLX(-DIMAG(Z), DREAL(Z)))
       CDERFC = CDEXP(-Z*Z) * F
       RETURN
       END
C
C
       SUBROUTINE VZERR(X, Y, IER)
C
C      ERROR MONITORING FOR SUBROUTINE COMERR - CALLED FOR OUT-OF-
C      RANGE ARGUMENTS IN DSIN, DCOS, OR DEXP
C
       DOUBLE PRECISION X, Y
       INTEGER IER, IUNIT
       DATA IUNIT /6/
C
  501  FORMAT (/ ' *** EXPONENTIAL OVERFLOW IN COMERR, X = ', 1PE15.7,
      X ' Y =', 1PE15.7 /)
  502  FORMAT (/ ' *** ARGUMENT FOR SIN/COS OUT-OF-RANGE IN COMERR, X =',
      X 1PE15.7, ' Y =', 1PE15.7 /)
C
       IF (IER .EQ. -2) GO TO 10
       WRITE (IUNIT, 501) X, Y
       GO TO 20
C
   10  WRITE (IUNIT, 502) X, Y
C
   20  RETURN
```

```
C
C
C      DOUBLE PRECISION FUNCTION DREAL(Z)
C
C      FIND THE REAL PART OF THE COMPLEX DOUBLE PRECISION NUMBER Z.
C
C      COMPLEX*16 Z, ZZ
       DOUBLE PRECISION X(2)
       EQUIVALENCE (ZZ, X)
C
       ZZ = Z
       DREAL = X(1)
       RETURN
       END
C      DOUBLE PRECISION FUNCTION DIMAG(Z)
C
C      FIND THE IMAGINARY PART OF THE DOUBLE PRECISION COMPLEX NUMBER
C      Z.
C
C      COMPLEX*16 Z, ZZ
       DOUBLE PRECISION X(2)
       EQUIVALENCE (ZZ, X)
C
       ZZ = Z
       DIMAG = X(2)
       RETURN
       END
C ************************ END OF COMERR *****************************************
       REAL LLSWID,LSWID,MODSP
       COMPLEX*16 COMERR,FRDCNT,CDERFC,FRDCN,Z,ZZ
       DOUBLE PRECISION PLASF(2),X(2),FRK,FIK
       EQUIVALENCE (FRDCN,PLASF)
       EQUIVALENCE (ZZ,X)
C ALL THE DATA SHOULD BE ENTERED IN WAVENUMBERS.
C THE SEQUENCE IS:LASER-LW(FWHM),MODE-SPACING,
C DOPPLERWIDTH(FWHM),ATOMIC-LINEWIDTH(FWHM),
C THE MAX.DETUNING FROM THE RESON. OMO2=2*OMO,
C THE INCREMENT OF THE FREQUENCY OMO.
```

- 174 -

```
      READ,LLSWID,MODSP,DDOWID,ATLW,DETMAX,DOMO
      PRINT10,LLSWID,MODSP,DDOWID,ATLW,DETMAX,DOMO
10 FORMAT('1','LASERWIDTH=',F6.3/' ','MODE-SPACING=',
  XF6.3/' ','DOPPLER-WIDTH=',F6.3/' ','ATOMIC-LINEWIDTH=',
  XF6.3/' ','MAX.-DETUNING=',F6.3/' ','INCREMENT OF ',
  X'INPUT-FREQUENCY=',F6.3)
      PRINT20
20 FORMAT('0',15X,'DETUNING',17X,'EFFICIENCY'/'0')
      LSWID=1.2*LLSWID
      DOWID=.4247*DDOWID
      L=INT(LSWID/MODSP)
C CALCULATION OF THE AVERAGE POWER IN THE INCOMING FIELD
C
      PAV=.8862*L
C ********************************************************
C CALCULATION OF THE RESONANCE PROFILE.FOR EACH FREQUENCY
C A SUM OVER K HAS TO BE PERFORMED.FOR GIVEN K AN ADDITIONAL
C SUM OVER N MUST BE DONE.
C
      DET=DETMAX
2 RESPR=0.
      K=-L
C CALCULATION OF FR(K) AND FI(K)
C
3 X(1)=(-DET+K*MODSP)/(1.414*DOWID)
      X(2)=.5*ATLW/(1.414*DOWID)
      Z=ZZ
      FRDCN=FRDCNT(Z)
      FRK=1.77245*PLASF(1)
      FIK=1.77245*PLASF(2)
C
C CALCULATION OF THE CONVOLUTION OF THE POWER SPECTRUM
C FOR GIVEN K
C
      AK=FLOAT(K)
      B=2*(AK/L)*(AK/L)
      GSOK=.6267*L*EXP(-B)
C
C EVALUATION OF THE SUM OVER K
```

```
C         DRESPR=GSQK*(FRK*FRK+FIK*FIK)/(PAV*PAV)
          RESPR=RESPR+DRESPR
          K=K+1
          IF(K.LE.L) GO TO 3
C
C THIS IS THE END OF THE CALCULATION FOR A GIVEN OMO.
C PRINT THE RESULT
C
          PRINT100,DET,RESPR
100 FORMAT(' ',F20.2,20X,E10.3)
C
C NOW INCREMENT THE FREQUENCY OMO
C
          DET=DET-2*DOMO
          IF(DET.GE.(-.1)) GO TO 2
          STOP
          END
$DATA
.1,.005,.03,.01,2.0,.05
/*
```

```fortran
      INTEGER IER, IUNIT
      DATA IUNIT /6/
C
  501 FORMAT (/ ' *** EXPONENTIAL OVERFLOW IN COMERR, X = ', 1PE15.7,
     X ' Y =', 1PE15.7 /)
  502 FORMAT (/ ' *** ARGUMENT FOR SIN/COS OUT-OF-RANGE IN COMERR, X =',
     X 1PE15.7, ' Y =', 1PE15.7 /)
C
      IF (IER .EQ. -2) GO TO 10
      WRITE (IUNIT, 501) X, Y
      GO TO 20
C
   10 WRITE (IUNIT, 502) X, Y
C
   20 RETURN
      END
C
C
C     DOUBLE PRECISION FUNCTION DREAL(Z)
C
C     FIND THE REAL PART OF THE COMPLEX DOUBLE PRECISION NUMBER Z.
C
      COMPLEX*16 Z, ZZ
      DOUBLE PRECISION X(2)
      EQUIVALENCE (ZZ, X)
C
      ZZ = Z
      DREAL = X(1)
      RETURN
      END
C     DOUBLE PRECISION FUNCTION DIMAG(Z)
C
C     FIND THE IMAGINARY PART OF THE DOUBLE PRECISION COMPLEX NUMBER
C     Z.
C
      COMPLEX*16 Z, ZZ
      DOUBLE PRECISION X(2)
      EQUIVALENCE (ZZ, X)
C
```

```
      ZZ = Z
      DIMAG = X(2)
      RETURN
      END
C ****************** END OF COMERR ****************************
      REAL LLSWID,LSWID,MODSP
      COMPLEX*16 COMERR,FRDCNT,CDERFC,FRDCN,Z,ZZ
      DOUBLE PRECISION PLASF(2),X(2),FRK,FIK
      EQUIVALENCE (FRDCN,PLASF)
      EQUIVALENCE (ZZ,X)
C ALL THE DATA SHOULD BE ENTERED IN WAVENUMBERS.
C THE SEQUENCE IS:LASER-LW(FWHM),MODE-SPACING,
C DOPPLERWIDTH(FWHM),MAX ATOMIC-LINEWIDTH(FWHM),
C THE .DETUNING FROM THE RESON. OM02-2*OMO,
C THE INCREMENT OF THE ATOMIC LINEWIDTH
      READ,LLSWID,MODSP,DDOWID,ATLWMX,DET,DATLW
      PRINT10,LLSWID,MODSP,DDOWID,ATLWMX,DET,DATLW
   10 FORMAT('1','LASERWIDTH=',F6.3/' ','MODE-SPACING=',
     XF6.3/' ','DOPPLER-WIDTH=',F6.3/' ','MAX.-ATOMIC-LINEWIDTH=',
     XF6.3/' ','DETUNING=',F6.3/' ','INCREMENT OF ',
     X'ATOMIC LINEWIDTH=',F6.3)
      PRINT20
   20 FORMAT('0',11X,'ATOMIC LINEWIDTH',13X,'EFFICIENCY'/'0')
      LSWID=1.2*LLSWID
      DOWID=.4247*DDOWID
      L=INT(LSWID/MODSP)
C CALCULATION OF THE AVERAGE POWER IN THE INCOMING FIELD
C
      PAV=.8862*L
C *****************************************************
C CALCULATION OF THE RESONANCE PROFILE.FOR EACH FREQUENCY
C A SUM OVER K HAS TO BE PERFORMED.FOR GIVEN K AN ADDITIONAL
C SUM OVER N MUST BE DONE.
C
      ATLW=0.0001
    2 RESPR=0.
      K=-L
C CALCULATION OF FR(K) AND FI(K)
C
```

```
    3 X(1)=(-DET+K*MODSP)/(1.414*DOWID)
      X(2)=.5*ATLW/(1.414*DOWID)
      Z=ZZ
      FRDCN=FRDCNT(Z)
      FRK=1.77245*PLASF(1)
      FIK=1.77245*PLASF(2)
C
C CALCULATION OF THE CONVOLUTION OF THE POWER SPECTRUM
C FOR GIVEN K
C
      AK=FLOAT(K)
      B=2*(AK/L)*(AK/L)
      GSQK=.6267*L*EXP(-B)
C
C EVALUATION OF THE SUM OVER K
C
      DRESPR=GSQK*(FRK*FRK+FIK*FIK)/(PAV*PAV)
      RESPR=RESPR+DRESPR
      K=K+1
      IF(K.LE.L) GO TO 3
C
C THIS IS THE END OF THE CALCULATION FOR A GIVEN OMO.
C PRINT THE RESULT
C
      PRINT100,ATLW,RESPR
  100 FORMAT(' ',F20.4,20X,E10.3)
C
C NOW INCREMENT THE ATOMIC LINEWIDTH
C
      ATLW=ATLW+DATLW
      IF(ATLW.LE.ATLWMX)GO TO 2
      STOP
      END
$DATA
2.0,.028,.115,.5,0.,.48
/*
```

- 179 -

APPENDIX B

RESOLUTION OF A TYPE III UP-CONVERTER

We calculate the magnification of an up-converter using a Type III optical system, and the effect of its finite length on its resolution. Figure 19 shows a diagram of the complete optical system. The IR field in the up-converter is the Fourier transform of the field in the object plane. The nonlinear polarization in the medium varies spatially as the product of this IR field and the square of the pump field. Assuming a Gaussian pump profile:

$$dP \propto U_{ir} \times e^{-2r^2/w_0^2} \, d\alpha \qquad (B.1)$$

where w_0 is the radius of the pump beam, and dP is the polarization set up in a thin slice of medium with thickness $d\alpha$. At first sight we have a problem in applying the results of Fourier optics[39] to this case, since we are given a polarization in some plane instead of an electric field. This problem can be solved by the following observation. The relation between the electric fields in two planes of an optical system is given by a Huygens-Fresnel integral. For small angles, however, this integral has exactly the same form as the
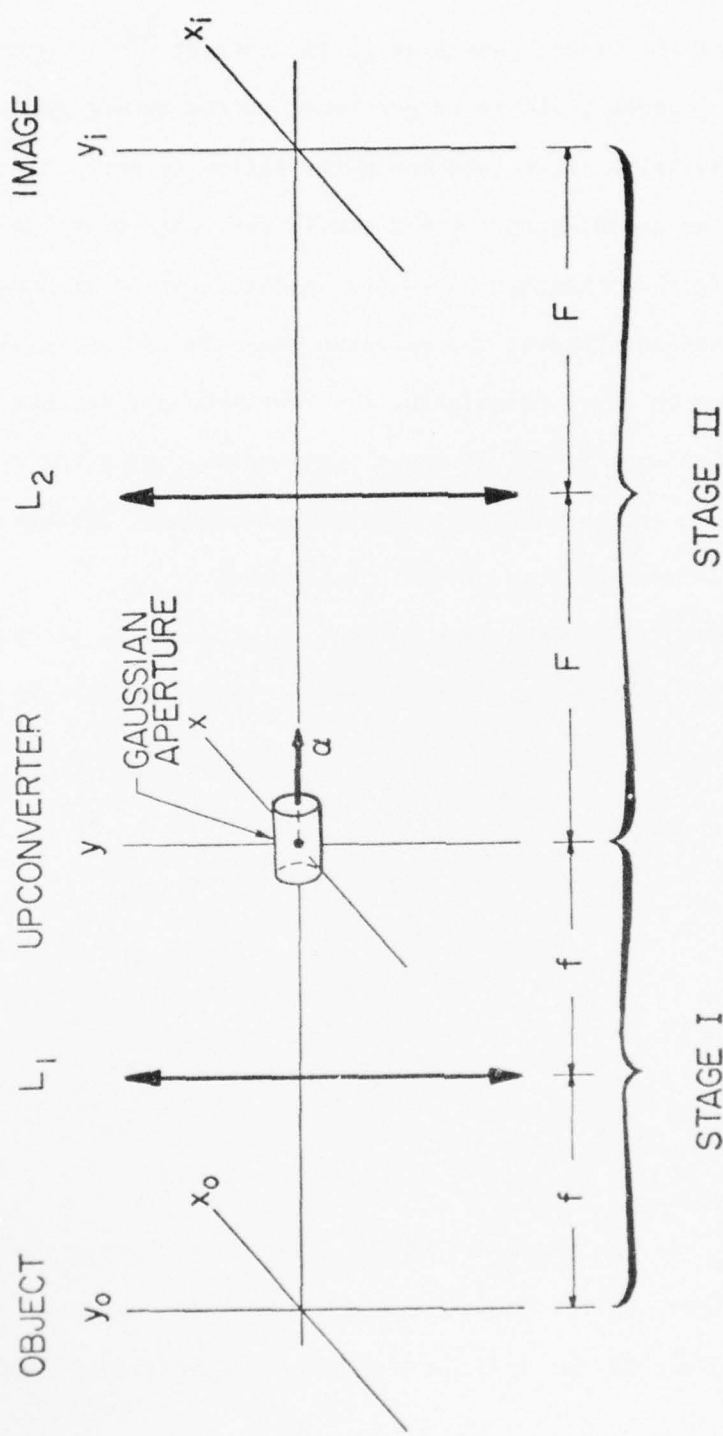
Fig. 19—Schematic of Type III up-converter.

integral relating the vector potential to the current.[39,40] Since, spatially, the electric field is proportional to the vector potential (the scalar potential is zero) and the polarization is proportional to the current, we conclude that the field in the image plane can be found by treating the polarization in the up-converter as an electric field. Our method for finding the electric field in the image plane will then consist in first calculating the contributions to that field due to different slices in the up-converting medium, using the results of Fourier optics, and then adding these contributions. Throughout the calculation, the formalism of Ref. 39 is used.

The electric field in the image plane, due to a slice of thickness $d\alpha$ at a distance α from the center plane of the up-converter, is proportional to:

$$dU_i \propto e^{\dfrac{ik_s\alpha(x_i^2 + y_i^2)}{2F^2}} \times \left[F_u\left(\frac{x_i}{\lambda_s F}, \frac{y_i}{\lambda_s F} \right) * A \right] d\alpha \qquad (B.2)$$

where

$$A = e^{-\dfrac{\pi^2 w_0^2(x_i^2 + y_i^2)}{2\lambda_s^2 F^2}}$$

The quantity F_u is the transform of the field in the cross section α of the up-converter, while A is the transform of the Gaussian aperture function. The field in the up-converter can be expressed in terms of

- 182 -

the field behind the lens L_1 :

$$F_u \propto e^{-\dfrac{i\pi\lambda_i(f + \alpha)(x_i^2 + y_i^2)}{\lambda_s^2 F^2}} \times F_{L_1}\left(\frac{x_i}{\lambda_s F}, \frac{y_i}{\lambda_s F}\right) \qquad (B.3)$$

where F_{L_1} is the transform of the field behind lens L_1 . Finally, the field behind L_1 can be expressed in terms of the field in the object plane:

$$F_{L_1} \propto U_0\left(\frac{x_i}{M}, \frac{y_i}{M}\right) e^{\dfrac{i\pi\lambda_i f(x_i^2 + y_i^2)}{\lambda_s^2 F^2}} \qquad (B.4)$$

where $M = (\lambda_s F/\lambda_i f)$. Combination of (B.2), (B.3), and (B.4) yields

$$dU_i \propto e^{\dfrac{i\pi\alpha(x_i^2 + y_i^2)}{\lambda_s F^2}}$$

$$\times \left[e^{\dfrac{-i\pi\lambda_i\alpha(x_i^2 + y_i^2)}{\lambda_s^2 F^2}} U_0\left(\frac{x_i}{M}, \frac{y_i}{M}\right) * A \right] d\alpha \qquad (B.5)$$

This result can be greatly simplified by realizing that the phase factor inside the brackets can only be allowed to vary less than π from the center of the image to the edge, and thus can be considered constant over the aperture function A and taken out of the brackets.

Hence, to an excellent approximation:

$$dU_i \propto e^{\frac{i\pi\alpha}{\lambda_s F^2}\left(1 - \frac{\lambda_i}{\lambda_s}\right)(x_i^2 + y_i^2)} \times \left[U_0\left(\frac{x_i}{M}, \frac{y_i}{M}\right) * A \right] d\alpha \qquad (B.6)$$

The total field in the image plane is found by integration over α.
The result is:

$$U(x_i, y_i) \propto \left[U_0\left(\frac{x_i}{M}, \frac{y_i}{M}\right) * A \right] \text{sinc} \left[\frac{B(x_i, y_i)L}{2} \right]$$

where

$$B(x_i, y_i) = \frac{\pi(1 - \lambda_i/\lambda_s)(x_i^2 + y_i^2)}{\lambda_s F^2} \qquad (B.7)$$

We find that, if there were no change in wavelength, i.e., $\lambda_i = \lambda_s$,
the image would simply be a magnified replica of the object, with a
loss in resolution, however, due to diffraction through the Gaussian
aperture. Because of the change in wavelength, however, the image
gets modulated by a function that depends on the length of the medium.
The effect of this finite length will be small if the sinc function
is close to unity over the entire image. This requires:

$$\frac{\pi \lambda_i r_{i_{max}}^2 L}{2\lambda_s F^2} \lesssim \frac{\pi}{2}$$

Using

$$A_i = \pi r_{i_{max}}^2$$

$$M = \lambda_s F / \lambda_i F$$

$$A_0 = A_i / M^2$$

this can be rewritten as:

$$\boxed{\Delta\Omega_u \lesssim \pi\lambda_i / L}$$ (B.8)

Note that the requirement $B_{max} L/2 \lesssim \pi/2$ limits the change between $r_i = 0$ and $r_i = r_{i_{max}}$ of the phase factor mentioned above indeed to less than π , and thus taking that phase factor out of the convolution was permitted.

We can now easily calculate the number of resolution elements in the image as the ratio of the area of the image to the area of a diffraction spot. The area of the image is simply the area of the object times the magnification:

$$A_i = A_0 M^2$$

The area of the diffraction spot could (for example) be defined as the

area between the 50% points of the Gaussian, i.e.,

$$a_i = \ln 2 \frac{\lambda_s^2 F^2}{\pi w_0^2/2} = \ln 2 \frac{\lambda_s^2 F^2}{A_p}$$

where A_p is the area of the pump beam. The resulting resolution is:

$$R \equiv \frac{A_i}{a_i} = \frac{1}{\ln 2} \times \frac{A_p A_0}{\lambda_i^2 f^2} = \frac{1}{\ln 2} \times \frac{A_p \Delta\Omega_u}{\lambda_i^2}$$

using $f^2 \Delta\Omega_u = A_0$. Hence, approximately:

$$R \simeq \frac{A_p \Delta\Omega_u}{\lambda_i^2} \tag{B.9}$$

Using the maximum value for the solid angle of the up-converter, given by (B.8):

$$R \simeq \frac{\pi A_p}{\lambda_i L} \tag{B.10}$$

The resolution found using the above criterion is a factor of two higher than what is commonly used, i.e., $R = A \times \Delta\Omega/\lambda_i^2$, where for our case $A = A_p/2$. This more conservative value has been used in resolution calculations.

APPENDIX C

CHROMATIC ABERRATION

In Appendix B we found that the up-converter magnifies the object by a wavelength dependent factor:

$$M = \frac{\lambda_s}{\lambda_i} \times \frac{F}{f} \qquad (C.1)$$

To find a criterion for chromatic aberration, we will consider an object that only has one (arbitrary) spatial frequency (in one dimension), but is illuminated by two different IR frequencies. We take the amplitudes of these two frequencies to be the same. The field in the object plane can then be written as

$$U_0 = \cos(k_{x1}x_0) + \cos(k_{x2}x_0)$$

with

$$k_{x1} = k_{x2}$$

or

$$\frac{\theta_1}{\lambda_{i1}} = \frac{\theta_2}{\lambda_{i2}} \tag{C.2}$$

in terms of the angles θ_1 and θ_2 between the z direction and the k vectors of the two IR waves. The magnified field in the image plane is given by:

$$U_i \propto \cos\left(k_{x1} \frac{x_i}{M_1}\right) + \cos\left(k_{x2} \frac{x_i}{M_2}\right) \tag{C.3}$$

So at the output we have two different spatial frequencies, and there will be a beating between those. Clearly what we want is that the beating period is longer than the size of the image. Let's first rewrite (C.3) such that the beating period is shown:

$$U_i \propto \cos\left(x_i \frac{k_{x1}/M_1 + k_{x2}/M_2}{2}\right) \cos\left(x_i \frac{k_{x1}/M_1 - k_{x2}/M_2}{2}\right) \tag{C.4}$$

If we limit the phase of the beating factor to $\pi/4$, then the intensity in the image plane, at the edge of the image, will be half the value in the center. So we require:

$$\frac{(k_{x1}/M_1 - k_{x2}/M_2)r_i}{2} \lesssim \frac{\pi}{4} \tag{C.5}$$

MICROCOPY RESOLUTION TEST CHART
NATIONAL BUREAU OF STANDARDS-1963-A
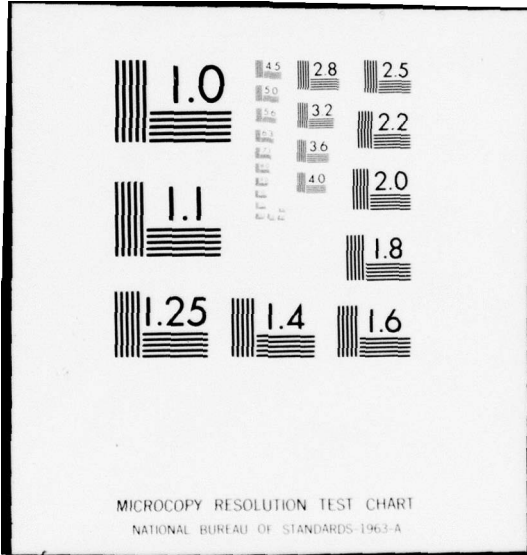
If we let:

$$\omega_{i2} = \omega_{i1} + \Delta\omega_i$$

$$\omega_{s2} = \omega_{s1} + \Delta\omega_i$$

this condition can be rewritten as:

$$\frac{\Delta\omega_i}{\omega_i} \lesssim \frac{1}{4} \frac{\lambda_s F}{f\theta_0 r_i} \qquad (C.6)$$

for all angles $\theta \lesssim \theta_{0_{max}}$ in the object plane. Clearly the aberration is most severe for large θ_0, i.e., large spatial frequencies. Expressing the radius of the image in terms of the radius of the object and the magnification, the condition (C.6) for the maximum angle θ_0 can be rewritten as:

$$\frac{\Delta\omega_i}{\omega_i} \lesssim \frac{1}{4} \frac{\lambda_i}{r_0 \theta_{0_{max}}} \qquad (C.7)$$

Using:

$$A_0 = \pi r_0^2$$

$$\Delta\Omega_0 = \pi\theta_{0_{max}}^2$$

$$R \simeq A_0 \Delta\Omega_0 / \lambda_i^2$$

- 189 -

TABLE VII

IR BANDWIDTHS ALLOWED BY CHROMATIC ABERRATION

IN A TYPE III UP-CONVERTER

ω_i (cm^{-1}) \ R	10^3	10^4	10^5
3300 (Cs)	10^4	33	10.4
1000 (Na)	31.6	10	3.2

this can be rewritten as:

$$\frac{\Delta\omega_i}{\omega_i} \lesssim \frac{\pi}{4} \times \frac{1}{\sqrt{R}} \qquad (C.8)$$

The criterion for chromatic aberration can then be written as:

$$\boxed{\frac{\Delta\omega_i}{\omega_i} \lesssim \frac{1}{\sqrt{R}}} \qquad (C.9)$$

The aberration is most visible near the edge of the image, and is worse for higher spatial frequencies.

The IR bandwidths, as allowed by chromatic aberration, for $3\ \mu$ and $10\ \mu$ up-conversion, and for various resolutions, are shown in Table VII.

APPENDIX D

PRESSURE BROADENING ESTIMATES

The formalism developed in Ref. 41 was used to estimate the pressure broadening of the 6s-7s and 7s-7p transitions in cesium. Matrix elements were taken from Ref. 19.

A. TRANSITION $6s^2S_{1/2} - 7s^2S_{1/2}$

Paths used for the shift of $6s^A + 6s^B$

Atom A	Atom B
6s - 6p	6s - 6p

Paths used for the shift of $6s^A + 7s^B$

Atom A	Atom B
6s - 6p	7s - 6p
6s - 6p	7s - 7p

One finds:

$$\frac{\Delta C_6}{\hbar} = 1.1 \times 10^{-41}$$

$$\gamma = 5 \times 10^{-26} \times N \; [\text{cm}^{-1}]$$

where N is in $[\text{m}^{-3}]$.

B.   TRANSITION $7s^2S_{1/2} - 7p^2P_{3/2}$

Paths used for the shift of $6s^A + 7s^B$

Atom A	Atom B
6s - 6p	7s - 6p
6s - 6p	7s - 7p

Paths used for the shift of $6s^A + 7p^B$

Atom A	Atom B
6s - 7p	7p - 6s
- - - -	- - - -
	7p - 6s
	7p - 7s
	7p - 8s
6s - 6p	7p - 9s
	7p - 5d
	7p - 6d
	7p - 7d
	7p - 8d

One finds:

$$\frac{\Delta C_6}{\hbar} = 2 \times 10^{-41}$$

$$\frac{C_3}{\hbar} = 5.5 \times 10^{-16}$$

If only the $1/R^6$ potentials are used, $\rho_{Om} = 24$ Å . If the $1/R^6$ and $1/R^3$ potentials are used with the same sign, $\rho_{Om} = 27$ Å . If the $1/R^6$ and $1/R^3$ potentials are used with opposite signs, $\rho_{Om} = 21$ Å . The resulting linewidth varies between $4.7 \times 10^{-26} \times N$ [cm^{-1}] and $7.7 \times 10^{-26} \times N$ [cm^{-1}] , where N is in [m^{-3}].

APPENDIX E

DEPENDENCY OF SUSCEPTIBILITIES ON POLARIZATION

A. INTRODUCTION

In this appendix we study the effect of the polarization of the electric fields used in linear and nonlinear processes on their susceptibilities. Although most of the results derived are intuitively quite obvious, it is interesting to see how they are derived quantum-mechanically. Some of the results are:

- The dipole moment set up in a first order process is parallel to the exciting electric field, and has a magnitude independent of the polarization of this field.

- The magnitudes of the third order susceptibilities $\chi^{(3)}_{zzzz}$ and $\chi^{(3)}_{xzzx}$ for a path $s \to p \to s \to p \to s$ are equal, i.e., it does not make a difference whether the electric field used in the third step is parallel to or orthogonal to the field used in the first two steps. The generated dipole moment is also parallel to the field used in the third step.

- If, in the previous process, a path $s \to p \to d \to p \to s$ is used, then the susceptibility for the case of the three fields parallel

is a factor of two higher than for the other case. This becomes
understandable if one looks at the spatial distributions of the
wave functions used in both processes.

The expressions for the linear and nonlinear susceptibilities are
given in Ref. 12. For this discussion we are not interested in consid-
ering all the permutations of the electric fields, so we drop the S
operator (= symmetrization operator). Then we still have to sum over
all the atomic levels. If an atomic level is $(2m + 1)$ fold degen-
erate, it has to be looked at as consisting of $(2m + 1)$ different
levels, all at the same energy, and we have to sum the contributions
of all of them. Except for this summation, we also have to sum over
all the possible paths (e.g., $1s \rightarrow 2p$, but also $1s \rightarrow 3p$, etc.
for a first order process in H). We will also drop this last sum-
mation because it is irrelevant.

B.   DEPENDENCE OF THE DIPOLE MOMENT GENERATED IN A FIRST ORDER
     PROCESS ON THE POLARIZATION OF THE ELECTRIC FIELD

From Ref. 12:

$$\chi_{\mu\alpha}^{(1)}(\omega) \;=\; -\frac{N}{\hbar} \sum_{a,b} \rho_{aa}^{o} \left(\frac{R_{ab}^{\alpha} R_{ba}^{\mu}}{\omega_{ab} - \omega} + \frac{R_{ab}^{\mu} R_{ba}^{\alpha}}{\omega_{ab} + \omega} \right) \qquad (E.1)$$

- 196 -

where

μ = direction of generated dipole moment

(along x,y, or z)

α = polarization of electric field

a,b = atomic energy levels

eR_{ab}^{μ} = matrix element between a,b of the μ component of
the dipole moment operator

N = atomic number density

ρ_{aa}^{o} = equilibrium occupancy of level a ; we set $\rho_{aa}^{o} = 1$
in what follows

For our purposes, as discussed in Section A:

$$\chi_{\mu\alpha}^{(1)}(\omega) = -\frac{N}{\hbar} \sum_{\text{m-deg.}} \left(\frac{R_{ab}^{\alpha} R_{ba}^{\mu}}{\omega_{ab} - \omega} + \frac{R_{ab}^{\mu} R_{ba}^{\alpha}}{\omega_{ab} + \omega} \right) \qquad (E.2)$$

Using this expression for the first order susceptibility, we will:

(a) Calculate the dipole moment set up in the z-direction by an
electric field in the z-direction.

(b) Calculate the dipole moment set up in the x-direction by an
electric field in the x-direction.

(c) Calculate the dipole moment set up in the y-direction by an
electric field in the x-direction.

- 197 -

(d) Prove that the linear dipole moment set up by an electric
field is parallel to that field, and that its magnitude is
independent of the polarization of the field.

1. The Dipole Moment Set Up in the z-Direction by an Electric Field
in the z-Direction is:[12]

$$P_z(t) = \int_{-\infty}^{\infty} d\omega E_z(\omega) \, \chi_{zz}^{(1)}(\omega) \, e^{-i\omega t}$$

where

$$\chi_{zz}^{(1)}(\omega) = -\frac{N}{\hbar} \sum_{\text{m-deg.}} \left(\frac{|z_{sp}|^2}{\omega_{01} - \omega} + \frac{|z_{sp}|^2}{\omega_{01} + \omega} \right) \qquad (E.3)$$

from Section D:

$$\langle s|z|p, m = 0 \rangle = 1/\sqrt{3}$$

$$\langle s|z|p, m = \pm 1 \rangle = 0$$

so in this case the sum only contains one term; for $m = 0$:

$$\chi_{zz}^{(1)}(\omega) = -\frac{N}{\hbar} \frac{1}{3} \left(\frac{1}{\omega_{01} - \omega} + \frac{1}{\omega_{01} + \omega} \right) \qquad (E.4)$$

- 198 -

2. <u>The Dipole Moment Set Up in the x-Direction by an Electric Field in the x-Direction is:</u>

$$P_x(t) = \int_{-\infty}^{\infty} d\omega E_x(\omega) \, \chi_{xx}^{(1)}(\omega) \, e^{-i\omega t}$$

where

$$\chi_{xx}^{(1)}(\omega) = -\frac{N}{\hbar} \sum_{m\text{-deg.}} \left(\frac{|x_{sp}|^2}{\omega_{01} - \omega} + \frac{|x_{sp}|^2}{\omega_{01} + \omega} \right) \qquad (E.5)$$

from Section D:

$$\langle s|x|p, m = 0 \rangle = 0$$

$$\langle s|x|p, m = \pm 1 \rangle = \mp 1/\sqrt{6}$$

hence, summing over m :

$$\chi_{xx}^{(1)}(\omega) = -\frac{N}{\hbar} \left(|\langle s|x|p, m = -1 \rangle|^2 + |\langle s|x|p, m = 1 \rangle|^2 \right)$$

$$\times \left(\frac{1}{\omega_{01} - \omega} + \frac{1}{\omega_{01} + \omega} \right)$$

$$= -\frac{N}{\hbar} \left(\frac{1}{6} + \frac{1}{6} \right) \left(\frac{1}{\omega_{01} - \omega} + \frac{1}{\omega_{01} + \omega} \right) = \chi_{zz}^{(1)}(\omega) \qquad (E.6)$$

One shows similarly: $\chi_{yy}^{(1)}(\omega) = \chi_{zz}^{(1)}(\omega) = \chi_{xx}^{(1)}(\omega)$.

3. The Dipole Moment Set Up in the y-Direction by an Electric Field in the x-Direction is:

$$P_y(t) = \int_{-\infty}^{\infty} d\omega E_x(\omega)\, \chi_{yx}^{(1)}(\omega)\, e^{-i\omega t}$$

where

$$\chi_{yx}^{(1)}(\omega) = -\frac{N}{\hbar} \sum_{m\text{-deg.}} \left(\frac{x_{sp} y_{ps}}{\omega_{01} - \omega} + \frac{y_{sp} x_{ps}}{\omega_{01} + \omega} \right) \qquad (E.7)$$

from Section D:

$$\langle s|x|p, m = 0 \rangle = 0 \qquad\qquad \langle s|y|p, m = 0 \rangle = 0$$

$$\langle s|x|p, m = \pm 1 \rangle = \mp 1/\sqrt{6} \qquad\qquad \langle s|y|p, m = \pm 1 \rangle = -i/\sqrt{6}$$

hence, summing over m :

$$\chi_{yx}^{(1)}(\omega) = -\frac{N}{\hbar} \left[\frac{\langle s|x|p, m=-1 \rangle \langle p, m=-1|y|s \rangle + \langle s|x|p, m=1 \rangle \langle p, m=1|y|s \rangle}{\omega_{01} - \omega} \right.$$

$$\left. + \frac{\langle s|y|p, m=-1 \rangle \langle p, m=-1|x|s \rangle + \langle s|y|p, m=1 \rangle \langle p, m=1|x|s \rangle}{\omega_{01} + \omega} \right]$$

$$= -\frac{N}{\hbar} \left[\frac{(1/\sqrt{6})(i/\sqrt{6}) + (-1/\sqrt{6})(i/\sqrt{6})}{\omega_{01} - \omega} \right.$$

$$\left. + \frac{(-i/\sqrt{6})(1/\sqrt{6}) + (-i/\sqrt{6})(-1/\sqrt{6})}{\omega_{01} + \omega} \right] = 0 \qquad (E.8)$$

- 200 -

One shows similarly that all the other off-diagonal elements of the linear susceptibility tensor are zero.

4. **The Dipole Moment is Parallel to the Electric Field, and Its Magnitude is Independent of the Polarization of the Electric Field**

This follows immediately from Sections 1, 2, and 3. A formal proof that takes into account the frequency dependence of $\chi^{(1)}(\omega)$ goes as follows:

Specify the electric field by its direction cosines, i.e., $\bar{E}(E \cos \alpha , E \cos \beta , E \cos \gamma)$, with $\cos^2 \alpha + \cos^2 \beta + \cos^2 \gamma = 1$; then:

$$P_x(t) = \cos \alpha \int d\omega \; \chi_{xx}^{(1)}(\omega) \; E(\omega) \; e^{-i\omega t}$$

$$P_y(t) = \cos \beta \int d\omega \; \chi_{yy}^{(1)}(\omega) \; E(\omega) \; e^{-i\omega t}$$

$$P_z(t) = \cos \gamma \int d\omega \; \chi_{zz}^{(1)}(\omega) \; E(\omega) \; e^{-i\omega t}$$

since $\chi_{xx}^{(1)}(\omega) = \chi_{yy}^{(1)}(\omega) = \chi_{zz}^{(1)}(\omega)$, it follows

$$P_x(t) = I \cos \alpha$$

$$P_y(t) = I \cos \beta$$

$$P_z(t) = I \cos \gamma$$

- 201 -

where

$$I(t) = \int\limits_{-\infty}^{\infty} d\omega \, \chi_{xx}^{(1)}(\omega) \, E(\omega) \, e^{-i\omega t}$$

hence

$$\overline{P}(t) // \overline{E}(t)$$

$$|\overline{P}(t)| = I \quad , \quad \text{independent of the direction} \qquad (E.9)$$
$$\text{of the electric field}$$

C.   EXAMPLES OF THE DEPENDENCY OF THE THIRD ORDER NONLINEAR SUSCEPTI-
BILITY ON THE POLARIZATION OF THE ELECTRIC FIELDS

Since the number of possible third order processes is very large,
we will only do a few specific examples. The third order suscepti-
bility, as given in Ref. 12, has four terms. For convenience we will
only consider one of them, more specifically the one that has three
minus signs in the denominator, which is usually the dominant one.
Again we do not permute the frequencies, i.e., we apply the fields
in a well defined order, e.g.: in the first two steps we apply a
field of frequency ω_p along the z axis, in the third step and
at frequency ω_i along the x axis. We also do not sum over all
the atomic levels as explained in Section A. So for our purposes

(Ref. 12):

$$P_\mu^{(3)}(t) = \iiint\limits_{-\infty}^{\infty} d\omega_1 d\omega_2 d\omega_3 \, \chi_{\mu\alpha\beta\gamma}^{(3)}(\omega_1,\omega_2,\omega_3) E_\alpha(\omega_1) E_\beta(\omega_2) E_\gamma(\omega_3) \, e^{-it\left(\sum\limits_k \omega_k\right)}$$

where

$$\chi_{\mu\alpha\beta\gamma}^{(3)}(\omega_1,\omega_2,\omega_3) = -\frac{N}{6\hbar^3} \sum_{m\text{-deg.}} \frac{R_{ab}^\alpha R_{bc}^\beta R_{cd}^\gamma R_{da}^\mu}{(\omega_{ab}-\omega_1)(\omega_{ac}-\omega_1-\omega_2)(\omega_{ad}-\omega_1-\omega_2-\omega_3)}$$

$$(E.10)$$

Using this expression for the third order susceptibility, we will do the following examples:

For a path $s \to p \to s \to p \to s$

(a) Dipole moment along z when all fields are along z , i.e., $\chi_{zzzz}^{(3)}$.

(b) Dipole moment along x when the fields used in the first two steps are along z , and the third field is along x , i.e., $\chi_{xzzx}^{(3)}$.

For a path $s \to p \to d \to p \to s$

(a) Dipole moment along z when all fields are along z , i.e., $\chi_{zzzz}^{(3)}$.

(b) Dipole moment along x when all fields are along x , i.e., $\chi_{xxxx}^{(3)}$.

(c) Dipole moment along x when the fields used in the first two steps are along z, and the third field is along x, i.e., $\chi_{xzzx}^{(3)}$.

To shorten the algebra, we will represent the resonance denominator $(\omega_{01} - \omega_1)(\omega_{02} - \omega_1 - \omega_2)(\omega_{03} - \omega_1 - \omega_2 - \omega_3)$ by one symbol, say D.

1. <u>Process Using a Path $s \rightarrow p \rightarrow s \rightarrow p \rightarrow s$</u>

(a) Calculation of $\chi_{zzzz}^{(3)}$

$$\chi_{zzzz}^{(3)} = -\frac{N}{6\hbar^3} \sum_{m\text{-deg.}} \frac{z_{sp} z_{ps} z_{sp} z_{ps}}{D} \qquad (E.11)$$

From Section D:

$$\langle s|z|p, m = 0 \rangle = 1/\sqrt{3}$$

$$\langle s|z|p, m = \pm 1 \rangle = 0$$

hence, summing over m:

$$\chi_{zzzz}^{(3)} = -\frac{N}{6\hbar^3} \left(\frac{1}{\sqrt{3}}\right)^4 \frac{1}{D} = -\frac{N}{6\hbar^3} \left(\frac{1}{9}\right)\left(\frac{1}{D}\right) \qquad (E.12)$$

(b) Calculation of $\chi_{xzzx}^{(3)}$

$$\chi_{xzzx}^{(3)} = -\frac{N}{6\hbar^3} \sum_{m\text{-deg.}} \frac{z_{sp} z_{ps} x_{sp} x_{ps}}{D} \qquad (E.13)$$

From Section D:

$$\langle s|z|p, m = 0 \rangle = 1/\sqrt{3} \qquad \langle s|x|p, m = 0 \rangle = 0$$

$$\langle s|z|p, m = \pm 1 \rangle = 0 \qquad \langle s|x|p, m = \pm 1 \rangle = \mp 1/\sqrt{6}$$

hence, summing over m :

$$\chi^{(3)}_{xzzx} = -\frac{N}{6\hbar^3} \frac{1}{D} \left\{ \begin{array}{l} \langle s|z|p, m = 0 \rangle \langle p, m = 0|z|s \rangle \\ \times \left[\langle s|x|p, m = -1 \rangle \langle p, m = -1|x|s \rangle \right. \\ + \left. \langle s|x|p, m = 1 \rangle \langle p, m = 1|x|s \rangle \right] \end{array} \right\}$$

$$= -\frac{N}{6\hbar^3} \frac{1}{D} \left[\frac{1}{3} \left(\frac{1}{6} + \frac{1}{6} \right) \right]$$

$$= -\frac{N}{6\hbar^3} \left(\frac{1}{9} \right) \left(\frac{1}{D} \right) = \chi^{(3)}_{zzzz} \qquad (E.14)$$

So it does not make a difference in this case whether the third field is parallel to or orthogonal to the first two. This could be expected since the vibration set up in the second step (s level) is spatially symmetric. It can also easily be shown that $\chi^{(3)}_{zzzx}$ and $\chi^{(3)}_{yzzx}$ are zero, i.e., the generated dipole moment is parallel to the third field.

2. **Process Using a Path $\quad s \to p \to d \to p \to s$**

  (a) Calculation of $\chi^{(3)}_{zzzz}$

$$\chi^{(3)}_{zzzz} = -\frac{N}{6\hbar^3} \sum_{m\text{-deg.}} \frac{z_{sp} z_{pd} z_{dp} z_{ps}}{D} \tag{E.15}$$

From Section D:

$$\langle s|z|p,m = 0 \rangle = 1/\sqrt{3} \qquad\qquad \langle p,m = 0|z|d,m = 0 \rangle = 2/\sqrt{15}$$

$$\langle s|z|p,m = \pm 1 \rangle = 0 \qquad\qquad \langle p,m = 0|z|d,m = \pm 1 \rangle = 0$$

$$\langle p,m = 0|z|d,m = \pm 2 \rangle = 0$$

hence, summing over m :

$$\chi^{(3)}_{zzzz} = -\frac{N}{6\hbar^3} \frac{(1/\sqrt{3})(2/\sqrt{15})(2/\sqrt{15})(1/\sqrt{3})}{D}$$

$$= -\frac{N}{6\hbar^3} \left(\frac{4}{45}\right)\left(\frac{1}{D}\right) \tag{E.16}$$

  (b) Calculation of $\chi^{(3)}_{xxxx}$

$$\chi^{(3)}_{xxxx} = -\frac{N}{6\hbar^3} \sum_{m\text{-deg.}} \frac{x_{sp} x_{pd} x_{dp} x_{ps}}{D} \tag{E.17}$$

$$\chi^{(3)}_{xxxx} = -\frac{N}{6\hbar^3}\left(\frac{1}{D}\right)$$

$$\times \begin{bmatrix} \langle s|x|p,m=-1\rangle\langle p,m=-1|x|d,m=0\rangle\langle d,m=0|x|p,m=-1\rangle\langle p,m=-1|x|s\rangle \\ + \langle s|x|p,m=-1\rangle\langle p,m=-1|x|d,m=0\rangle\langle d,m=0|x|p,m=1\rangle\langle p,m=1|x|s\rangle \\ + \langle s|x|p,m=-1\rangle\langle p,m=-1|x|d,m=-2\rangle\langle d,m=-2|x|p,m=-1\rangle\langle p,m=-1|x|s\rangle \\ + \langle s|x|p,m=1\rangle\langle p,m=1|x|d,m=0\rangle\langle d,m=0|x|p,m=-1\rangle\langle p,m=-1|x|s\rangle \\ + \langle s|x|p,m=1\rangle\langle p,m=1|x|d,m=0\rangle\langle d,m=0|x|p,m=1\rangle\langle p,m=1|x|s\rangle \\ + \langle s|x|p,m=1\rangle\langle p,m=1|x|d,m=2\rangle\langle d,m=2|x|p,m=1\rangle\langle p,m=1|x|s\rangle \end{bmatrix}$$

$$(E.18)$$

Using the values for the matrix elements given in Section D:

$$\chi^{(3)}_{xxxx} = -\frac{N}{6\hbar^3}\left(\frac{1}{D}\right)$$

$$\times \begin{bmatrix} (1/\sqrt{6})(-1/\sqrt{30})(-1/\sqrt{30})(1/\sqrt{6}) \\ + (1/\sqrt{6})(-1/\sqrt{30})(1/\sqrt{30})(-1/\sqrt{6}) \\ + (1/\sqrt{6})(1/\sqrt{5})(1/\sqrt{5})(1/\sqrt{6}) \\ + (-1/\sqrt{6})(1/\sqrt{30})(-1/\sqrt{30})(1/\sqrt{6}) \\ + (-1/\sqrt{6})(1/\sqrt{30})(1/\sqrt{30})(-1/\sqrt{6}) \\ + (-1/\sqrt{6})(-1/\sqrt{5})(-1/\sqrt{5})(-1/\sqrt{6}) \end{bmatrix}$$

(Cont'd)

$$= -\frac{N}{6\hbar^3} \left(\frac{1}{D}\right) \left(\frac{4}{45}\right)$$

$$= \chi^{(3)}_{zzzz} \tag{E.19}$$

(c) Calculation of $\chi^{(3)}_{xzzx}$

$$\chi^{(3)}_{xzzx} = -\frac{N}{6\hbar^3} \sum_{\text{m-deg.}} \frac{z_{sp} z_{pd} x_{dp} x_{ps}}{D} \tag{E.20}$$

$$\chi^{(3)}_{xzzx} = -\frac{N}{6\hbar^3} \left(\frac{1}{D}\right)$$

$$\times \left[\langle s|z|p,m = 0\rangle \langle p,m = 0|z|d,m = 0\rangle \right]$$

$$\times \left[\langle d,m = 0|x|p,m = -1\rangle \langle p,m = -1|x|s\rangle \right.$$
$$\left. + \langle d,m = 0|x|p,m = 1\rangle \langle p,m = 1|x|s\rangle \right] \tag{E.21}$$

Using the values for the matrix elements given in Section D:

$$\chi^{(3)}_{xzzx} = -\frac{N}{6\hbar^3} \left(\frac{1}{D}\right) \left[(1/\sqrt{3})(2/\sqrt{15}) \right.$$
$$\left. \times \left[(-1/\sqrt{30})(1/\sqrt{6}) + (1/\sqrt{30})(-1/\sqrt{6}) \right] \right]$$

$$= -\frac{N}{6\hbar^3} \left(\frac{1}{D}\right) \left(\frac{-2}{45}\right) = -\frac{1}{2} \chi^{(3)}_{zzzz} \tag{E.22}$$

The susceptibility for the case where the three fields are parallel is a factor of two higher than in the case where the third field is orthogonal to the first two. This is not too surprising if one looks at the spatial form of the wave functions involved.

D. MATRIX ELEMENTS OF THE DIPOLE-MOMENT OPERATOR

Since only first and third order processes are considered, only s, p, and d levels are involved, i.e., $\ell = 0, 1, 2$. For an electron moving in a spherically symmetrical potential the wave functions can be written as (Ref. 43):

$$\Psi(r,\theta,\varphi) = R_{n1}(r) Y_{\ell}^{m}(\theta,\varphi) \quad \left\{ \begin{array}{l} \ell = 0, 1, \ldots, n-1 \\ m = -\ell, -\ell+1, \ldots, \ell-1, \ell \end{array} \right. \tag{E.23}$$

The $Y_{\ell}^{m}(\theta,\varphi)$ for $\ell = 0, 1, 2$ are (Ref. 42):

$$Y_{0}^{0} = \frac{1}{\sqrt{4\pi}}$$

$$Y_{1}^{0} = \sqrt{\frac{3}{4\pi}} \cos\theta$$

$$Y_{1}^{\pm 1} = \mp \sqrt{\frac{3}{8\pi}} e^{\pm i\varphi} \sin\theta$$

$$Y_{2}^{0} = \sqrt{\frac{5}{16\pi}} (3\cos^2\theta - 1) \qquad \text{(Cont'd)}$$

$$Y_2^{\pm 1} = \mp \sqrt{\frac{15}{8\pi}} \; e^{\pm i\varphi} \sin\theta \cos\theta$$

$$Y_2^{\pm} = \sqrt{\frac{15}{32\pi}} \; e^{\pm i2\varphi} \sin^2\theta \qquad\qquad (E.24)$$

The matrix elements of the position operator are defined by:

$$\langle n\ell m | \vec{r} | n'\ell'm' \rangle$$

where $|n\ell m\rangle = R_{n\ell}(r)Y_\ell^m(\theta,\varphi)$. Since for this discussion the value of the radial integral is irrelevant, we will set its value equal to one. So we have to evaluate the following integrals:

$$\text{for:} \quad \begin{bmatrix} z & : & \langle \ell m | \cos\theta | \ell'm' \rangle \\[1.5em] x & : & \langle \ell m | \sin\theta \cos\varphi | \ell'm' \rangle \\[1.5em] y & : & \langle \ell m | \sin\theta \sin\varphi | \ell'm' \rangle \end{bmatrix}$$

The $Y_\ell^m(\theta,\varphi)$ are given by:

$$Y_\ell^m(\theta,\varphi) = P_\ell^m(\cos\theta) \; e^{im\varphi}$$

From this follows the selection rule for ℓ : $\Delta\ell = \pm 1$. Since for this discussion the selection rule for m is important, we will derive

- 210 -

it here. The φ part of the matrix elements is of the form:

$$\langle\, e^{im\varphi}\, \left|\begin{array}{c} z \\ x \\ y \end{array}\right|\, e^{im'\varphi}\, \rangle\; =\; \int\limits_{0}^{2\pi} e^{-im\varphi}\begin{pmatrix} 1 \\ \cos\varphi \\ \sin\varphi \end{pmatrix} e^{im'\varphi}\, d\varphi$$

$$=\; \int\limits_{0}^{2\pi} e^{-im\varphi}\begin{pmatrix} 1 \\ (e^{i\varphi} + e^{-i\varphi})/2 \\ (e^{i\varphi} - e^{-i\varphi})/2 \end{pmatrix} e^{im'\varphi}\, d\varphi$$

hence:

$$\text{for:}\; \left[\begin{array}{lll} z & : & \Delta m = 0 \\[2mm] x & : & \Delta m = \pm 1 \\[2mm] y & : & \Delta m = \pm 1 \end{array}\right.$$

List of relevant matrix elements:

(1) s → p

$$\langle s|z|p, m = 0\rangle\; =\; 1/\sqrt{3}$$

$$\langle s|z|p, m = \pm 1\rangle\; =\; 0$$

$$\langle s|x|p, m = 0\rangle\; =\; 0$$

$$\langle s|x|p, m = \pm 1\rangle\; =\; \mp 1/\sqrt{6}$$

$$\langle s|y|p, m = 0 \rangle = 0$$

$$\langle s|y|p, m = \pm 1 \rangle = -i/\sqrt{6}$$

(2) $\underline{p \to d}$ (only the non-zero ones are given)

$$\langle p, m = 0|z|d, m = 0 \rangle = 2/\sqrt{15}$$

$$\langle p, m = \pm 1|z|d, m = \pm 1 \rangle = 1/\sqrt{5}$$

$$\langle p, m = 0|x|d, m = \pm 1 \rangle = \mp 1/\sqrt{10}$$

$$\langle p, m = -1|x|d, m = 0 \rangle = -1/\sqrt{30}$$

$$\langle p, m = -1|x|d, m = -2 \rangle = 1/\sqrt{5}$$

$$\langle p, m = 1|x|d, m = 0 \rangle = 1/\sqrt{30}$$

$$\langle p, m = 1|x|d, m = 2 \rangle = -1/\sqrt{5}$$

$$\langle p, m = 0|y|d, m = \pm 1 \rangle = \pm i/\sqrt{10}$$

$$\langle p, m = -1|y|d, m = 0 \rangle = -i/\sqrt{30}$$

$$\langle p, m = -1|y|d, m = -2 \rangle = i/\sqrt{5}$$

$$\langle p, m = 1|y|d, m = 0 \rangle = -i/\sqrt{30}$$

$$\langle p, m = 1|y|d, m = 2 \rangle = i/\sqrt{5}$$

APPENDIX F

CONVERSION OF LINE STRENGTHS, OSCILLATOR STRENGTHS

AND EINSTEIN COEFFICIENTS TO MATRIX ELEMENTS

USED IN PERTURBATION CALCULATIONS

A.   INTRODUCTION

In this appendix we address the problem of calculating the matrix elements to be used in each step of a perturbation sequence, given the relevant line strengths, oscillator strengths or Einstein coefficients. Since in practice we are almost always concerned with transitions s-p or p-d , only these are discussed. We consider two cases:

Case 1: The frequency detuning is much larger than the term split-
         tings of the multiplet. In this case one can use the to-
         tal matrix element for the transition $(n\ell) - (n'\ell')$.

Case 2: The frequency detuning is comparable to or smaller than
         the term splittings of the multiplet. In this case one
         has to take into account the fine structure of the multi-
         plet, i.e., one has to calculate the matrix elements for
         each of the transitions $(n\ell j) - (n'\ell'j')$, and after-
         wards sum over j and j' . The results in this appendix

also show how to distribute the total line strength of a

multiplet among its various lines.

Clearly, if one neglects the energy difference between the levels of

a term, after summing over j and j′ in the second case one should

find the same final result as in the first case. We demonstrate this

by calculating a third order nonlinearity in both schemes, after first

considering the effect of spin.

All the results are valid for atoms with ne electron in the outer

shell, for which the unperturbed wave functions are products of a ra-

dial part and a spherical harmonic. Also, the electric fields used in

the perturbation sequence must all have the same polarization; if this

is not the case, the combination of the results of Appendix E and the

techniques illustrated here will still lead to the answer, but each

case has to be solved separately.

B.   CALCULATION OF MATRIX ELEMENTS FROM TOTAL LINE STRENGTHS,

     DISREGARDING TERM SPLITTINGS

Remarks:

— The line strength S is defined between two levels (Sections

G and H), e.g., $(s, j = 1/2) - (p, j = 3/2)$. However, if we sum the

line strengths of the transitions $(n\ell j) - (n′\ell′j′)$ over all possible

pairs $(j, j′)$, then this total S is by definition $\Sigma |\langle a | \overline{P} | b \rangle|^2$

between the configurations $(n\ell)$ and $(n′\ell′)$ (usually it is this

total S which is given in tables). From this total line strength

we will find the matrix element to be used in the transition $(n\ell)$ - $(n'\ell')$.

— The eigenstates used in this calculation are $\left| n\ell s m_\ell m_s \right\rangle$ states. Since $s = 1/2$ and n is irrelevant for this discussion, we will usually omit these two quantum numbers. The numerical values used in the following calculations are taken from Ref. 45.

— Selection rules:

$$\begin{cases} \Delta\ell = \pm 1 \\ \Delta m_\ell = 0 , \pm 1 \\ \Delta m_s = 0 \end{cases}$$

1. s - p Transitions

$$S = e^2 \sum_{a,b} \left(|x_{ab}|^2 + |y_{ab}|^2 + |z_{ab}|^2 \right)$$

— Calculation of $\Sigma |z_{ab}|^2$ using $\Delta m_\ell = 0$:

$$\sum = 2|\langle s\ 0\ 1/2|z|p\ 0\ 1/2\rangle|^2 = 2\ (1/3) = 2/3$$

— Calculation of $\Sigma |x_{ab}|^2$ using $\Delta m_\ell = \pm 1$:

$$\sum = 2[|\langle s\ 0\ 1/2|x|p\ 1\ 1/2\rangle|^2 + |\langle s\ 0\ 1/2|x|p\ -\ 1\ 1/2\rangle|^2]$$

$$= 2\ (1/6 + 1/6) = 2/3$$

hence

$$\sum |x_{ab}|^2 = \sum |y_{ab}|^2 = \sum |z_{ab}|^2$$

as it should be. As a consequence S must be divided by 3 if linearly polarized light is used. We will see in Section D that another factor of 2 appears because of the equal distribution of the atoms in the first level used in the process between the two spin states.

Example: Lithium

Transition	S	$\sqrt{S/6}$	$\langle z\rangle$ (Ref. 19)	Difference in %
2s − 2p	33.3	2.36	2.34	0.8
2p − 3s	18.5	1.76	1.71	3.0

2. **p – d Transitions**

$$d \quad \overline{}_{0} \quad \overline{}_{1} \quad \overline{}_{-1} \quad \overline{}_{2} \quad \overline{}_{-2} \qquad \overline{}_{0} \quad \overline{}_{1} \quad \overline{}_{-1} \quad \overline{}_{2} \quad \overline{}_{-2}$$

$$p \quad \overline{}_{0} \quad \overline{}_{1} \quad \overline{}_{-1} \qquad \qquad \overline{}_{0} \quad \overline{}_{1} \quad \overline{}_{-1}$$

$$\underline{m_s = 1/2} \qquad \qquad \underline{m_s = -1/2}$$

— Calculation of $\Sigma |z_{ab}|^2$ using $\Delta m_\ell = 0$:

$$\sum = 2 \left\{ \begin{array}{l} |\langle p\ 0\ 1/2 | z | d\ 0\ 1/2 \rangle|^2 + |\langle p\ 1\ 1/2 | z | d\ 1\ 1/2 \rangle|^2 \\ + |\langle p - 1\ 1/2 | z | d - 1\ 1/2 \rangle|^2 \end{array} \right\}$$

$$= 2\,(4/15 + 1/5 + 1/5) = 2\,(4/15 + 6/15) = 4/3$$

— Calculation of $\Sigma |x_{ab}|^2$ using $\Delta m_\ell = \pm 1$:

$$\sum = 2 \left\{ \begin{array}{l} |\langle p\ 0\ 1/2 | x | d\ 1\ 1/2 \rangle|^2 + |\langle p\ 0\ 1/2 | x | d - 1\ 1/2 \rangle|^2 \\ + |\langle p\ 1\ 1/2 | x | d\ 0\ 1/2 \rangle|^2 + |\langle p\ 1\ 1/2 | x | d\ 2\ 1/2 \rangle|^2 \\ + |\langle p - 1\ 1/2 | x | d\ 0\ 1/2 \rangle|^2 + |\langle p - 1\ 1/2 | x | d - 2\ 1/2 \rangle|^2 \end{array} \right\}$$

$$= 2\,\{(1/10 + 1/10) + (1/30 + 1/5) + (1/30 + 1/5)\}$$

$$= 4/3$$

- 217 -

hence

$$\sum |x_{ab}|^2 \;=\; \sum |y_{ab}|^2 \;=\; \sum |z_{ab}|^2$$

and S must be divided by 3 for linearly polarized light.

Now consider a nonlinear process starting in a s-level, and with a transition p → d in some intermediate step, e.g., in the second step; assume also that the electric field is polarized along the z axis (for convenience):

Identical
Diagram
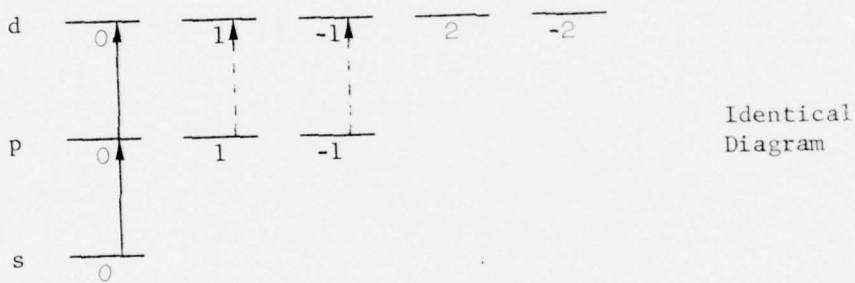
$$m_s = 1/2 \qquad\qquad m_s = -1/2$$

Because of the selection rule $\Delta m_\ell = 0$, not all the $|z_{ab}|^2$'s can be used in going from p to d . The fraction used is:

$$\frac{(0 \to 0)}{(0 \to 0) + (1 \to 1) + (-1 \to -1)} = \frac{4/15}{4/15 + 6/15} = 2/5$$

As a consequence, in a perturbation sequence step as this one, the line strength S has to be divided by 2.5, besides the factor of 3 because of polarization. Also again an extra factor of 2 appears because of spin as will be explained later.

Example: Lithium

Transition	S	$\sqrt{S/15}$	(z) (Ref. 19)	Difference in %
2p - 3d	80.4	2.32	2.26	2.5
2p - 4d	11.1	0.86	0.86	0.0
3p - 5d	30.9	1.44	1.45	1.0

C. CALCULATION OF MATRIX ELEMENTS BETWEEN PAIRS OF LEVELS OF TWO TERMS, GIVEN THE TOTAL LINE STRENGTH OF THE MULTIPLET

Remarks:

— From a mathematical point of view, one can always transform from one complete basis set to another one, in our case from $(n\ell s m_\ell m_s)$ to $(n\ell s j m_j)$. Clearly the magnitude of physical quantities calculated in both schemes should be the same. The reason why the $(n\ell s j m_j)$ scheme is a good scheme to use in the presence of spin-orbit interaction is that the total Hamiltonian $H_0 + H_{L-S}$ is to an excellent approximation diagonal in this scheme (Ref. 44). As a consequence the L-S interaction does not mix states with different j values, but only gives them different energies. If this had not been the case,

- 219 -

the matrix elements calculated between two pure j-levels would have
been incorrect for real atoms where the L-S interaction is impor-
tant.

— To calculate matrix elements between $(n\ell s j m_j)$ eigenstates,
one has to express them in terms of $(n\ell s m_\ell m_s)$ eigenstates. The
coefficients of this linear transformation are the Clebsch-Gordan
coefficients. They are tabulated in Section I for the cases of in-
terest to us, i.e.:

$$- s = 1/2$$

$$- \ell = 0, 1, 2$$

— A useful property of matrix elements in the $(j m_j)$ scheme,
that follows immediately from a symmetry argument, is:

$$\left| \langle \ell j m_j | \bar{r} | \ell' j' m_j' \rangle \right| = \left| \langle \ell j - m_j | \bar{r} | \ell' j' - m_j' \rangle \right|$$

We will frequently make use of it to simplify the calculations.

— We will use spectroscopic notation, but omit the superscript
$2s + 1 = 2$ for convenience, i.e., we will write, e.g., $P_{3/2}$ in-
stead of $^2P_{3/2}$.

— The selection rules in this scheme are:

$$\begin{cases} \Delta j = 0, \pm 1 \quad (0-0 \text{ forbidden}) \\ \Delta m_j = 0, \pm 1 \\ \Delta m_s = 0 \end{cases}$$

Since $m_j = m_\ell + m_s$, $\Delta m_j = \Delta m_\ell + \Delta m_s = \Delta m_\ell$.

— Numerical values for matrix elements are taken from Ref. 45.

1. <u>s - p Transitions</u>

Levels	Spectroscopic Notation
s $j = 1/2$	$^2S_{1/2}$
p $j = 1/2$	$^2P_{1/2}$
$j = 3/2$	$^2P_{3/2}$

The transitions allowed by the selection rule on j are:

$$S_{1/2} - P_{1/2} \qquad \Delta j = 0$$

$$S_{1/2} - P_{3/2} \qquad \Delta j = \pm 1$$

a. $\underline{S_{1/2} - P_{1/2} \text{ Transitions}}$

$P_{1/2}$ $\overline{\quad 1/2 \quad}$ $\overline{\quad -1/2 \quad}$

$S_{1/2}$ $\overline{\quad 1/2 \quad}$ $\overline{\quad -1/2 \quad}$

— Calculation of $\Sigma |z_{ab}|^2$ using $\Delta m_j = 0$, $\Delta m_s = 0$:

$$\sum = 2 \, |\langle s \; 1/2 \; 1/2 |z| p \; 1/2 \; 1/2 \rangle|^2$$

$$= 2 \, | - \sqrt{1/3} \; \langle s \; 0 \; 1/2 |z| p \; 0 \; 1/2 \rangle$$

$$+ \sqrt{2/3} \; \langle s \; 0 \; 1/2 |z| p \; 1 \; - 1/2 \rangle |^2$$

$$= 2/9$$

The second term in the sum vanishes because of $\Delta m_s = 0$.

— Calculation of $\Sigma |x_{ab}|^2$ using $\Delta m_j = \pm 1$, $\Delta m_s = 0$:

$$\sum = 2 \, |\langle s \; 1/2 \; 1/2 |x| p \; 1/2 \; - 1/2 \rangle|^2$$

$$= 2 \, |- \sqrt{2/3} \; \langle s \; 0 \; 1/2 |x| p \; - 1 \; 1/2 \rangle |^2$$

$$= 2/9$$

hence

$$\sum |x_{ab}|^2 = \sum |y_{ab}|^2 = \sum |z_{ab}|^2$$

as in the other scheme, and of course as it should be. As a consequence S must be divided by 3 for linearly polarized light.

b. $\underline{S_{1/2} - P_{3/2} \text{ Transitions}}$

$P_{3/2}$ $\overline{1/2}$ $\overline{-1/2}$ $\overline{3/2}$ $\overline{-3/2}$

$S_{1/2}$ $\overline{1/2}$ $\overline{-1/2}$

— Calculate $\Sigma |z_{ab}|^2$ using $\Delta m_j = 0$, $\Delta m_s = 0$:

$$\sum = 2 |\langle s \ 1/2 \ 1/2 |z| p \ 3/2 \ 1/2 \rangle|^2$$

$$= 2 | \sqrt{2/3} \ \langle s \ 0 \ 1/2 |z| p \ 0 \ 1/2 \rangle|^2 = 4/9$$

One shows again

$$\sum |x_{ab}|^2 = \sum |y_{ab}|^2 = \sum |z_{ab}|^2$$

and hence S must be divided by 3 for linearly polarized light.

Conclusion

Comparing the results of (1) and (2), we see that the line strength for the $S_{1/2} - P_{1/2}$ transition is twice as large as the one for the $S_{1/2} - P_{3/2}$ transition. Hence the total line strength is divided among the two lines of the doublet as follows:

Transition	Fraction
$S_{1/2} - P_{1/2}$	1/3
$S_{1/2} - P_{3/2}$	2/3

This result agrees with numerical examples taken from Ref. 45.

Example: Na 3s-3p

Transition	Line Strength	Fraction
s-p	38.1	1
$S_{1/2} - P_{1/2}$	12.7	1/3
$S_{1/2} - P_{3/2}$	25.4	2/3

2.   p - d Transitions

Levels		Spectroscopic Notation
p	$j = 1/2$	$^2P_{1/2}$
	$j = 3/2$	$^2P_{3/2}$
d	$j = 3/2$	$^2D_{3/2}$
	$j = 5/2$	$^2D_{5/2}$

The transitions allowed by the selection rule on   j   are:

$$P_{1/2} - D_{3/2} \qquad \Delta j = \pm 1$$

$$P_{3/2} - D_{3/2} \qquad \Delta j = 0$$

$$P_{3/2} - D_{5/2} \qquad \Delta j = \pm 1$$

a. $\underline{P_{1/2} - D_{3/2}}$ Transitions

$D_{3/2}$ $\overline{1/2}$ $\overline{-1/2}$ $\overline{3/2}$ $\overline{-3/2}$

$P_{1/2}$ $\overline{1/2}$ $\overline{-1/2}$

- 225 -

– Calculation of $\Sigma |z_{ab}|^2$ using $\Delta m_j = 0$, $\Delta m_s = 0$

$$\sum = 2 \ |\langle p \ 1/2 \ 1/2 |z| d \ 3/2 \ 1/2 \rangle|^2$$

$$= 2 \ | \ \sqrt{2/5} \ \sqrt{1/3} \ \langle p \ 0 \ 1/2 |z| d \ 0 \ 1/2 \rangle$$

$$+ \ \sqrt{3/5} \ \sqrt{2/3} \ \langle p \ 1 \ - 1/2 |z| d \ 1 \ - 1/2 \rangle|^2$$

$$= 2 \ (26/225 + 24/225) \ = \ 4/9$$

One shows again that S must be divided by 3 for linearly polarized light.

Consider a nonlinear process starting in a $S_{1/2}$ level, and with a transition $P_{1/2} - D_{3/2}$ as some intermediate step. Assume that the electric field is along the z axis:
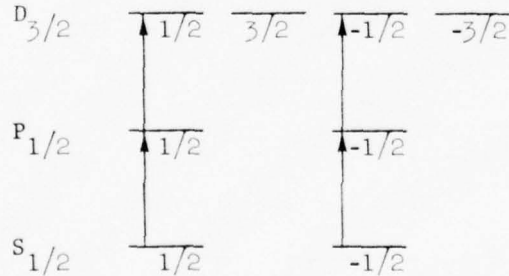
In this case of a transition $P_{1/2} - D_{3/2}$, the line strength must not be divided by an additional factor because of the fact that $\Delta m_j = 0$ for all the steps of the sequence. This will not be so for the transitions $P_{3/2} - D_{3/2}$ and $P_{3/2} - D_{5/2}$.

b. $P_{3/2} - D_{3/2}$ Transitions

$D_{3/2}$ $\overline{1/2}$ $\overline{3/2}$ $\overline{-1/2}$ $\overline{-3/2}$

$P_{3/2}$ $\overline{1/2}$ $\overline{3/2}$ $\overline{-1/2}$ $\overline{-3/2}$

— Calculation of $\Sigma |z_{ab}|^2$ using $\Delta m_j = 0$, $\Delta m_s = 0$:

$$\sum = 2 \left(|\langle p\,3/2\,1/2|z|d\,3/2\,1/2 \rangle|^2 + |\langle p\,3/2\,3/2|z|d\,3/2\,3/2 \rangle|^2 \right)$$

$$= 2 \left\{ \begin{array}{l} | -\sqrt{2/5}\ \sqrt{2/3}\ \langle p\,0\,1/2|z|d\,0\,1/2 \rangle \\[4pt] +\sqrt{3/5}\ \sqrt{1/3}\ \langle p\,1\,-1/2|z|d\,1\,-1/2 \rangle|^2 \\[4pt] + | -\sqrt{1/5}\ \langle p\,1\,1/2|z|d\,1\,1/2 \rangle|^2 \end{array} \right\}$$

$$= 2\,(1/225 + 9/225) = 4/45$$

Again a factor of 3 comes in for linearly polarized light.

Consider a nonlinear process starting in a $S_{1/2}$ level, and with
a transition $P_{3/2} - D_{3/2}$ as some intermediate step. Assume that the

electric field is along the z axis:

$D_{3/2}$ $1/2$ $3/2$ $-1/2$ $-3/2$

$P_{3/2}$ $1/2$ $3/2$ $-1/2$ $-3/2$
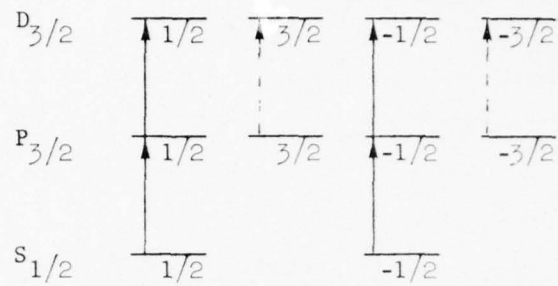
$S_{1/2}$ $1/2$ $-1/2$

Because of the selection rule $\Delta m_j = 0$, not all the $\left| z_{ab} \right|^2$'s can be used in going from $P_{3/2}$ to $D_{3/2}$. The fraction used is:

$$\frac{(1/2 - 1/2)}{(1/2 - 1/2) + (3/2 - 3/2)} = \frac{1}{1 + 9} = 1/10$$

c. $\underline{P_{3/2} - D_{5/2} \text{ Transitions}}$

$D_{5/2}$ $1/2$ $3/2$ $5/2$ $-1/2$ $-3/2$ $-5/2$

$P_{3/2}$ $1/2$ $3/2$ $-1/2$ $-3/2$
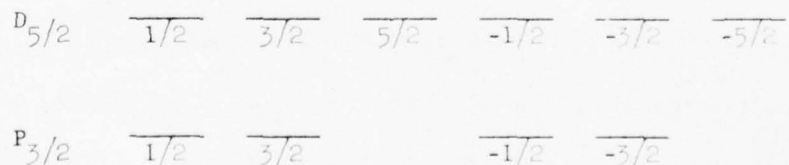
— Calculation of $\Sigma |z_{ab}|^2$ using $\Delta m_j = 0$, $\Delta m_s = 0$:

$$\Sigma = 2 \left(|\langle p\ 3/2\ 1/2 |z| d\ 5/2\ 1/2 \rangle|^2 + |\langle p\ 3/2\ 3/2 |z| d\ 5/2\ 3/2 \rangle|^2 \right)$$

$$= 2 \left\{ \begin{array}{l} |\ \sqrt{3/5}\ \sqrt{2/3}\ \langle p\ 0\ 1/2 |z| d\ 0\ 1/2 \rangle \\[2mm] +\ \sqrt{2/5}\ \sqrt{1/3}\ \langle p\ 1\ -1/2 |z| d\ 1\ -1/2 \rangle |^2 \\[2mm] +\ |\ \sqrt{4/5}\ \langle p\ 1\ 1/2 |z| d\ 1\ 1/2 \rangle |^2 \end{array} \right\}$$

$$= 2\ (54/225 + 36/225)\ =\ 4/5$$

Again a factor of 3 comes in for linearly polarized light.

Consider a nonlinear process starting in a $S_{1/2}$ level, and with a transition $P_{3/2} - D_{5/2}$ as some intermediate step. Assume that the electric field is along the z axis:
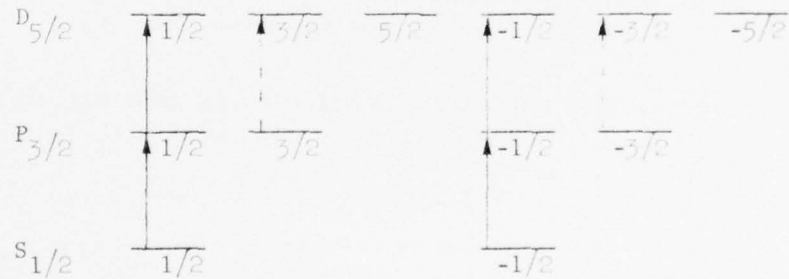

The fraction used in this case is:

$$\frac{(1/2 - 1/2)}{(1/2 - 1/2) + (3/2 - 3/2)} = \frac{54}{54 + 36} = 6/10$$

Conclusion

Let's compare $\Sigma |z_{ab}|^2$ for the three lines:

Line	$\Sigma |z_{ab}|^2$
$P_{1/2} - D_{3/2}$	4/9
$P_{3/2} - D_{3/2}$	4/45
$P_{3/2} - D_{5/2}$	4/5

hence the total line strength of the multiplet is divided among the three lines as follows:

Line	Fraction
$P_{1/2} - D_{3/2}$	5/15
$P_{3/2} - D_{3/2}$	1/15
$P_{3/2} - D_{5/2}$	9/15

This result agrees with numerical examples taken from Ref. 45.

Example: Na 3p-3d

Transition	Line Strength	Fraction
p-d	135.0	1
$P_{1/2} - D_{3/2}$	44.7	5/15
$P_{3/2} - D_{3/2}$	9.0	5/15
$P_{3/2} - D_{5/2}$	81.0	9/15

D.   EFFECT OF SPIN ON THE CALCULATION OF MATRIX ELEMENTS

FROM LINE STRENGTHS

As was mentioned in the Introduction, we require that all the electric fields used in the process have the same polarization; for mathematical convenience we take them all along the z axis (of course this does not have an effect on the final result). The diagrams in Sections B and C may help in clarifying the discussion in this section.

1. $(\ell m_\ell m_s)$ Scheme

In the calculation of a linear or nonlinear process, one always has to perform a sum over all possible paths. In the $(\ell m_\ell m_s)$ scheme, this sum can be subdivided into two parts: one part with spin up $(m_s = 1/2)$ and one with spin down $(m_s = -1/2)$. Because of the selection rule $\Delta m_s = 0$ these two parts are uncoupled. The expressions for susceptibilities (and related quantities) can then be written as:

$$\chi \approx \begin{pmatrix} \text{fraction of the population with } m_s = 1/2 \\ \text{in the first level of the process} \end{pmatrix}$$

$$\times \sum_{\text{paths}} \begin{pmatrix} \text{product of matrix} \\ \text{elements} \end{pmatrix} \qquad \text{(Cont'd)}$$

- 231 -

$$+ \begin{pmatrix} \text{fraction of the population with } m_s = -1/2 \\ \text{in the first level of the process} \end{pmatrix}$$

$$\times \sum_{\text{paths}} \begin{pmatrix} \text{product of matrix} \\ \text{elements} \end{pmatrix}$$

Since the electronic matrix elements in both terms of this sum are equal, we can write equivalently:

$$\chi \approx \begin{pmatrix} \text{total population in the first level of} \\ \text{the process} \end{pmatrix}$$

$$\times \sum_{\text{paths}} \begin{pmatrix} \text{product of matrix} \\ \text{elements} \end{pmatrix}$$

This means that equivalently we can assign all the population of the first level to either one of the spin states, and consider the other one empty, i.e., we only use one-half of the diagrams in Section I. Because the line strength includes a summation over spin, since it is defined in the $(\ell j m_j)$ scheme, this implies that for each step of a perturbation sequence the line strength must be divided by two to find the effective matrix element for that step.

2. $(\ell j m_j)$ Scheme

In this scheme we cannot in general make a subdivision as in the other scheme, i.e., states with positive and negative m_j values are not uncoupled, e.g., $(s\ 1/2\ 1/2 | x | p\ 1/2 - 1/2) \neq 0$. However, if we assume all the electric fields polarized along the z axis, then states with m_j values of opposite sign are uncoupled $(\Delta m_j = 0)$, and we

- 232 -

can make an argument analogous to the one used in the other scheme, i.e.:

$$X \simeq \begin{pmatrix} \text{fraction of the population with total angular} \\ \text{momentum up in the first step of the process} \end{pmatrix}$$

$$\times \sum_{\text{paths}} \begin{pmatrix} \text{product of matrix} \\ \text{elements} \end{pmatrix}$$

$$+ \begin{pmatrix} \text{fraction of the population with total angular} \\ \text{momentum down in the first step of the process} \end{pmatrix}$$

$$\times \sum_{\text{paths}} \begin{pmatrix} \text{product of matrix} \\ \text{elements} \end{pmatrix}$$

The rest of the argument is analogous to the previous case, and the conclusion is the same.

E.   SUMMARY OF RULES FOR CONVERSION FROM LINE STRENGTHS TO
      MATRIX ELEMENTS

<u>Remarks</u>:

— Only the absolute value of the matrix elements can be found from the line strength; in the tables below the conversion is given from line strength to the square of the matrix element.

— For p-d transitions, we have to consider two cases (see Sections B and C for an explanation):

<u>Case 1</u>: None of the preceding steps in the perturbation sequence uses a s-p transition.

<u>Case 2</u>: At least one of the preceding steps uses a s-p transition.

1. $(\ell m_\ell m_s)$ Scheme, Linearly Polarized Light

Transition		Fraction of S
s-p		1/6
p-d	Case 1	1/6
	Case 2	1/15

2. $(\ell j m_j)$ Scheme, Linearly Polarized Light

Transition		Fraction of Total S of the Multiplet	Fraction of S of the Line
$S_{1/2} - P_{1/2}$		1/18	1/6
$S_{1/2} - P_{3/2}$		1/9	1/6
$P_{1/2} - D_{3/2}$	Case 1	1/18	1/6
	Case 2	1/18	1/6
$P_{3/2} - D_{3/2}$	Case 1	1/90	1/6
	Case 2	1/900	1/60
$P_{3/2} - D_{5/2}$	Case 1	1/10	1/6
	Case 2	3/50	1/10

F. CALCULATION OF A THIRD ORDER SUSCEPTIBILITY IN THE

$(\ell m_\ell m_s)$ AND $(\ell j m_j)$ SCHEMES

The purpose of this section is to demonstrate with an example that, if j-degeneracy is assumed, susceptibilities calculated in both schemes have the same value, as they should. One must assume j-degeneracy to make the detunings for the various transitions between levels of two terms identical. From a practical point of view it follows that, in the case of detunings much larger than the doublet splittings, susceptibilities can be calculated in either scheme, the calculations in the $(\ell m_\ell m_s)$ scheme being much simpler however. This calculation is also a numerical check on the results of the previous sections.

− Path: s - p - d - p - s

− We assume an electric field parallel with the z axis, hence

$$\chi \simeq \sum_{\text{paths}} \langle s|z|p \rangle \langle p|z|d \rangle \langle d|z|p \rangle \langle p|z|s \rangle$$

− Symbols:

S_1 = total line strength for the s-p multiplet

S_2 = total line strength for the p-d multiplet

1. $(\ell m_\ell m_s)$ Scheme
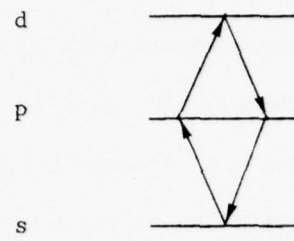
$$X \simeq \sqrt{s_1/6} \; \sqrt{s_2/15} \; \sqrt{s_2/15} \; \sqrt{s_1/6} \; = \; s_1 s_2/90$$

2. $(\ell j m_j)$ Scheme
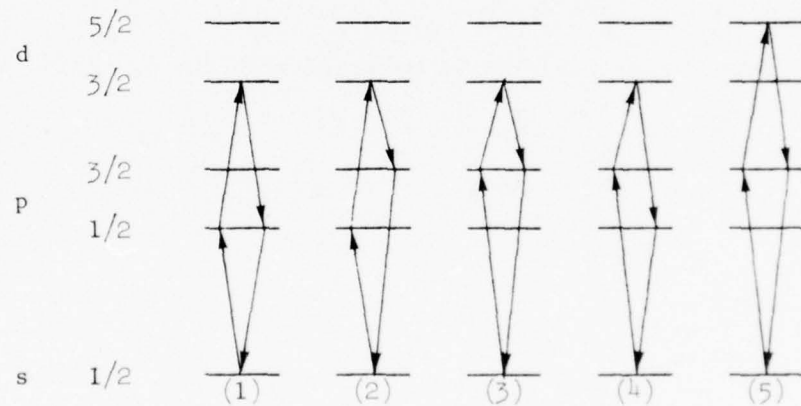
(1) $\quad \sqrt{s_1/18} \; \sqrt{s_2/18} \; \sqrt{s_2/18} \; \sqrt{s_1/18} \; = \; s_1 s_2/324$

(2) $\quad \sqrt{s_1/18} \; \sqrt{s_2/18} \; \sqrt{s_2/900} \; \sqrt{s_1/9} \; = \; s_1 s_2/1620$

(3) $\sqrt{S_1/9} \ \sqrt{S_2/900} \ \sqrt{S_2/900} \ \sqrt{S_1/9} = S_1 S_2/8100$

(4) $\sqrt{S_1/9} \ \sqrt{S_2/900} \ \sqrt{S_2/18} \ \sqrt{S_1/18} = S_1 S_2/1620$

(5) $\sqrt{S_1/9} \ \sqrt{3S_2/50} \ \sqrt{3S_2/50} \ \sqrt{S_1/9} = S_1 S_2/150$

$X \simeq S_1 S_2 \ (1/324 + 1/1620 + 1/8100 + 1/1620 + 1/150)$

$= S_1 S_2 \ (90/8100) = S_1 S_2/90$

G. DEFINITIONS[44]

— Level: Set of $(2j + 1)$ <u>states</u>, each characterized by a dif-
ferent m_j value. If the atom is unperturbed by ex-
ternal fields, the $(2j + 1)$ states are degenerate.
When the atom is perturbed they can have different
energies.

— Line: Radiation associated with all possible transitions be-
tween the states belonging to two levels. The radiation
resulting from a transition between a particular pair of
states is called a <u>component</u> of the line.

— Configuration: The quantum numbers (n, ℓ) are said to specify
the configuration of the electron.

- Term: The (one or) two levels into which each configuration is split because of spin-orbit interaction are said to constitute a doublet term.

- Multiplet: Ensemble of all lines connected with transitions from one term characterized by L,S to another characterized by L',S' .

H. LINE STRENGTH, OSCILLATOR STRENGTH AND EINSTEIN COEFFICIENT[44]

1. Line Strength

Given two levels A and B , each consisting of several states (respectively $2j_A + 1$ and $2j_B + 1$), the line strength is defined as:

$$S(A,B) \ = \ S(B,A) \ = \ S \ = \ \sum_{a,b} \ |\langle a|\overline{P}|b\rangle|^2$$

where $\overline{P} = - e \sum_{i} \overline{r}_i$ is the dipole moment operator. If only one electron is involved, $\overline{P} = - e\overline{r}$ and

$$S \ = \ e^2 \ \sum_{a,b} \ (|x_{ab}|^2 + |y_{ab}|^2 + |z_{ab}|^2)$$

The summation is over all states a,b of the levels A,B .

<u>Example</u>:

p,j = 3/2 $\overline{3/2}$ $\overline{1/2}$ $\overline{-1/2}$ $\overline{-3/2}$ ← 4 states

s,j = 1/2 $\overline{1/2}$ $\overline{-1/2}$ ← 2 states

Note that S is symmetrical to the initial and final levels. The physical origin of this definition of S is that the total intensity of a line in natural excitation (equal numbers of atoms in all the states of the same level) is given by:

$$I(A,B) = N(a)\ h\nu\ \frac{64\pi^4\nu^3}{3hc^3} \sum_{a,b} |\langle a|\overline{P}|b\rangle|^2$$

$$\simeq N(a)\ S(A,B)$$

2.   <u>Oscillator Strength</u>

Given two levels (αj) and $(\alpha' j')$, the oscillator strength is defined as:

$$f(\alpha' j',\alpha j) = \frac{8\pi^2\mu}{3e^2 h}\ \frac{\nu(\alpha' j',\alpha j)\ S(\alpha j,\alpha' j')}{2j+1}$$

where

$$(\alpha j) \quad = \quad \text{lower level}$$

$$(\alpha' j') \quad = \quad \text{higher level}$$

$$v(\alpha' j', \alpha j) \quad = \quad \text{frequency of the transition}$$

Note that the oscillator strength is defined between two levels, each having a particular j value. The physical origin of this definition of oscillator strength is: it is the ratio of the contribution of the spectral line $(\alpha' j', \alpha j)$ to the atomic polarizability, and the polarizability of a classical harmonic oscillator with a resonant frequency equal to the frequency $v(\alpha' j', \alpha j)$ of the transition. Using more common notation:

$$(\alpha j) \quad = \quad i$$

$$(\alpha' j') \quad = \quad k$$

$$2j + 1 \quad = \quad g_i$$

$$v(\alpha' j', \alpha j) \quad = \quad c/\lambda$$

and substituting numerical values for the constants:

$$f_{ik} = 303.7 \; \frac{S}{g_i \lambda} \qquad (F.1)$$

$$S = 3.292 \times 10^{-3} \; g_i \lambda f_{ik} \qquad (F.2)$$

where

- λ in $\overset{\circ}{A}$

- S in a.u. (i.e., in units of $a_0 e$);
  conversion to Int. System:
  $$\mu = 8.46 \times 10^{-30} \sqrt{S}$$

Expressions (F.1) and (F.2) agree with those given in the conversion table in Ref. 45. Note that the oscillator strength is not symmetrical in the initial and final levels, since S is symmetrical and g_i refers to the lower level. However, if f_{ik} is known, one can always find S using (F.2). As a consequence it was sufficient to give all the results in Section E in terms of S .

3. Einstein Coefficient

Given two levels A and B , the Einstein coefficient is defined as:

$$G(A,B) = \frac{64\pi^4 \nu^3}{3hc^3} \cdot \frac{S(A,B)}{2j_A + 1}$$

where

$$A = \text{initial level} = \text{higher level}$$

$$B = \text{final level} = \text{lower level}$$

Just as the oscillator strength, an Einstein coefficient is defined between two levels, each having a particular j value. The physical origin of this definition of Einstein coefficient is: the total intensity of the line $A \to B$ is given by:

$$I(A,B) = N(A) \, h\nu \, G(A,B)$$

where $N(A)$ is the total population of level A (the reader is urged to read pp. 97 and 98 in Ref. 44 at this point to get the complete picture). Using more common notation:

$$A = k$$

$$B = i$$

$$2j_A + 1 = g_k$$

and substituting numerical values for the constants:

$$G_{ki} = 2.026 \times 10^{18} \frac{S}{g_k \lambda^3} \qquad (F.3)$$

$$S = 4.935 \times 10^{-19} g_k \lambda^3 G_{ki} \qquad (F.4)$$

where

- λ in $\overset{o}{A}$

- S in a.u.

Expressions (F.3) and (F.4) agree with those given in the conversion table in Ref. 45. Just as in the case of the oscillator strength, the Einstein coefficient is not symmetric in the initial and final levels. However, given G , one finds S using (F.4), and again there is no loss in generality by expressing everything in terms of S .

I. CLEBSCH-GORDAN COEFFICIENTS

One goes from the basis set $|n\ell sm_\ell m_s\rangle$ to the basis set $|n\ell sjm_j\rangle$ by a linear transformation. The coefficients used in this transformation are the Clebsch-Gordan coefficients. Clearly the number of eigenstates in the second scheme has to be equal to the number of eigenstates in the first scheme, since all the eigenstates are orthogonal in the

first scheme; this can be shown very easily:

$$|m_\ell m_s\rangle \quad \text{basis: degeneracy} = \underset{\text{spin}}{2} \times \underset{m_\ell \text{ degeneracy}}{(2\ell + 1)}$$

$$|jm_j\rangle \quad \text{basis: degeneracy} = \sum_j \underset{m_j \text{ degeneracy}}{(2j + 1)}$$

$$= 2(\ell - 1/2) + 1 + 2(\ell + 1/2) + 1$$

$$= 2(2\ell + 1)$$

The coefficients given in the following table were calculated using Table 1[3] on p. 76 in Ref. 44.

<u>Transformation Matrices</u>

I. <u>s-state</u>

$$\ell = 0 \quad , \quad m_\ell = 0 \quad ; \quad j = 1/2 \quad , \quad m_j = \pm 1/2$$

$$
\begin{array}{cc} j & m_j \end{array}
\qquad\qquad
\begin{array}{cc} m_\ell & m_s \end{array}
$$

$$
\begin{pmatrix} |1/2 \quad 1/2\rangle \\ |1/2 \quad -1/2\rangle \end{pmatrix} = \begin{pmatrix} 1 & 0 \\ 0 & 1 \end{pmatrix} \begin{pmatrix} |0 \quad 1/2\rangle \\ |0 \quad -1/2\rangle \end{pmatrix}
$$

II. p-state

$\ell = 1$, $m_\ell = 0$, ± 1 ; $\begin{cases} j = 1/2 & m_j = \pm 1/2 \\ j = 3/2 & m_j = \pm 1/2 , \pm 3/2 \end{cases}$

$$
\begin{bmatrix}
|1/2 \;\; 1/2\rangle \\
|1/2 \;\; -1/2\rangle \\
|3/2 \;\; 3/2\rangle \\
|3/2 \;\; -3/2\rangle \\
|3/2 \;\; 1/2\rangle \\
|3/2 \;\; -1/2\rangle
\end{bmatrix}
=
\begin{bmatrix}
-\sqrt{1/3} & \sqrt{2/3} & 0 & 0 & 0 & 0 \\
0 & 0 & \sqrt{1/3} & -\sqrt{2/3} & 0 & 0 \\
0 & 0 & 0 & 0 & 1 & 0 \\
0 & 0 & 0 & 0 & 0 & 1 \\
\sqrt{2/3} & \sqrt{1/3} & 0 & 0 & 0 & 0 \\
0 & 0 & \sqrt{2/3} & \sqrt{1/3} & 0 & 0
\end{bmatrix}
\begin{bmatrix}
|0 \;\; 1/2\rangle \\
|1 \;\; -1/2\rangle \\
|0 \;\; -1/2\rangle \\
|-1 \;\; 1/2\rangle \\
|1 \;\; 1/2\rangle \\
|-1 \;\; -1/2\rangle
\end{bmatrix}
$$

III. d-state

$$\ell = 2 \,,\quad m_\ell = 0 \,,\ \pm 1 \,,\ \pm 2 \,;\quad
\begin{cases}
j = 3/2 & m_j = \pm 1/2 \,,\ \pm 3/2 \\[4pt]
j = 5/2 & m_j = \pm 1/2 \,,\ \pm 3/2 \,,\ \pm 5/2
\end{cases}$$

	$\lvert 0\ 1/2\rangle$	$\lvert 0\ -1/2\rangle$	$\lvert 1\ 1/2\rangle$	$\lvert 1\ -1/2\rangle$	$\lvert -1\ 1/2\rangle$	$\lvert -1\ -1/2\rangle$	$\lvert 2\ 1/2\rangle$	$\lvert 2\ -1/2\rangle$	$\lvert -2\ 1/2\rangle$	$\lvert -2\ -1/2\rangle$
$\lvert 3/2\ \ 1/2\rangle$	$-\sqrt{2/5}$	0	0	$\sqrt{3/5}$	0	0	0	0	0	0
$\lvert 3/2\ -1/2\rangle$	0	$\sqrt{2/5}$	0	0	$-\sqrt{3/5}$	0	0	0	0	0
$\lvert 3/2\ \ 3/2\rangle$	0	0	$-\sqrt{1/5}$	0	0	0	0	$\sqrt{4/5}$	0	0
$\lvert 3/2\ -3/2\rangle$	0	0	0	0	0	$\sqrt{1/5}$	0	0	$-\sqrt{4/5}$	0
$\lvert 5/2\ \ 1/2\rangle$	$\sqrt{3/5}$	0	0	$\sqrt{2/5}$	0	0	0	0	0	0
$\lvert 5/2\ -1/2\rangle$	0	$\sqrt{3/5}$	0	0	$\sqrt{2/5}$	0	0	0	0	0
$\lvert 5/2\ \ 3/2\rangle$	0	0	$\sqrt{4/5}$	0	0	0	0	$\sqrt{1/5}$	0	0
$\lvert 5/2\ -3/2\rangle$	0	0	0	0	0	$\sqrt{4/5}$	0	0	$\sqrt{1/5}$	0
$\lvert 5/2\ \ 5/2\rangle$	0	0	0	0	0	0	1	0	0	0
$\lvert 5/2\ -5/2\rangle$	0	0	0	0	0	0	0	0	0	1

REFERENCES

1. D. A. Kleinman and G. D. Boyd, J. Appl. Phys. 40, 546 (1969).

2. J. Warner, Opto-Electronics 3, 37 (1971).

3. A. F. Milton, Appl. Optics 11, 2311 (1972).

4. R. T. Hodgson, P. P. Sorokin, and J. J. Wynne, Phys. Rev. Lett. 32, 343 (1974).

5. S. E. Harris and D. M. Bloom, Appl. Phys. Lett. 24, 229 (1974).

6. D. M. Bloom, J. T. Yardley, J. F. Young, and S. E. Harris, Appl. Phys. Lett. 24, 427 (1974).

7. F. Biraben, B. Cagnac, and G. Grynberg, Phys. Rev. Lett. 32, 643 (1974).

8. M. D. Levenson and N. Bloembergen, Phys. Rev. Lett. 32, 645 (1974).

9. T. W. Hänsch, K. C. Harvey, G. Meisel, and A. L. Schawlow, Opt. Comm. 11, 50 (1974).

10. D. Pritchard, J. Apt, and T. W. Ducas, Phys. Rev. Lett. 32, 641 (1974).

11. D. B. Lidow, R. W. Falcone, J. F. Young, and S. E. Harris, Phys. Rev. Lett. 36, 462 (1976).

12. P. N. Butcher, Nonlinear Optical Phenomena, Ch. 8, Bulletin 200, Engineering Experiment Station, Ohio State University, Columbus, Ohio (1965).

13. B. D. Fried and S. D. Conte, The Plasma Dispersion Function (New York: Academic Press, 1961).

14. R. Bracewell, The Fourier Transform and Its Applications (New York: McGraw-Hill Book Co., 1965).

15. F. Zernike and J. E. Midwinter, Applied Nonlinear Optics (New York: John Wiley and Sons, 1973).

16. K. S. Krishnan and J. S. Ostrem, "Evaluation of Technologies for Infrared Imaging," Stanford Research Institute, Menlo Park, California (1976).

17. J. Falk and W. B. Tiffany, J. Appl. Phys. 43, 3762 (1972).

18. R. A. Andrews, IEEE J. Quant. Elect. QE-6, 68 (1970).

19. R. B. Miles and S. E. Harris, IEEE J. Quant. Elect. QE-9, 470 (1973).

20. N. N. Kostin and V. A. Khodovoi, Seriya Fizicheskaya, 37, 2093 (1973).

21. J. Reintjes, private communication.

22. N. N. Kostin and V. A. Khodovoi, Seriya Fizicheskaya 37, 2083 (1973).

23. A. N. Nesmeyanov, Vapor Pressure of Chemical Elements (New York: Elsevier Publishing Co., 1963).

24. S. E. Harris, "Principles of Nonlinear Optical Devices," Note Set 5, Department of Electrical Engineering Course EE 346, Stanford University, Stanford, California.

25. S. E. Harris, Proc. IEEE 57, 2096 (1969).

26. C. S. Chang, Phys. Rev. A $\underline{9}$, 1769 (1974).

27. Nan Mohan and S. N. Hague, Phys. Rev. A $\underline{9}$, 725 (1974).

28. J. Bakos, A. Kiss, L. Snabo, and M. Tendler, Phys. Lett. $\underline{41A}$, 163 (1972).

29. B. Held, C. Mainfray, C. Manus, J. Norellec, and F. Sanchez, Phys. Rev. Lett. $\underline{30}$, 423 (1973).

30. S. E. Harris, Phys. Rev. Lett. $\underline{31}$, 341 (1973).

31. S. E. Harris and D. M. Bloom, Appl. Phys. Lett. $\underline{24}$, 229 (1974).

32. N. Bloembergen, Nonlinear Optics (New York: Benjamin Book Co., 1965), Chap. 2.

33. C. E. Moore, Atomic Energy Levels, Volume I, NSRDS-NBS-4 (U.S. GPO, Washington, D.C., 1966).

34. W. L. Wiese, M. W. Smith, and B. M. Glennon, Atomic Transition Probabilities: Volume I — Hydrogen Through Neon, NSRDS-NBS-4 (U.S. GPO, Washington, D.C., 1966).

35. J. F. Ward and G. H. C. New, Phys. Rev. Lett. $\underline{19}$, 556 (1967); R. B. Miles and S. E. Harris, IEEE J. Quant. Elect. QE-$\underline{9}$, 470 (1973).

36. H. B. Bebb and A. Gold, Phys. Rev. $\underline{143}$, 1 (1966).

37. V. M. Morton, Proc. Phys. Soc. Lond. $\underline{92}$, 301 (1967).

38. E. A. Stappaerts, Phys. Rev. A $\underline{11}$, 1664 (1975).

39. J. W. Goodman, Introduction to Fourier Optics (New York: Mc-Graw-Hill Book Co., 1968).

40. S. Ramo, J. R. Whinnery, and T. Van Duzer, <u>Fields and Waves in Communication Electronics</u> (New York: John Wiley and Sons, 1967).

41. S. E. Harris, "Slow Collisions Between Atoms," Department of Electrical Engineering Course EE 392F, Stanford University, Stanford, California.

42. E. Merzbacher, <u>Quantum Mechanics</u> (New York: John Wiley and Sons, 1961), Chap. 9.

43. L. I. Schiff, <u>Quantum Mechanics</u> (New York: McGraw-Hill Book Co., 1968), Chap. 4, p. 76.

44. E. U. Condon and G. H. Shortley, <u>The Theory of Atomic Spectra</u> (New York: Cambridge University Press, 1970), Chaps. 3 and 4.

45. W. L. Wiese, M. W. Smith, and B. M. Glennon, <u>Atomic Transition Probabilities: Volume I — Nitrogen Through Neon</u>, NSRDS-NBS-4 (U.S. GPO, Washington, D.C., 1966); and W. L. Wiese, M. W. Smith, and B. M. Miles, <u>Atomic Transition Probabilities: Volume II — Sodium Through Calcium</u>, NSRDS-NBS-22 (U.S. GPO, Washington, D.C., 1969).

46. C. E. Moore, <u>Atomic Energy Levels: Volume III</u>, NSRDS-NBS-35 (U.S. GPO, Washington, D.C., 1966).

APPENDIX B

PUBLICATIONS

1. E. A. Stappaerts, "Dependency of Susceptibilities on Polarization," Internal Memorandum, Microwave Laboratory Report No. 2438, Stanford University, Stanford, California (May 1975).

2. E. A. Stappaerts, "Conversion of Line Strengths, Oscillator Strengths and Einstein Coefficients to Matrix Elements Used in Perturbation Calculations," Internal Memorandum, Microwave Laboratory Report No. 2439, Stanford University, Stanford, California (May 1975).

3. E. A. Stappaerts, "Infrared Image Up-Conversion in Alkali Metal Vapors," Ph.D. Dissertation, Ginzton Laboratory Report No. 2569, Stanford University, Stanford, California (May 1976).

4. E. A. Stappaerts, G. W. Bekkers, J. F. Young, and S. E. Harris, "The Effect of Linewidth on the Efficiency of Two-Photon-Pumped Frequency Converters," IEEE J. Quant. Elect. QE-12, 330 (June 1976).

5. E. A. Stappaerts, S. E. Harris, and J. F. Young, "Infrared Image Up-Conversion in Alkali Metal Vapors," presented at the 9th International Quantum Electronics Conference, Amsterdam, The Netherlands, June 14-18, 1976.

6. E. A. Stappaerts, S. E. Harris, and J. F. Young, "Efficient IR Image Up-Conversion in Two-Photon Resonantly Pumped Cs Vapor," Appl. Phys. Lett. (to be published).

APPENDIX C

PUBLICATIONS UNDER RELATED CONTRACTS

Contract F19628-73-C-0025

1. J. F. Young, R. B. Miles, S. E. Harris, and R. W. Wallace, "Pump Linewidth Requirement for Optical Parametric Oscillators," J. Appl. Phys. 42, 497 (January 1971).

2. S. E. Harris and R. B. Miles, "Proposed Third Harmonic Generation in Phase-Matched Metal Vapors," Appl. Phys. Lett. 19, 385 (November 1971).

3. J. F. Young, G. C. Bjorklund, A. H. Kung, R. B. Miles, and S. E. Harris, "Third Harmonic Generation in Phase Matched Rb Vapor," Phys. Rev. Lett. 27, 1551 (December 1971).

4. J. Pinard and J. F. Young, "Interferometric Stabilization of an Optical Parametric Oscillator," Optics Comm. 4, 425 (March 1972).

5. R. B. Miles, "Optical Third Harmonic Generation in Metal Vapors," Ph.D. Dissertation, Microwave Laboratory Report No. 2069, Stanford University, Stanford, California (June 1972).

6. A. H. Kung, J. F. Young, G. C. Bjorklund, and S. E. Harris, "Generation of Vacuum Ultraviolet Radiation in Phase Matched Cd Vapor," Phys. Rev. Lett. 29, 985 (October 1972).

7. A. H. Kung, J. F. Young, and S. E. Harris, "Generation of 1182 Å Radiation in Phase Matched Mixtures of Inert Gases," Appl. Phys. Lett. 22, 301 (March 1973).

8. R. B. Miles and S. E. Harris, "Optical Third Harmonic Generation in Alkali Metal Vapors," IEEE J. Quant. Elect. QE-9, 470 (April 1973).

9. S. E. Harris, "Generation of Vacuum Ultraviolet and Soft X-Ray Radiation Using High-Order Nonlinear Optical Polarizabilities," Phys. Rev. Lett. 31, 341 (August 1973).

10. S. E. Harris, A. H. Kung, E. A. Stappaerts, and J. F. Young, "Stimulated Emission in Multiple-Photon-Pumped Xenon and Argon Excimers," Appl. Phys. Lett. 23, 232 (September 1973).

11. S. E. Harris, J. F. Young, A. H. Kung, D. M. Bloom, and G. C. Bjorklund, "Generation of Ultraviolet and Vacuum Ultraviolet Radiation," in Laser Spectroscopy, R. G. Brewer and A. Mooradian, eds. (New York: Plenum Publishing Corp., 1974), p. 59.

12. D. M. Bloom, James T. Yardley, J. F. Young, and S. E. Harris, "Infrared Up-Conversion With Resonantly Two-Photon Pumped Metal Vapors," Appl. Phys. Lett. 24, 427 (May 1974).

Contract F19(628)-67-C-0038

1. S. E. Harris, "Threshold of Phase-Locked Parametric Oscillators," IEEE J. Quant. Elect. QE-3, 205 (May 1967).

2. R. L. Byer and S. E. Harris, "Power and Bandwidth of Spontaneous Parametric Emission," Phys. Rev. 168, 1064 (April 1968).

3. R. W. Wallace, S. E. Harris, and C. F. Quate, "Acousto-Optic Tuning and Phase Matching of Optical Parametric Oscillators," Microwave Laboratory Report No. 1647, Stanford University, Stanford, California (June 1968).

4. R. L. Byer, M. K. Oshman, J. F. Young, and S. E. Harris, "Visible CW Parametric Oscillator," Appl. Phys. Lett. 13, 109 (August 1968).

5. J. Falk and J. E. Murray, "Single Cavity Noncollinear Parametric Oscillation," Appl. Phys. Lett. 14, 245 (April 1969).

6. S. E. Harris, "Method to Lock an Optical Parametric Oscillator to an Atomic Transition," Appl. Phys. Lett. 14, 335 (June 1969).

7. R. W. Wallace and S. E. Harris, "Oscillation and Doubling of the .946 μ Line in Nd^{3+}:YAG," Appl. Phys. Lett. 15, 111 (August 1969).

8. S. E. Harris, "Tunable Optical Parametric Oscillators," Proc. IEEE 57, 2096 (December 1969).

9. R. W. Wallace, "0.473 μ Light Source Using the Second Harmonic of the 0.946 μ Line in Nd^{3+}:YAG," Microwave Laboratory Report No. 1808, Stanford University, Stanford, California (December 1969).

MISSION
of
Rome Air Development Center

RADC plans and conducts research, exploratory and advanced
development programs in command, control, and communications
(C^3) activities, and in the C^3 areas of information sciences
and intelligence. The principal technical mission areas
are communications, electromagnetic guidance and control,
surveillance of ground and aerospace objects, intelligence
data collection and handling, information system technology,
ionospheric propagation, solid state sciences, microwave
physics and electronic reliability, maintainability and
compatibility.